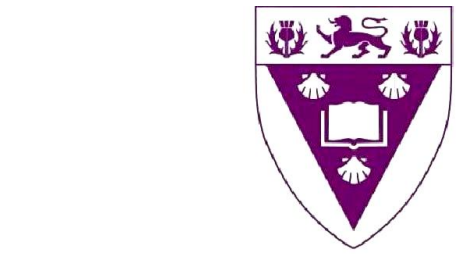

RHODES UNIVERSITY

Where leaders learn

Gold nanoparticle–based colorimetric probes for dopamine detection

A thesis submitted to Rhodes University in fulfilment of the requirements for the degree of

Doctor of Philosophy (Science)

By

Nokuthula Ngomane

Supervised by

Prof Rui Krause

Co–supervised by

Prof Nelson Torto and Dr Sibulelo Vilakazi

April 2015

DEDICATION

This thesis is dedicated to my whole family with love.

Acknowledgements

Psalm 28: 7 “The LORD *is* my strength and my shield; my heart trusted in him, and I am helped: therefore my heart greatly rejoiceth; and with my song will I praise him” (KJB). King James puts it better…thanks Daddy.

To my supervisor Professor Rui Krause, thank you so much for the chance to work under your supervision. I will forever be grateful for all the opportunities you presented to me including the trip to Malta.

I would like to express my sincere gratitude to my Honours and Masters supervisor Professor Nelson Torto for his supervision. Thank you so much for all the opportunities you gave me and the training. Not meaning to blow my own trumpet, but I believe that I am now a better researcher and individual because of your training and guidance. Thank you so much for believing in me and for the opportunity to be part of your group. It was an honour to work under you supervision, thank you.

I would like to extend my appreciation to my co-supervisor Dr Sibulelo Vilakazi for all the academic support and making sure that I had everything I needed when I visited at MINTEK for HRTEM characterization. This work would not have been a success without all you scientific contribution. From the bottom of my heart, I thank you.

I am deeply indebted to Dr Shima Batlokwa, who was my mentor in my honours level. Thank you so much doc for convincing me to continue with my studies. You also went all out to make sure that I understand the concept of molecular imprinting. Thank you.

To my colleagues in F22 and former F12 colleagues: thank you so much for all your professional critics of my work during the course of the MSc and PhD period, you have helped broaden my view and knowledge, you are highly appreciated.

MINTEK, for the financial support, thank you. I also appreciate Siyasanga (also from MINTEK) for running my samples. I know it was not easy and took much of your time, thank you so much for your patience.

Dr Mashazi, thank you so much for helping with the XPS analysis.

To my mother, thank you so much Dlamini for taking your parenting duty serious. You are such a wonderful blessing to me. I love you!

To my family Sibusiso, Sabelo, Nonduduzo, Musomuhle, Sboniso and Themba: you are the best guys, thank you so much for all the support and encouragement. I thank my heavenly father every time I think of you. I am truly blessed having you as my brothers and sister.

To my family in Grahamstown: particularly Yolanda and Melody; all my friends and brethren who were always there for me and never forgot me in their prayers. May the Lord reward you according to His riches in glory.

I am thankful to NRF, DST/MINTEK and the Henderson Postgraduate Scholarship for financial assistance.

Last but not least, I am very thankful to the Nelson Mandela Metropolitan University, the physics department in particular for assistance with the high resolution scanning electron microscopy analysis.

Abstract

Colorimetric probes have become important tools in analysis and biomedical technology. This thesis reports on the development of such probes for the detection of dopamine (DA). Liquid and different solid state probes were developed utilizing un–functionalized gold nanoparticles (UF–AuNPs). The liquid state probe is based on the growth and aggregation of the UF–AuNPs in the presence of DA. Upon addition of the UF–AuNPs to various concentrations of DA, the shape, size and colour change results in spectral shifts from lower to higher wavelengths. The analyte can be easily monitored by the naked eye from 5.0 nM DA with a calculated limit of detection of 2.5 nM (3σ) under optimal pH. Ascorbic acid (AA) has a potential to interfere with DA detection in solution since it is often present in biological fluids, but in this case the interference was limited to solutions where its concentration was beyond 200 times greater than that of DA. Since most of the previously reported colorimetric probes, especially those for DA are solution based, the main focus of the thesis was in the development of a solid state based colorimetric probe in the form of nanofibre mats. To overcome the interference challenges experienced in the solution studies (the interference by high concentrations of AA), the suitability of molecularly imprinted polymers (MIPs) for the selective detection of DA was investigated. The results showed that the MIPs produced did not play a significant role in enhancing the selectivity towards DA. A probe composed of just the UF–AuNPs and Nylon–6 (UF–AuNPs + N6) was also developed. The UF–AuNPs were synthesized following an *in situ* reduction method. The probe was only selective to DA and insensitive to other catecholamines at physiological pH. Thus, the probe did not require any addition functionalities to achieve selectivity and sensitive to DA. The liquid state probe and the composite UF–AuNPs + N6 nanofibre probe were successfully applied to a whole blood sample and showed good selectivity towards DA. The simple, sensitive and selective probe could be an excellent alternative for on–site and immediate detection of DA without the use of instrumentation. For quantification of DA using the solid state probe, open–source software imageJ was used to assist in the analysis of the nanofibre colours. It was observed that the intensity of the colour increased with the increase in concentration of DA in a linear fashion. The use of imageJ can also be a great alternative where the colour changes are not so clear or for visually impaired people. The solid state probe developed can detect DA qualitatively and

quantitatively. The work also forms a good foundation for development of such probes for other analyte.

Table of contents

List of abbreviations

3-MCA	3−mercaptopropionic acid
3-MCA-AuNPs	3−mercaptiopropionic acid stabilized gold nanoparticles
µM	micro molar
nM	nano molar
AA	ascorbic acid
AgNPs	silver nanoparticles
AHMT	4−amino−3−hydrazino−5−mercapto−1,2,4−trazole
AIBN	azobisisobutyronotrile
AuNPs	gold nanoparticles
CAT	3,4−dihydroxy−L−phenylalanine
CE	capillary electrophoresis
CL	chemiluminescence
DA	dopamine
DMABA	4−(dimethylamino)benzaldehy
DMAP	4−dimethylaminopyridine
DMF	N,N−dimethyleformide
EDGMA	ethylene glycol dimethacrylate
EPI	(−)−epinephrine
ES	electrospinning
$HAuCl_4$	tetrachloauric acid
HCl	hydrochloric acid
HPLC	high liquid chromatography
HRSEM	high resolution scanning electron microscopy
HRTEM	high resolution transmission electron microscopy
IAE	immuno−affinity extraction
L-DOPA	3,4−dihydroxyphenylalanine

LOD	limit of detection
MAA	methacrylic acid
MBAA	N,N−methylenebiscrylamide
MIPs	molecularly imprinted polymers
MSA	mercaptosuccinic acid
MSA-AuNPs	mercaptosuccinic acid stabilized gold nanoparticles
N6	nylon 6
$NaBH_4$	sodium hydride
NIP	non–imprinted polymers
NORE	(−)−norepinephrine
NPs	nanoparticles
PAN	polyacrylonitrile
PDA	polydiacetylene
RAMs	restricted access materials
SPE	solid phase extraction
TOAB	tetraoctylamonium bromide
TSC	trisodium citrate dehydrate
TSC-AuNPs	trisodium citrate stabilized gold nanoparticles
UA	uric acid
UF−AuNPs	un−functionalized gold nanoparticles
UV/vis	ultraviolet visible

List of figures

Chapter 1: Introduction

1.0 Background

Dopamine (3,4–dihydroxyphenylethylamine) is a biogenic catecholamine neurotransmitter [1]. It was first synthesized by George Barger and James Hill in 1910 at The Wellcome Laboratories in London, England by decarboxylation of 3,4–dihydroxyphenylalanine which is also known as L–DOPA. The name dopamine (DA) was first suggested by Henry Dale in 1952 [2]. Before the mid–1950s, DA was known as just a precursor in the formation of norepinephrine. However, in the late 1950s DA began to be recognized as having important physiological effects in its own right. Further studies on DA by Carlsson *et al.* led to the realization that it is a neurotransmitter [3].

DA is naturally produced and widely distributed in the central nervous system (olfactory bulb, *substantia nigra*, ventral tegmental area, and the retina) of mammals. It plays a number of significant roles in the function of human metabolism, cardiovascular, central nervous, renal, as well as hormonal systems [4]. DA affects the fundamental functions of the brain such as learning, movement, emotions, the sense of smell, sensitivity to light, and the ability to experience pain. DA is also an integral to higher brain functions such as salience, euphoria, pleasure and appetitive and consummatory aspects of reward. Moreover, abnormal levels of DA in the body fluids are indications of various serious diseases and disorders such as Parkinson's disease, Huntington's disease, and Schizophrenia [5-7]. Furthermore, DA coexists with ascorbic acid (AA) and uric acid (UA) in biological fluids such as urine and blood. The basal concentration of AA and UA is generally much higher (100–1000 times) than that of DA (0.01–0.1 μM) and results in poor selectivity as well as sensitivity for DA detection [1, 8, 9]. It is therefore essential to develop analytical methods that will detect dopamine in the presence of interfering substances.

1.1 Analytical chemistry methods

An analytical method generally consists of several steps, including sample handling (involves sampling, extraction and pre–concentration and sample work-up) and detection. Sample handling refers to any action applied to the sample prior to instrumental analysis. Sampling is a process of selecting a representative portion of material (the sample) from a larger quantity of interest instead of the entire material. Biological samples are usually characterized by dirty and complex matrices that introduce severe challenges during separation and detection steps. After sampling, the analyte of interest will be isolated from the matrix to make it suitable for detection. Selective and sensitive sample preparation is therefore important, especially in detecting analytes on trace levels such as in pharmaceutical samples, organics and metal ions [10]. The sample preparation must be tailored to the final analysis, considering the instrument to be used and the degree of accuracy required. Generally, sample preparation is dependent on the matrix and analyte. The sampling and sample preparation process generally accounts for 80% of the whole analysis time [11].

A sample preparation technique namely extraction is used to separate analyte(s) from complex components of the matrix thereby simplifying the detection process. The extraction technique is applicable in liquids, solids and gaseous samples. Employing the extraction technique, one can separate the analyte of interest from the sample matrix with an optimum yield and selectivity, in order to minimize the quantity of the interfering species that are carried through to the analytical separation stage [12]. Extraction methods such as solvent extraction from solids and liquid-liquid extraction (LLE) from solids are used. Other sample extraction techniques include: Soxhlet, super-critical fluid, pressurized liquid and microwave assisted extraction. Selectivity is usually achieved by changing the extraction temperature or pressure or through the use of pH and additives. This often changes the solubility of the analyte in the given solvent system. In other extraction methods, such as solid phase extraction, immuno–affinity and imprinted polymers, selectivity for specific functional groups or mimicking of biological selectivity is attained. Furthermore, biological analytes are normally found to be at trace levels in real samples. A pre–concentration step is usually required to bring the analye(s) to detectable level using instruments.

After sample preparation, the analyte can be detected using techniques such as electrochemical, spectroscopic or colorimetric methods depending on the analyte or the developed method.

There are various conventional analytical techniques that have been reported for detecting DA. These conventional techniques include chemiluminescent, fluorescent, spectrophotometric and electrochemical detection and are reported next (Section **1.2**).

1.2 Conventional detection techniques

1.2.1 Chemiluminescent detection

Chemiluminescence (CL) is light emitted by chemical reactions. In principle, the light can be emitted from the ultraviolet to the infrared region, but is most commonly emitted as visible. The energy levels in CL are identical with those involved in fluorescence phenomena, except for the mode of excitation. CL reactions normally yield a product in an electrochemically excited state that produces light. Therefore, only exothermic reactions can generate the required energies. Most CL reactions utilize oxygen, hydrogen peroxides or similar potential oxidants. Peroxides, particularly cyclic peroxides, are prevalent in light emitting reactions due to their relatively weak bond (O–O) that is easily cleaved resulting in molecular reorganization that releases a large quantity of energy. The attractiveness of CL as an analytical tool is its inherent strengths such as sensitivity, simplicity and wide dynamic range, as well as applicability to a range of analytical chemistry applications in biomedical and environmental analysis. Detection of CL signals can also be accomplished in several ways including direct methods (e.g. naked–eye), and indirect methods such as emission in flow injection, chromatographic and immunoassays [13-16].

Autoxidation of DA produces dopaminequinone and superoxides while enzyme oxidation of DA by monoamine oxidase generate hydrogen peroxide. This is due to the two phenolic hydroxyl groups that are easily oxidized under physiological conditions to generate hydrogen peroxide and other radicals (e.g. OH^{-}) [17]. CL could therefore be applied to detect DA. In one study [18],

imidazole was utilized to generate hydrogen peroxide from DA, and peroxyoxalate CL detected the hydrogen peroxide. Nozaki *et al.*[19], used amines to generate hydrogen peroxide from DA. Recently, Liu and co–workers developed a method based on electrogenerated CL for determining DA and the limit of detection (LOD) of 9.2 x10^{-10} M was achieved [20].

Although CL detection is highly sensitive, it is time consuming owing to its reliance on enzymatic reactions that are dynamic and change over–time [21]. Lack of selectivity towards the analyte of interest may occur when a CL reagent yields a significant emission for more than one analyte. Furthermore, CL emission intensities are sensitive to a number of environmental factors such as temperature, solvent, ionic strength, as well as pH. Consequently, there will be a mismatch of the separation conditions (e.g. high performance liquid chromatography, HPLC) and the optimum CL conditions.

1.2.2 Fluorescence detection of DA

Fluorescence detection methods have led to major improvements in bioanalytical applications owing to their extraordinary selectivity. The conventional fluorescent probes used are organic dyes; a lot of methods have been reported for bioimaging [22, 23] and biosensor [24] utilizing semiconductor nanocrystals as substituent for the organic dyes which are usually associated with low sensitivity. Quantum dots and noble metal nanoclusters are also promising materials as substitutes for organic dyes. Both quantum dots and noble metal nanoclusters are characterized by enhanced sensitivity for the analyte of interest. Mu *et al*. [25] reported a sensor for the sensitive detection of DA based on adenosine capped cadmium selenium/ zinc sulphate (CdSe/ZnS) quantum dots. The method exhibited high selectivity in the presence of amino acid, UA and glucide. An LOD of 29.3 nM was achieved and the sensor was applied in urine samples. Another fluorescence probe for sensitive detection of catecholamines based on the fluorescence quenching of CdSe nanocrystals was reported by Ma *et al*. [26]. Although low LOD have been reported for the fluorescence probe, fluorescence measurements require the use of expensive and somewhat complicated instrumentation.

1.2.3 Spectrophotometric detection of DA

Spectrophotometry deals with visible light, near-ultraviolet and near–infrared. However, spectrophotometric methods of determination based on ultraviolet and visible absorption are used more often and for a wide variety of substances compared to any other analytical method [27]. Due to the interferences that are normally observed during the detection of 1,2–diphenolic compounds by direct measurements of the UV absorption, new spectrophotometric methods are being developed to address the challenge. The newly developed methods involve conversion of the drugs to coloured derivatives prior to measurement to permit absorption in the visible spectrum. The spectrophotometric detection technique has been applied in the determination of DA–like compounds [28]. El–Dien *et al.* [29] employed the spectrophotometric detection technique to assay derivatives of DA in pharmaceutical and biological samples of schizophrenic patients utilizing copper tetramine complex and triiodide reagent. The method was based on coupling of 4–aminoantipyrine with one of the DA derivatives (levadopa for example) to produce a new ligand that reacts with copper tetramine complex and so as to generate an intensely coloured chelated ligand. Consequently, the coloured products were quantified spectrophotometrically. Recently, a method based on the oxidation of thionine by bromate in acidic media and the inhibitory effect of DA on this reaction was proposed [30]. There are a number of reports in literature for the determination of DA employing spectrophotometric methods, however, the limitations have been low sensitivity [31, 32] and the need for suitable instrumentation.

1.2.4 Electrochemical detection of DA

Electrochemical methods have received considerable interest owing to the fast detection, simplicity, reproducibility and potential for miniaturizing. To improve the sensitivity, nanomaterials are most commonly used for the design of sensing devices [33, 34]. The electrochemical technique suffer from low selectivity towards the analyte of interest. For instance, in the case of DA, overlapping voltammetric responses for the oxidation of a mixture of AA, UA and DA are usually observed. However, there are reports on the application of

electrochemical methods for the selective detection of DA. Most of the detection limits reported in literature are in the μM range [8, 35, 36].

1.2.5 Colorimetric detection

Methods developed utilizing conventional techniques have challenges including the use of analytically specific instrumentations that are difficult to operate and follow time-consuming procedures. It is therefore essential to develop an analytical method that is simple yet selective and sensitive for diagnostic application. As a better alternative method, colorimetric probes are being developed for routine analysis. Colorimetric detection relies on colour changes of materials induced by the presence of the targeted analyte and will be discussed in detail in chapter 2.

1.3 Objectives of the thesis

Gold nanoparticles stabilized with various stabilizing agents have been used in the development of colorimetric probes for dopamine. However, there are no studies that applied un-functionalized gold nanoparticles more especially in the synthesis of solid state based colorimetric probes. The main objective of the studies carried out in this thesis was to develop a simple, rapid, sensitive and selective colorimetric probe for the detection of DA. The specific aims of this thesis were to develop:

(i) A probe based on colloidal un–functionalized AuNPs (UF–AuNPs)

(ii) A probe based on electrospun molecularly imprinted polymers containing the same gold nanoparticles (UF–AuNPs/electrospun nylon 6) as electrospun composite nanofibres (MIPs + UF–AuNPs + N6).

(iii) A probe based on electrospun fibres containing the UF–AuNPs. A further objective was to explore how the probes work in order to understand the development of similar probes for other analytes.

The liquid state colorimetric probe would be prepared using a reducing agent only and introduced to DA of various concentrations to evaluate if colour changes would occur. The probe would then be characterized using UV/vis spectroscopy and transmission electron microscopy to evaluate any morphological changes of the nanoparticles in the presence of DA. After understanding the solution based probe, solid state colorimetric probes would be fabricated employing the electrospinning technique. Studies would be carried out in order to evaluate the reaction mechanism of the nanofibre (solid state probe) to investigate:

- The arrangement of the nanoparticles within the nanofibre using TEM to prove or disprove dispersion of the nanoparticles.
- Any possible interactions between the functional groups of DA and the UF–AuNPs by conducting nitrogen 1s and oxygen 1s XPS analysis of the probe.
- The presence of Au^{+} by conducting Au4F XPS studies.
- Interaction between the gold atom and the nylon–6 using FTIR.
- Morphology before and after DA using scanning and transmission electron microscopy
- If the intensity of the colour changes with increase/decrease in concentration of DA by looking at the quantification of the colour and intensity using ImageJ.

Further investigations on the applications of the probe in real sample (human whole blood) would be carried out.

The next chapter will give a literature review including the motivations on why the main materials (gold nanoparticles, molecularly imprinted polymer and electrospun nanofibres) used in this thesis were chosen.

Chapter 2: Literature Review

2.1 Colorimetric detection of dopamine

Various methods for the detection of biological compounds have been reported [37-41]. The newly developed methods have been characterized by several advantages over conventional methods, particularly in sensitivity and selectivity [42-45]. Among these methods, colorimetric detection appears to be most commonly used for routine analysis because of its fascinating characteristics that include its simplicity, low cost and that detection can be achieved with the naked eye [46], thus complicated instruments are not required. Various colorimetric detection techniques have been documented, including strategies employing organic dyes (e.g. azo dyes) [47], colorimetric polymeric materials (e.g. polydiacetylene, PDA) [48] and metal NPs (e.g. silver and gold) [49]. Currently, colorimetric methods that are based on the use of PDA and metal NPs are the most attractive.

2.1.1 Polydiacetylene-based colorimetric probes

Polydiacetylene is an outstanding conjugated polymeric material possessing unique chromatic properties. These polymers are easily prepared from diacetylenic monomers, initiated by ultraviolet (UV) or γ-irradiation at room temperature. The resulting PDA is of high purity since the process does not involve the use of catalysts or chemical initiators. The colour of the PDA is intensely blue and changes to red under external stimuli such as pH [50, 51], temperature changes [52], and surface pressure [53]. The blue–to–red transitions are mainly characterized using UV/vis spectroscopy. The absorption maxima for the blue phase appears around 650 nm whilst for the red phase occur around 550 nm [54].

The lipodomimetic structural features of PDA, i.e. hydrophobic tail and hydrophilic head group yield biomimetic membranes and liposomes in water. The most applied PDA material designs for assay and detection of biological analytes are the PDA liposomes. These can be prepared by conjugating the bio-reactive species to the surface [55]. PDAs have both absorbance and

fluorescence properties for signal transduction. These properties are due to the presence of the conjugated (ene-yne) backbone (**Fig. 2.1.1**) and allows for the application of PDA in the formation of bio-sensing materials. PDA has been extensively utilized to colorimetrically detect influenza [56, 57], bacteria [58], mammalian peptides [59], antibodies [60] and enzymatic activity [61].

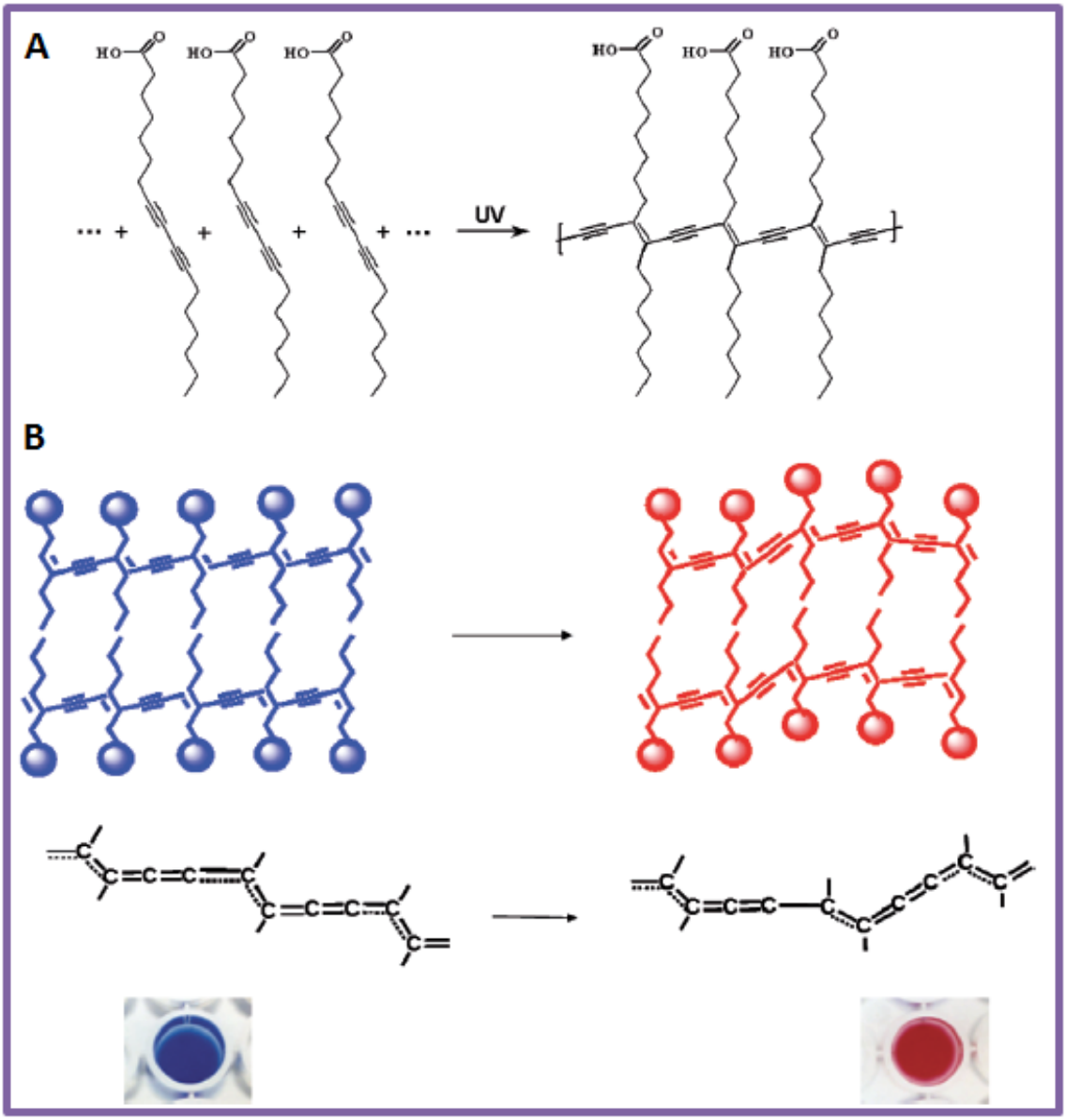

Figure 2.1.1: Structural features of polydiacetylene. (A) reaction of polymerized backbone from the diynoic acid monomers; (B) induction of the blue-red colour transitions [62].

A combination of PDA with phospholipids and other constituents of the cell membrane results in mixed lipid/PDA vesicles. These systems have proven to be advantageous in enhancing the use of the PDA technology to develop sensors for biological and pharmaceutical compounds. The benefits of using mixed lipid/PDA vesicles include the observation that the PDA framework can act as "scaffolding" for stabilization of additional lipophilic dyes and recognition elements that can be incorporated into the vesicles (rather than covalently attached to the polymer). Such organizations have been employed for high sensitive and selective detection of catecholamines. One example was reported by Kolusheva *et al*. [63]; the authors presented a method for sensitive and selective detection of norepinephrine and DA based on fluorescence induced from the phospholipid/PDA vesicles anchoring synthetic receptors. Unfortunately, the authors reported that they could not use the colorimetric aspect due to some practical challenges including the interference arising from the strong colours of the synthetic receptors.

2.1.2 Metal nanoparticle–based colorimetric probes

Metal nanoparticles have attracted great interest in science and technology mainly due to their unique properties and numerous applications. The areas of application include but are not limited to catalysis, electronics, optics [64], imaging, chemical sensors and biosensors [65]. Noble metal NPs particularly silver (AgNPs) and AuNPs are the subject of focused research owing to their optical and electronic features. Thanks to the remarkable properties of AuNPs and AgNPs that makes them ideal colorimetric probes in the development of analytical methods for detecting various analytes [66, 67]. Both AgNPs and AuNPs are extremely sensitive owing to their higher extinction coefficients compared with traditional organic chromophores [68].

However, until recently, AgNPs were mainly exploited for their antibacterial activity [69-71]. Hence, the few reports on the colorimetric detections based on AgNPs. The core challenge that has delayed the use of AgNPs as colorimetric probes is the susceptibility of the silver surface to oxidation, which makes it difficult to stabilize them for their analytical applications [65, 72, 73]. Recently, stabilization of AgNPs has been achieved through surface functionalization with appropriate ligands. Nevertheless, the studies conducted in this thesis focused on AuNPs.

2.1.3 Gold nanoparticles (AuNPs)

AuNPs have drawn considerable attention as colorimetric probes because they are easy to synthesize and functionalize, have distinct spectral features and, long-term stability [10, 74]. They have colours ranging from red to purple/blue and violet [75]. The colour change is highly sensitive to the size, shape, stabilizing agents, refractive index of the medium, as well as the aggregation state of the AuNPs. AuNP–based colorimetric probes have been widely applied in a variety of research fields including clinical diagnostics [76, 77], detection of DNA [78], proteins [79], metal ions and small molecules [67] and so on. In order to satisfy the desired application, various procedures are followed for the synthesis of the AuNPs.

2.1.3.1 Methods for the synthesis of gold nanoparticles

There are three main reagents for preparation of metal nanoparticles namely, a metal salt, a stabilizing or capping agent and a reducing agent. The function of the reducing agent is to reduce the metal ions to the atom that would precipitate to form nanoparticles. The stabilizing agent prevents formed nanoparticles from aggregating before their intended use. The reaction conditions also play a crucial role during the synthesis of the nanoparticles. Studies have shown that the method of synthesis of the AuNPs is important for both the mechanism of detection, their storage and may also determine their stability. As a result, depending on the intended use, AuNPs have been prepared under different conditions. For example, organic and inorganic solvents have been utilized as reaction media. Nanoparticles formed in solution are called colloidal nanopartcles. When specific shapes or sizes of AuNPs are required for a particular application, a method known as seed-grown synthesis is normally used. This method involves two or more steps (**Fig. 2.1.3.1.1**). Recently, an *in situ* strategy for the synthesis of NPs has been reported. The *in situ* method has received more attention since it involves formation of the NPs in one step. The two main chemical strategies for the synthesis of AuNPs are discussed in **2.1.3.1.1** and **2.1.3.1.2.**

2.1.3.1.1 Seed–growth method

As already mentioned in **2.1.3.1**, the seed–growth approach is employed to prepare nanoparticles with desired morphology. In a general seed–growth method, gold seeds or germ (small sized particles) are first prepared by chemical reduction of appropriate quantities of the gold salt using a suitable reducing agent in the presence of a stabilizing agent such as citrate and hexadecyltrimethyammonium bromide (CTAB) [80, 81]. The smaller particles are usually produced by using stronger reducing agents such as sodium borohydride ($NaBH_4$), phosphorus, or tetrakis(hydroxymethyl) phosphonium chloride [82-85]. The seeds are then added to a solution containing more metal salt. The reducing agent used in the second stage of the seed-growth process is a weaker one; for example, hydroxylamine and ascorbic acid [86, 87]. The weak reducing agents should reduce only the metal salt ions which are adsorbed onto the surface of the seed without forming any new nucleation or growth centres. Thus, the seeds serve as nucleation sites for the formation of particular sizes or shapes of the AuNPs [88, 89]. The whole process takes approximately 16 h or more [90]. There are various successful reports on the use of the method to produce different shapes and sizes of AuNPs.

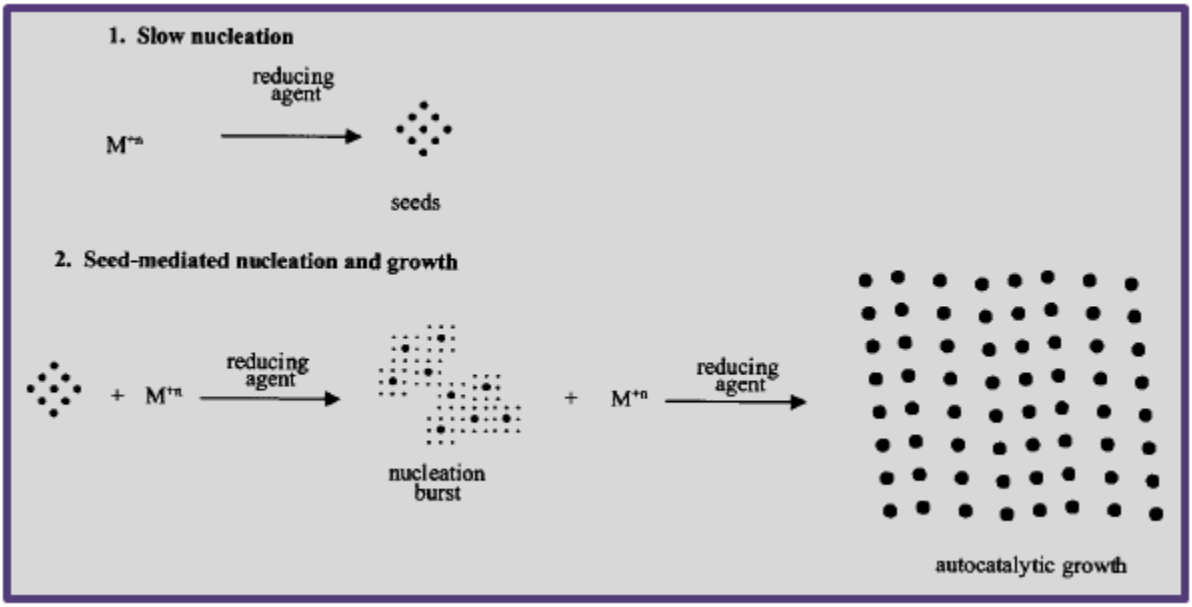

Figure 2.1.3.1.1: Generalized two-step mechanism for solution-phase AuNP synthesis [91].

2.1.3.1.2 *In situ* synthesis

In the *in situ* reduction method, both nucleation and growth are completed in a single step. There are two *in situ* reduction methods that have been applied to tetrachloauric acid ($HAuCl_4$) precursor namely photoreduction by UV irradiation and reduction by potassium (or sodium) borohydride. Reduction by UV irradiation in the presence of various stabilizing agents is a slow process and usually results in large particles; whereas the fast borohydride reduction method generally gives colloids that are stable for months with very small, spherical particles and narrower size distribution [92]. The size and shape of the nanoparticles is necessary in the development of colorimetric probes since they are the mostly affected when the analyte of interest interact with the AuNPs.

2.1.3.2 Gold nanoparticle–based colorimetric detection of dopamine

An ideal colorimetric probe must be simple, sensitive and selective towards the targeted analyte. Since AuNPs are naturally sensitive due to their high extinction coefficients, one needs to think about how to cater for selectivity. Selectivity of various analytes have been accomplished by choosing stabilizing agents that have functional groups which will allow selective binding of the target in the presence of interfering species. There are several reports for the colorimetric detection of DA employing AuNPs. Most of the approaches follow a two–step process. The first step is usually the *in situ* preparation of the AuNPs employing the citrate-mediated reduction of $HAuCl_4$. The citrate acts as both a reducing and stabilizing agent to produce wine–red solution. Basically, the citrate method involves heating of $HAuCl_4$ aqueous solution to vigorous boiling followed by the addition of sodium citrate solution under continuous stirring. The heating is stopped after boiling for few min to allow the solution to cool down to room temperature [93, 94]. In the second step, the citrate ion is exchanged for another ligand.

2.1.3.3 Literature examples of gold nanoparticle–based colorimetric probes for dopamine detection

For example, Liu *et al*. [95] synthesized dithiobis(succinimidylpropionate)-modified AuNPs following a ligand–exchange reaction. The probe showed good selectivity in the presence of some interfering compounds with a limit of detection (LOD) of 2 nM. Recently, Feng *et al*. [96] developed a probe based on 4–amino–3–hydrazino–5–mercapto–1,2,4–triazole (AHMT) functionalized AuNPs. The selectivity of the probe relied on the hydrogen bonding between the amine and hydroxyl groups of DA with AHMT. Employing the probe, the authors obtained an LOD of 0.07 μM. Another method utilizing AuNPs prepared via ligand–exchange reaction was reported by Lee *et al*. [97]. However, instead of following the citrate-mediated reduction, the AuNPs were prepared in a mixture of water and toluene in the presence of tetraoctylammonnium bromide (TOAB) as a stabilizing agent. In this case, $NaBH_4$ was used as a reducing agent. The TOAB–AuNPs were then mixed with a solution of 4–dimethyl–aminopyridine (DMAP). The hydrophilic DMAP molecules were replaced by the hydrophobic TOAB molecules on the surface of the AuNPs such that the DMAP–AuNPs moved into the water phase. Thus, achieving both ligand–exchange and phase transfer. The mechanism of detection by the probe is via the core etching of the DMAP–AuNPs by DA thereby resulting in a reduction in size of the prepared nanoparticles, causing colour change from red to green and an LOD of 5 nM was observed. Following the citrate reduction procedure, Zheng *et al*. [98] demonstrated a strategy for detecting DA employing a DA–binding aptamer as recognition element. Kong *et al*. [7] functionalized AuNPs with 4–mercaptophenylboronic acid and disthiobis(succinimidylpropionate) for double molecular recognition of DA. In another study [99], the citrate ion on the surface of the AuNPs was exchanged for dithiobis(sulfosuccinimidylpropionate) and the resulting nanoparticles were used in conjunction with Fe_3O_4 as recognition species for DA. Liu *et al*. [100] immobilized Ag^+ on the surface of gold nanorods (AuNR). The mechanism of detection involved the reduction of the Ag^+ to Ag^0 which resulted in the change of the dielectric function, the aspect ratio of the AuNR, and colour of the solution.

All the examples of AuNP–based colorimetric probes have shown undoubtable selectivity and sensitivity towards DA. However, they are somewhat complicated to prepare and the procedures

for obtaining the final probe are all fairly long. As a better alternative, this thesis proposed the use of *in situ* prepared un–functionalized AuNPs to develop a simple, yet sensitive and selective approach for the detection of DA.

2.1.4 Selectivity

Aptamers and ligands are not the only materials used to design methods that will be selective towards specific biological compounds. Selectivity towards different analytes has been achieved using solid phase extraction (SPE) sorbents such as restricted access materials, immuno-sorbents and molecularly imprinted polymers.

The principle of SPE involves partitioning of selected analytes between two phases, usually a liquid (solvent with analyte or sample matrix) and a solid (sorbent) phase. SPE is similar to liquid–liquid extraction (LLE) in the sense that they both involve separation of solutes between two phases [101]. SPE enables the concentration and purification of analytes from solution by sorption on a solid sorbent. It can be used to separate the targeted analytes from a wide variety of matrices such as urine, blood, animal tissue and soil [102-105]. SPE is currently one of the commonly used techniques for the pre–treatment of biological matrices.

A typical SPE procedure involves four steps (**Fig. 2.1.4.1**) namely (1) condition of the sorbent by passing through an appropriate solvent; (2) application of the sample (the analytes will be retained by the sorbent); (3) removal of interfering species and finally, (4) elution of the analytes [101]. Although SPE has offered several advantages over LLE in terms of selectivity, reproducibility and avoidance of emulsion formation; operation of the conventional SPE is still multistep, labour intensive and time consuming owing to the large number of samples. Moreover, a concentration step via solvent evaporation is often necessary, which may result in a loss of volatile components and generation of waste and hazards [106, 107].

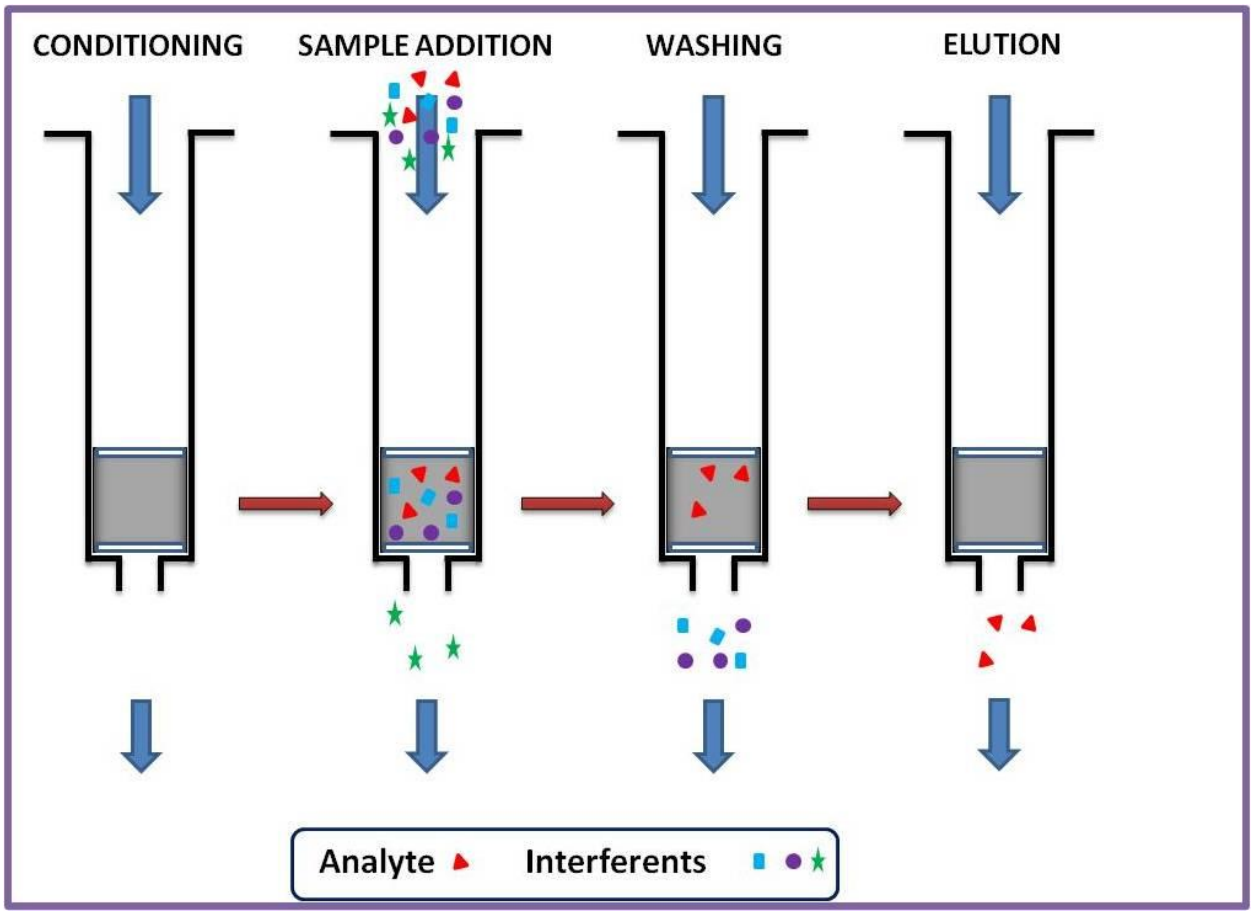

Figure 2.1.4.1: Schematic representation of SPE clean-up procedure [108].

There is a wide range of conventional SPE sorbents available commercially; these include C18 silica, graphitized carbon black, macroporous polystyrene divinylbenze (PS–DVB) [109]. The SPE sorbents are based either on physical loading or chemical binding of selected chelating reagents to different solid supports such as ion exchange resins, modified silica, modified clay, modified alumina and activated carbon. During the development of the method, the physical, chemical and thermodynamic dependencies concerning the targeted analyte, the solvent and sorbents are used to optimise the SPE process [110].

One of the limitations of SPE is that the packing must be uniform to avoid poor efficiency and although the pre–packed commercial cartridges are now considered reliable, automated systems can have difficulties with reproducibility for some sample types. The sample matrix can also affect the proficiency of the sorbent to 'extract' the analyte due to competition for retention.

Many conventional sorbents are limited in terms of selectivity and insufficient retention of very polar compounds. New adsorbents and modification of adsorbents by introducing polar groups are being developed to improve the extraction efficiency for polar compounds [11].

The main challenge with conventional SPE systems is that they are not selective enough and they give low extraction yields. Moreover, off–line SPE and extraction on alumina requires extensive washing procedures that could introduce variability in recoveries. There is therefore a demand for new selective SPE sorbents involving fewer one or step and give good recoveries in a short period. New selective sorbent materials based on molecular recognition (molecularly imprinted polymers and immune-sorbents) and size exclusion (restricted access materials) were developed with the aim to enhance selectivity.

Restricted access materials (RAMs) are a class of SPE sorbents that possess a biocompatible surface and a pore size that restricts large molecules from penetrating the interior extraction phase based on size. The inner pore surface has an extraction phase, which is responsible for the separation of low molecular weight analytes. RAMs were specifically developed for analysis of biological samples, such as plasma and serum. This is because they were developed to exclude large molecules such as proteins. The large molecules are separated either by a physical barrier or a chemical barrier created by the protein network at the outer surface of the particle. RAM can therefore be employed as a pre–column to preliminarily clean up the biological fluids and to pre-separate and pre–concentrate the target analyte from the biological matrices. With RAM-based on–line SPE, it is possible to directly inject the biological sample into flow–analysis systems without previous sample treatment [111, 112]. There are various publications reporting the application of RAMs as pre–columns in column switch systems for direct injection of biological samples such as plasma [113] and the determination of pharmaceuticals such as propranolol.

Immuno–sorbents with covalently immobilized antibodies or antigens have high affinity to the corresponding antigens, or antibodies. Immuno–sorbents can be designed for a single analyte [114] or antibodies that bind to related analytes with similar structures to the antigen or for a group of compounds [112, 115]. In immuno–affinity extraction techniques (IAE), SPE cartridges are loaded with antibodies specific to target analytes and bound onto silica-based sorbents.

Extraction, clean-up and trace enrichment of the targeted analyte from complex matrices is achieved in one step using the immuno–sorbents [116]. IAE coupled on-line to LC-MS has been employed to determine pharmaceuticals [117, 118] and hormones [119] in biological samples.

Although the immuno–sorbents are highly selective, they are unstable in most experimental conditions and are relatively expensive. Moreover, the need to first make the antibody makes it impractical for 'once–off' analyses and the process is tedious and time consuming. To overcome this challenge, extractants such as molecularly imprinted polymers (MIPs) have been developed. The MIPs are discussed in detail in the next section.

2.2 Molecular imprinting

2.2.0 Introduction

Molecular imprinting provides a way to synthesize polymers having specific molecular recognition properties for a target molecule. The target molecule is recognized based on complex formation by hydrogen bonding and electrostatic interaction or hydrophobic effects [120]. The highly selective recognition characteristics of MIPs are comparable to those of natural biological species such as receptors and antibodies. As a result, MIPs are normally referred to as synthetic antibodies [121]. Compared to other recognition materials such as immuno–sorbents, MIPs exhibit very good physical and chemical stability and can be used in harsh media such as in organic solvents, at extreme pH, high pressure and elevated temperatures where biological macromolecules are usually denatured [122-124]. Furthermore, they are cost effective and the synthesis procedures are relatively simple; making them an excellent alternative to the use of natural receptors [125].

MIPs can be synthesized by mixing the template (target) molecule with functional monomers, cross-linking monomers and a radical initiator in a suitable solvent, most often an aprotic and non–polar solvent. Subsequently, the pre–polymerization mixture is subjected to UV light or heat so as to initiate polymerization [126]. This results in a rigid polymer matrix with the embedded template. Removal of the template exposes permanent recognition sites specific to the template.

The binding sites are complementary in size, shape and chemical functionality to the target molecule; enabling selective rebinding of the template from a mixture of closely related molecules (**Fig. 2.2.1**) [127, 128].The accuracy of the binding cavity and the selectivity of the MIP are determined by the strength of the interaction between the template and the monomer [129].

2.2.1 Approaches for preparation of MIPs

To date, three approaches for preparation of MIPs have been reported, covalent, non–covalent and semi–covalent approaches. The covalent approach involves the formation of irreversible covalent bonds (such as boronate ester, ketal and acetyl, or Schiff base) between the template and monomers prior to polymerization. After polymerization, the covalent bond is chemically cleaved and the template is removed from the polymer. The same covalent bonds reform during re–binding of the analyte by the MIP. The template–monomer interaction (covalent bond) is highly stable; as a result the protocol yields a more homogenous distribution of recognition sites minimizing the existence of non–specific sites. However, the covalent imprinting approach is rather restrictive as the choice of irreversible covalent interactions and the potential templates suitable for the covalent approach are limited. Moreover, there is always a need for acid hydrolysis procedure to cleave the covalent bonds between the template and the functional monomer [128, 130-132]. Takeuchi *et al*. [133] developed a novel synthetic receptor for DA bearing bidentate binding sites by covalent imprinting using a disulfide linkage which was cleaved and oxidized to a non–covalent sulfoxide recognition group. Although the method showed good selectivity to DA, it is somewhat complicated.

On the other hand, the non–covalent imprinting approach developed by Arshady and Mosbach [134], utilizes only non–covalent interactions such as hydrogen bonds, ionic interactions and hydrophobic interactions for both the formation of recognition sites and for subsequent re–binding [135]. Of the three molecular imprinting approaches, the non–covalent approach is by far the most used for the preparation of MIPs, mainly because the experimental procedure is very easy and a variety of monomers to interact with any kind of template are commercially available [136]. Moreover, removal of the template is generally easy; it is usually accomplished by

continuous extraction. In addition, MIPs prepared by the non-covalent approach show rapid rebinding kinetics compared to those prepared by covalent approach.

An intermediate option is the semi–covalent approach. This approach combines the advantages of both covalent and non–covalent approaches. In the semi–covalent approach, a covalent template molecule is employed in the polymerization process but binding is entirely non-covalent in nature [120]. This process can be carried out in any solvent and is characterized by rapid re–binding kinetics. However, template removal from the polymer matrix can be a bottle neck; leading to low recovery of the templates and few of binding sites. The work reported in this thesis employed the non–covalent imprinting approach.

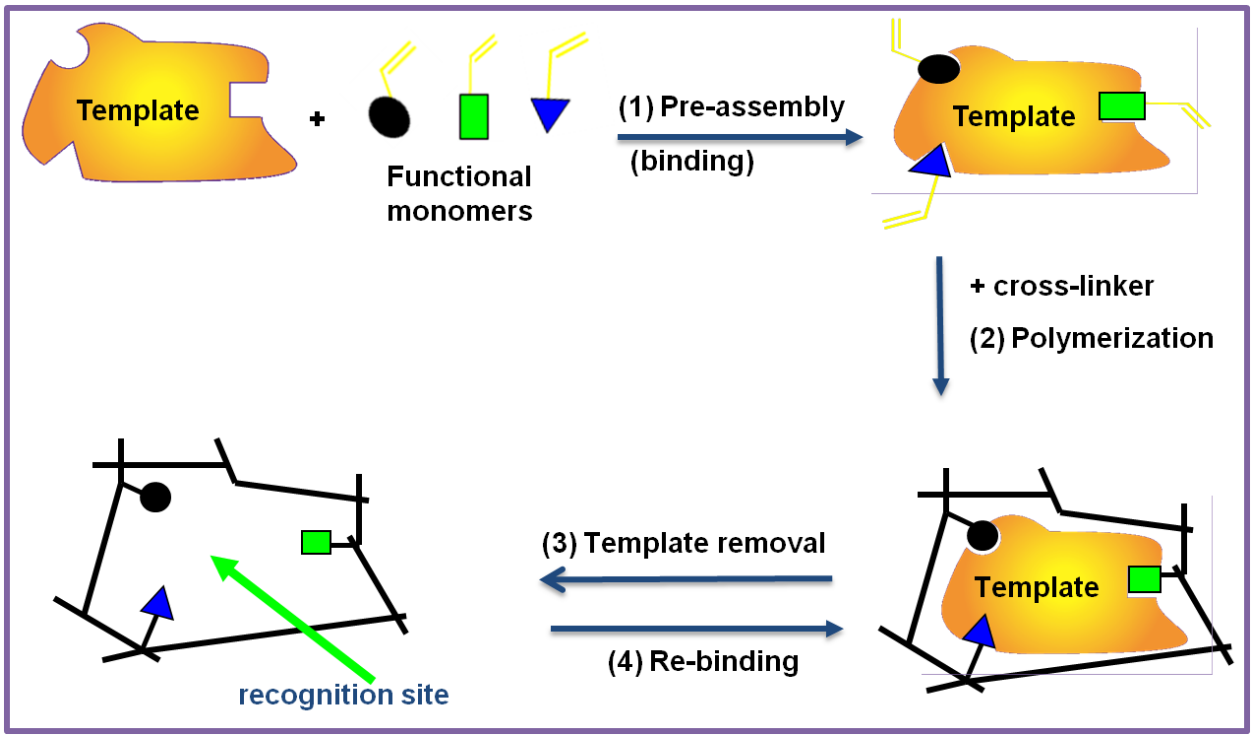

Figure 2.2.1: Schematic representation of a molecular imprinting process following the non-covalent. (1) The functional monomers are arranged around the template molecule as a result of the interactions between complementary chemical functionalities to form monomer-template complex. (2) Polymerization in the presence of a cross-linker fixes the monomer-template complex to form a template-defined recognition site. (3) Removal of the template molecule by extraction exposes the recognition site selective to the original template. (4) Recognition of the template during rebinding experiments.

2.2.2 Formation of the imprinted polymer structure

Polymerization reactions are known to be a very complex processes, which could be affected by a number of factors, such as type and concentration of the functional monomer, cross–linker and initiator, temperature and time of polymerization. In order to ensure a high level of molecular recognition, it is essential to have a good understanding of the chemical equilibrium, molecular recognition theory, thermodynamics and polymer chemistry. Thus, in order to prepare a MIP with perfect properties, numerous factors should be optimized, making the design and preparation of MIPs a time–consuming process. Fortunately, in some instances it is possible to rationally predict how changing any one such variable, for example, the ratio of the cross–linker is likely to impact these properties [137-140]. The selection of appropriate reagents is a crucial step during the molecular imprinting process.

2.2.2.1 Template (target analyte)

Generally, template molecules are target molecules in analytical processes. In all molecular imprinting processes, the template molecule is of central importance as it directs the arrangement of the functional groups pendent to the functional monomers in all molecular imprinting processes. An ideal template ought to gratify the following three questions: (1) does the template contain groups involved in or preventing polymerization? (2) Will the template exhibit excellent chemical stability and withstand elevated temperatures or exposure to UV irradiation? (3) Does it contain functional groups well adapted to assemble with function monomers? [132, 141].

In most cases, the amount of template used is high (often 1 mmol), therefore expensive templates or those that cannot be easily prepared are often substituted by a structurally simpler analogue to decrease the cost of the material. In non–covalent imprinting where the interactions involved are weak, the candidate template should present multiple functional sites to increase the strength of the template-monomer complex. In cases where a structural analogue is used as an alternative imprinting molecule, the process is known as dummy imprinting [142]. The resultant MIP should give rise to imprints that bind the target analyte. When a candidate template is selected, the choice of functional monomers to strongly bond it before polymerization is crucial. The strength of the interactions and the arrangement of the functional groups influence the binding properties

of the obtained polymer [143]. The template and structurally interfering molecules used in the thesis are shown in **Fig. 2.2.2.1**.

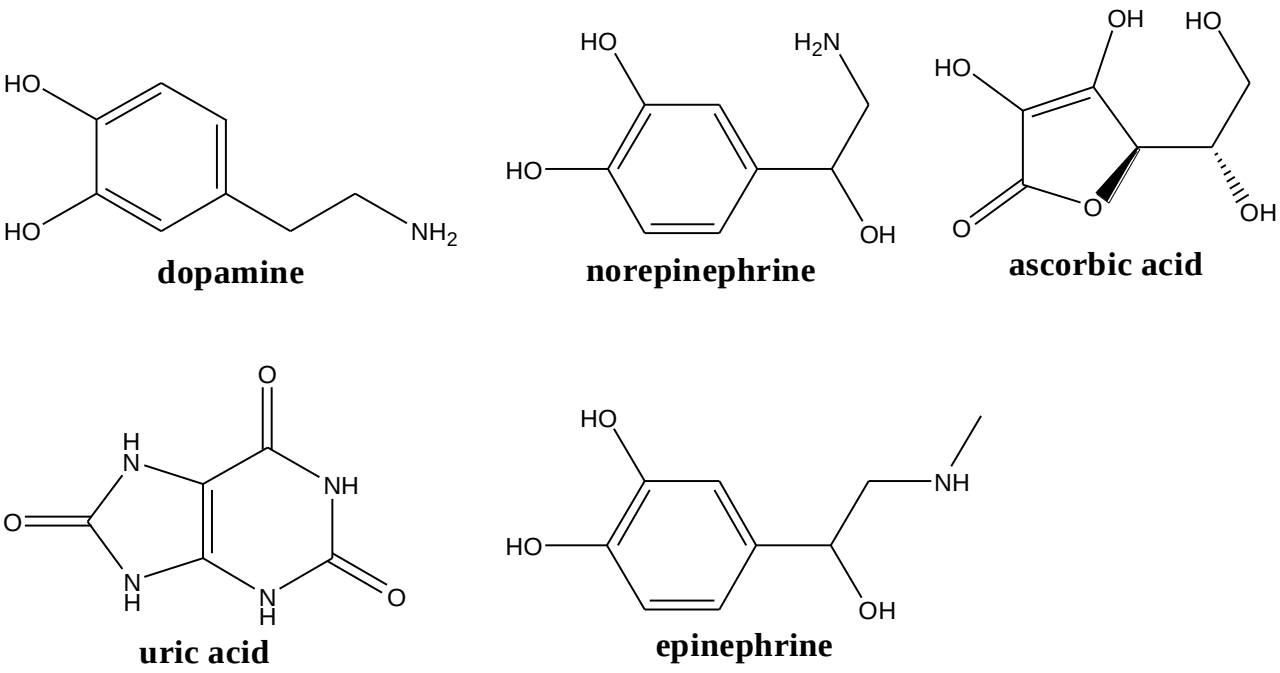

Figure 2.2.2.1: Structure of dopamine and the interfering molecules.

2.2.2.2 Monomers

The role of the monomer is to provide functional groups that can form a complex with the template by covalent or non–covalent interactions. The strength of the interactions between the template and the functional monomer affects the affinity of the MIPs, and determines the accuracy and selectivity of the recognition sites [144, 145]. Stronger interactions lead to more stable polymer complexes, resulting in higher binding capacity of the MIPs. It is therefore important to select the most suitable monomer. Since non–covalent interactions between the functional monomers and the templates are usually too weak (hydrogen bonding, Van de Waal forces and hydrophobic effects) for stable complexes to be formed; a large excess functional monomer relative to the number of moles of the template may be required to favour the formation of the template-monomer complex. This may result in the functional monomers being spread widely throughout the resulting polymer, rather than being restricted principally to the

binding site, thus increasing the degree of non–specific binding sites. Therefore, in order to gain high imprinting efficiency, the molar ratio of templates to functional monomer should be optimized. The most commonly used monomer in non-covalent molecular imprinting is methacrylic acid. This is because it can act as a hydrogen–bond donor and acceptor, and showing good suitability for ionic interactions [146-149]. Other functional monomers that have been reported in literature to give stable polymer complexes are listed in **Fig. 2.2.2.2**.

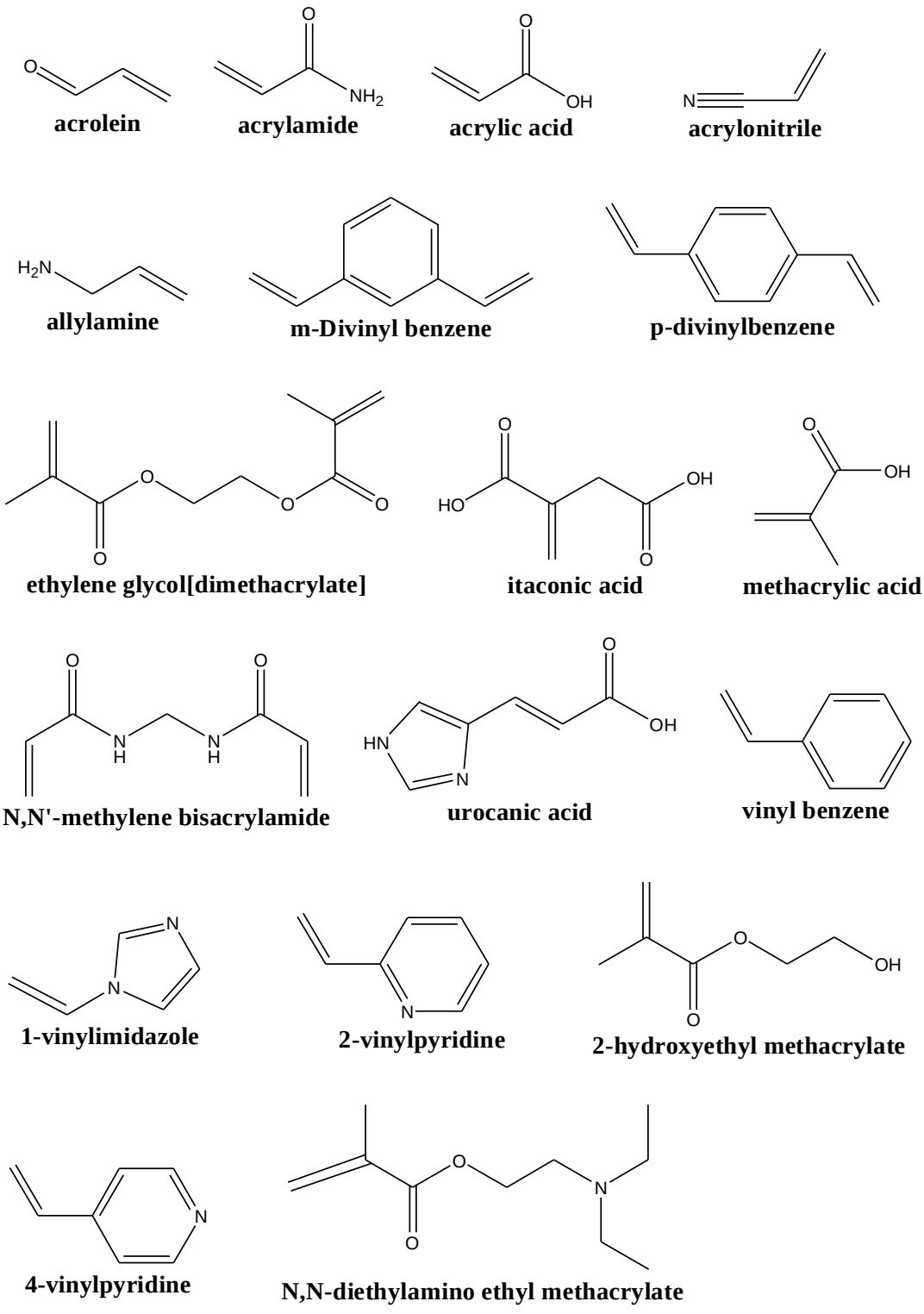

Figure 2.2.2.2: Structures of commonly used functional monomers in non-covalent molecular imprinting.

2.2.2.3 Cross-linkers

The role of the cross-linker is to affix the functional groups of the functional monomer, holding them in place after the template is removed thereby forming a highly cross–linked rigid polymer. The cross–linker has three major roles in an imprinted polymer: firstly, the cross-linker controls the morphology of the polymer matrix, whether it is gel–type, macroporous or a microgel powder. Secondly, it serves to stabilize the imprinted binding site. Finally, it imparts mechanical stability to the polymer matrix [126]. The kind and quantity of cross–linkers have profound influences on selectivity and binding capacity of the MIPs. When very small quantities are being used, the resulting MIPs cannot maintain stable cavity configurations due to the low degree of cross–linking. However, high quantities of cross–linkers can make accessibility to binding sites difficult and impossible to remove the template or for the binding sites to be used at all. The challenge can be minimized by selecting the appropriate cross–linker and optimization of the ratios. For easy accessibility of binding sites, porous cross–linkers or ones that can be broken into small pieces (pulverized) are normally used. The most commonly used cross–linker in non–covalent imprinting is ethylene glycol dimethacrylate (EGDMA). Other cross–linkers such as trimethylolpropane trimethacrylate, N,N–methylenebisacrylamide (MBAA) and divinylbenzene, have also been utilized producing MIPs of higher capacity and selectivity. Their structures are depicted in **Fig. 2.2.2.3**.

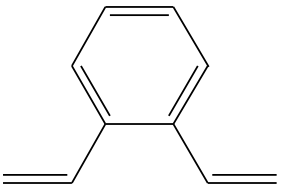

divinylbenzene

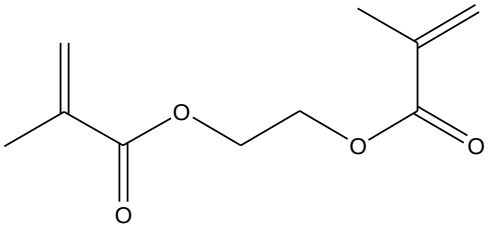

ethyleneglycol dimethacrylate

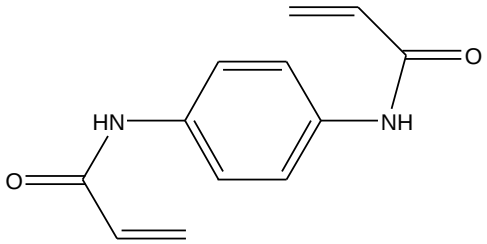

phenylene-diacrylamide

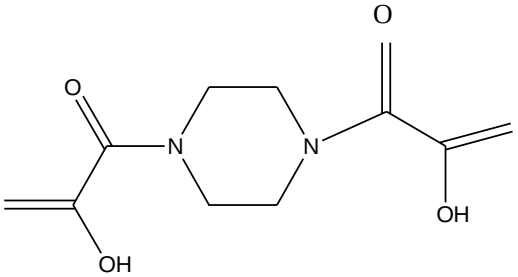

bisacrylol piperazine

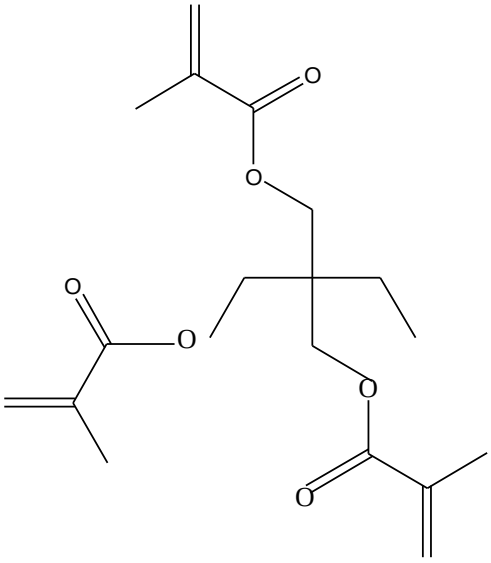

trimethylolpropanetrimethacrylate

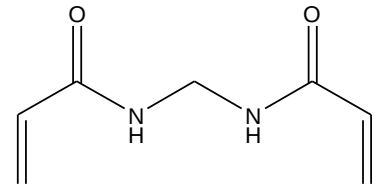

N,N'-methylene-bisacrylamide

Figure 2.2.2.3: Structures of commonly used cross-linkers in non-covalent imprinting.

2.2.2.4 Porogenic solvents

The role of a porogenic solvent during polymerization is to dissolve other polymerization reagents (template, functional monomer and the initiator) and to create the pore structure of the imprinted polymer. Thus, the choice of the solvent is often determined by the solubility of the template molecule, initiator, functional monomer and cross–linker [150]. In non-covalent interactions, the porogenic solvent also influences the bonding strength between functional monomers and templates, the property and morphology of the polymer. Most MIPs rely on hydrogen bonding and electrostatic interactions. As a result, in non–covalent molecular imprinting aprotic and low polarity solvents are normally used to reduce the interferences during the formation of template–monomer complex, and to obtain efficient imprinting. However, it must be noted that in some cases sufficiently strong template–monomer interactions have been observed in rather polar solvents (e.g. methanol/water) [132].

2.2.2.5 Initiators

To date, free radical polymerization is the most commonly used method to convert monomers to polymers. Various mechanical initiators with different chemical properties can be used as the radical source. The initiation process can be triggered and controlled by heat, light and by chemical or electrochemical means, depending upon the structural nature of the initiator [151]. Structures of common initiators are depicted in **Fig. 2.2.2.5**.

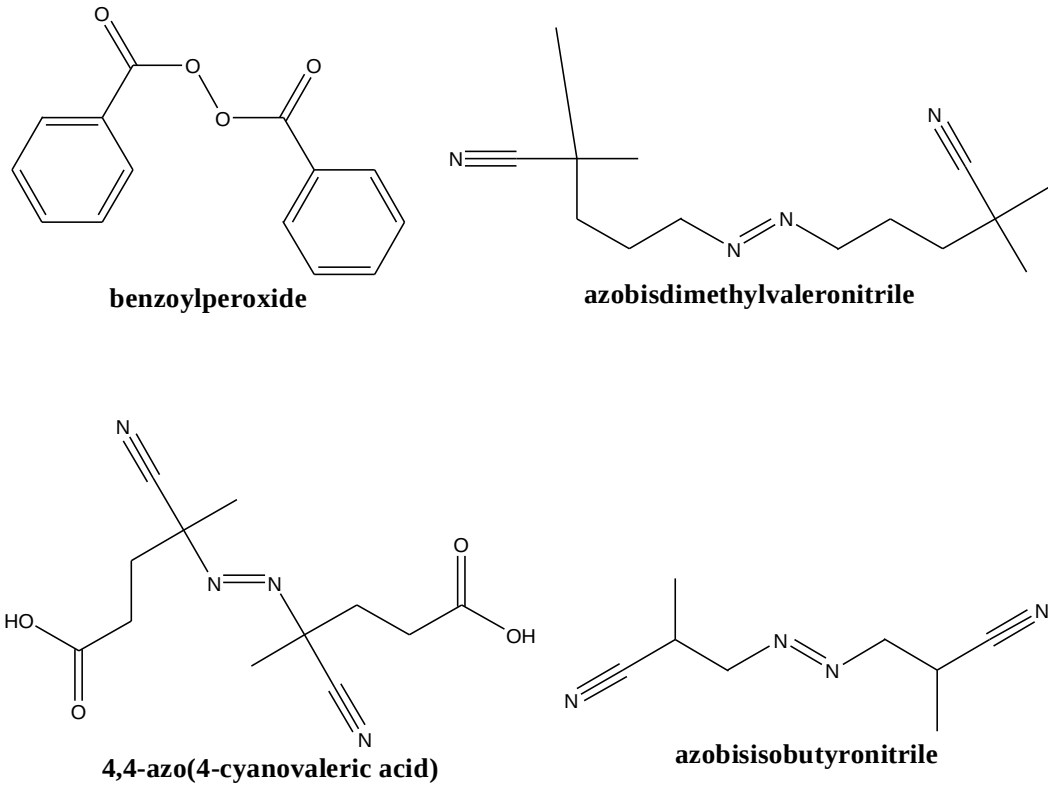

Figure 2.2.2.5: Structures of commonly used initiators.

2.2.3 Synthesis methods of MIPs

2.2.3.1 Bulk polymerization

The conventional method for synthesis of MIPs is by bulk polymerization, resulting in monolith macroporous materials. The monolith materials are crushed, ground and sieved to give particles of appropriate size ranges, with diameters usually in the μm range. This method is by far the most popular to prepare MIPs owing to its attractive properties such as, rapidity and simplicity in its practical execution, it does not require sophisticated or expensive instrumentation and particular operator skills. Moreover, the MIPs that are produced are normally pure. However, the bulk polymerization method presents many limitations. The grounding and sieving process can be time–consuming, the subsequent sedimentation process for the removal of fine particles resulting in a considerable loss of the polymer (only 30–40% of the polymer recover as usable material). Furthermore, the MIP particles obtained are irregular in shape, size and some binding

sites are destroyed during grounding. Bulk polymerization yields heterogeneous binding sites, and thus not ideal for some applications such as chromatography.

In order to overcome the challenges associated with the bulk polymerization approach, a variety of methods have been developed, including multi–step swelling polymerization, suspension polymerization, precipitation polymerization and surface imprinting.

2.2.3.2 Multi-step swelling polymerization

The multi–step swelling polymerization method is readily used to prepare mono–dispersed MIPs and to perform *in situ* modification [152]. The method is based on the swelling of uniformly sized particles to control the size distribution and the shape of the MIP particles more efficiently. Employing this approach, material lost in the form of small particles associated with bulk polymerization method is minimized [143]. The multi–swelling polymerization method was successfully employed to prepare uniform spherical particles [153, 154]. Although particles obtained using the multi−step swelling polymerization technique are well suited for chromatographic applications and are of controlled diameter, the procedures and reaction conditions for preparation are complicated and time-consuming. In addition, the use of aqueous suspensions in the multi–step swelling polymerization process as a continuous phase could interfere with the interactions between template molecules and functional monomers.

2.2.3.3 Suspension polymerization

Suspension polymerization is a heterogeneous radical polymerization process that utilizes mechanical agitation to mix a monomer or a mixture of monomers in a liquid phase while the monomers polymerize, forming sphere of polymer. Suspension polymerization is a rather simple method for preparation of MIPs. It produces spherical beads in a broad size range starting at a few µm and reaching up to a few hundred mm in diameter without the use of any mechanical grinding [155]. Traditionally, water is used as a continuous phase to suspend a droplet of pre-polymerization mixtures in the presence of a stabilizer or surfactant [156]. The use of water as a continuous phase normally introduces some interferences and may have unfavourable effect on

the non–covalent template–monomer complex. Consequently, the MIP microspheres may display poor recognition. To address the interference challenge faced by the multi–step swelling method, suspension polymerization in perfluorocarbons solvents has been studied. Using the suspension polymerization method in perfluorocarbons, regular molecularly imprinted microspheres were obtained. The polymer microspheres showed excellent chromatographic performance and good selectivity even at high flow rates. However, the specialized fluorocarbon solvent limits applicability and practicality of the method [126].

2.2.3.4 Precipitation polymerization

In order to obtain particles that are in the submicron range (0.3–10 μm), precipitation polymerization method could also be used. The method is based on the precipitation of the polymeric chains out of the solvent in the form of particles as they grow more and more insoluble in an organic continuous medium. The growing polymer chains do not coalesce due to the rigidity achieved from the cross–linking of the polymer, so an extra stabilizer is not required [157, 158]. When an adequate match between the solubility parameters of the polymer to be developed and the polarity of the porogen, the resulting polymer will have permanent pore structures and highly uniform particles sizes [159]. In precipitation polymerization, large quantities of solvents (> 95%, wt) are used compared to bulk polymerization.

2.2.3.5 *In situ* polymerization

The *in situ* polymerization approach bears advantages of both molecular imprinting technique and monolithic columns [160]. The procedure involves a one–step free–radical polymerization process directly within a chromatographic column without the tedious procedures of grinding, sieving, and column packing. After *in situ* polymerization, the monolith MIP is expected to advance separation and enable direct analysis with high–speed and high performance. The *in situ* polymerization method is simple and quick (the MIP monolith is prepared within 3 h) compared with the procedures described previously. The success of the synthesis relies on the presence of macropores to provide good flow–through properties and on the simultaneous generation of the selective binding sites [143].

The *in situ* polymerization technique was first used by Matsui *et al*. [161] for the preparation of molecularly imprinted monolith. The template, functional monomer, cross–linker and initiator were dissolved in a mixture of porogenic solvents (cyclohexanol and 1–dodecanol) and the mixture was degassed and poured into a stainless steel column. The template and porogenic solvent were removed by exhaustive washing with methanol–acetic acid. The *in situ*polymerization technique has attracted significant interest due to its ease of preparation, high reproducibility, high selectivity and sensitivity, and rapid mass transport. Moreover, the synthesis of this type of MIP is more cost effective, because of the lower quantity of the template required. In addition, their greater porosity, and hence good permeability, and high surface area are well suited for both small molecules and large biomolecules [162].
The work reported in this thesis followed the bulk polymerization method.

2.2.4 Template removal

Extraction methods such as liquid-liquid extraction, supercritical fluid extraction, pressurized liquid extraction, microwave assisted extraction, solid-phase extraction and Soxhlet extraction are normally used for the removal of the template molecule from the polymer matrix. In this thesis, the Soxhlet extraction technique was adopted (see section **2.2.4.1**).

2.2.4.1 Soxhlet extraction

The equipment used during Soxhlet extraction (the Soxhlet extractor) (**Fig. 2.2.4.1**), was originally designed to separate liquids from solid materials by Franz von Soxhlet in 1879 [163]. Since then, it has found applications in many areas where complete extraction of the analyte of interest out of the residual matrix was necessary. Saim *et al* employed the Soxhlet extraction technique to extract polycyclic aromatic hydrocarbons from soil [164]. It has also been used for analysis of heterocyclic aromatic amines in food [165]. The Soxhlet extraction process is quite slow (up to 24 – 48 h of extraction) but it results in complete/total recoveries and numerous extraction possibilities [166]. The Soxhlet equipment stimulated a great deal of interest because lengthy extractions could be performed unmonitored.

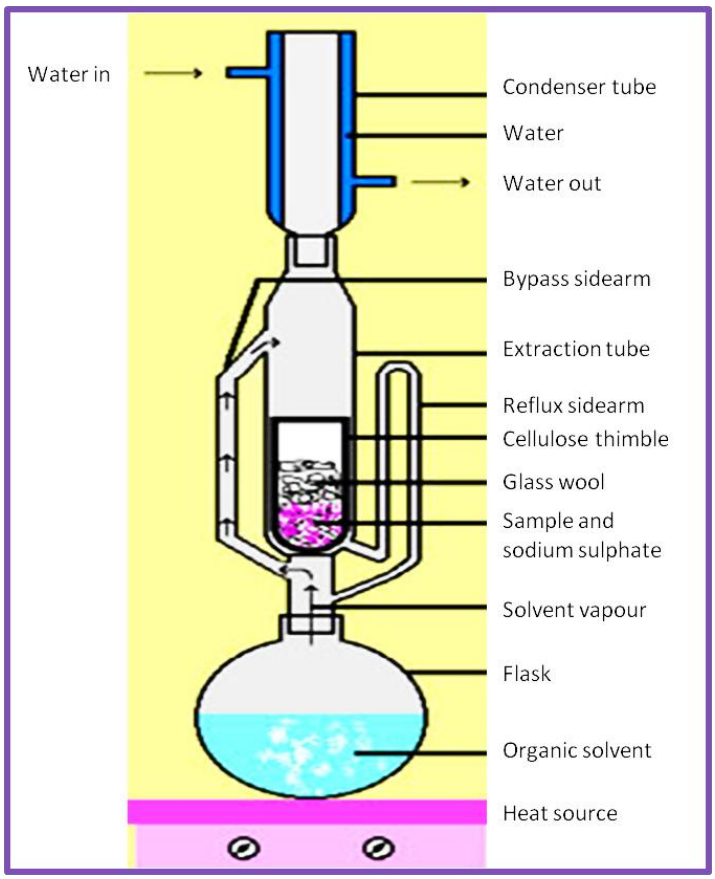

Figure 2.2.4.1: The conventional Soxhlet extractor [167].

2.2.5 Application of MIPs

The application of MIPs has become increasingly attractive in various fields of biology, chemistry and engineering, particularly as selective sorbents for SPE [168, 169], chromatographic separation [170], artificial antibodies [171] and sensor components [172]. Of interest in this thesis was the application of MIPs as sensor materials.

Due to the remarkable specificity associated with MIPs, the molecular imprinting technique has been incorporated in various analytical methods to design sensors that are selective and sensitive towards various analytes. In one study, Du *et al*. [173] utilized CL and molecular imprinting for the detection of epinephrine. After re–binding of epinephrine, luminal and potassium ferricyanide (CL reagents) were flowed passed through the polymer packed into a capillary.

Epinephrine binding to the polymer would produce a strong concentration dependent CL signal. Employing such a set–up, the authors obtained an LOD of 0.2 nM. There are many other studies based on the combination of CL and molecular imprinting [174, 175].

The incorporation of fluorescent components within MIP structures has also been intensely studied [176-179]. Wang and co–workers [180, 181] reported the imprinting of D–fructose employing a fluorescent anthracene–boronic acid conjugate bearing a methacrylate moiety. Boronic acid is known to bind molecules with a *cis*–diol structure; however its inclusion in the MIP enabled high selectivity towards D–fructose when compared to other analogues such as D–glucose or D–mannose. Claude and colleagues [182] reported on the analysis of urinary neurotransmitters by capillary electrophoresis CE. They showed that using field–amplified sample injection and MIP SPE, sensitivity could be enhanced. In another example of the molecular imprinting technique combined with CE, sensitive and selective determination of enrofloxacin residue in chicken muscle was achieved [183].

While literature is rich with reports about merging the special characteristics of other various detection techniques, there are very few reports based on the study of MIPs for colorimetric detection; more especially those that integrate the molecular imprinting technique with metal NPs. To date, there are less than three such studies that have been reported. Amongst the few, Matsui and co–workers reported a MIP with immobilized 11–mercaptoundecanoic acid stabilized AuNPs as colorimetric sensor material for detecting adrenaline [184]. The MIP was utilized as both a solid support and for selectivity. The method is based on the swelling of the MIP during analyte rebinding, which resulted in colour change.

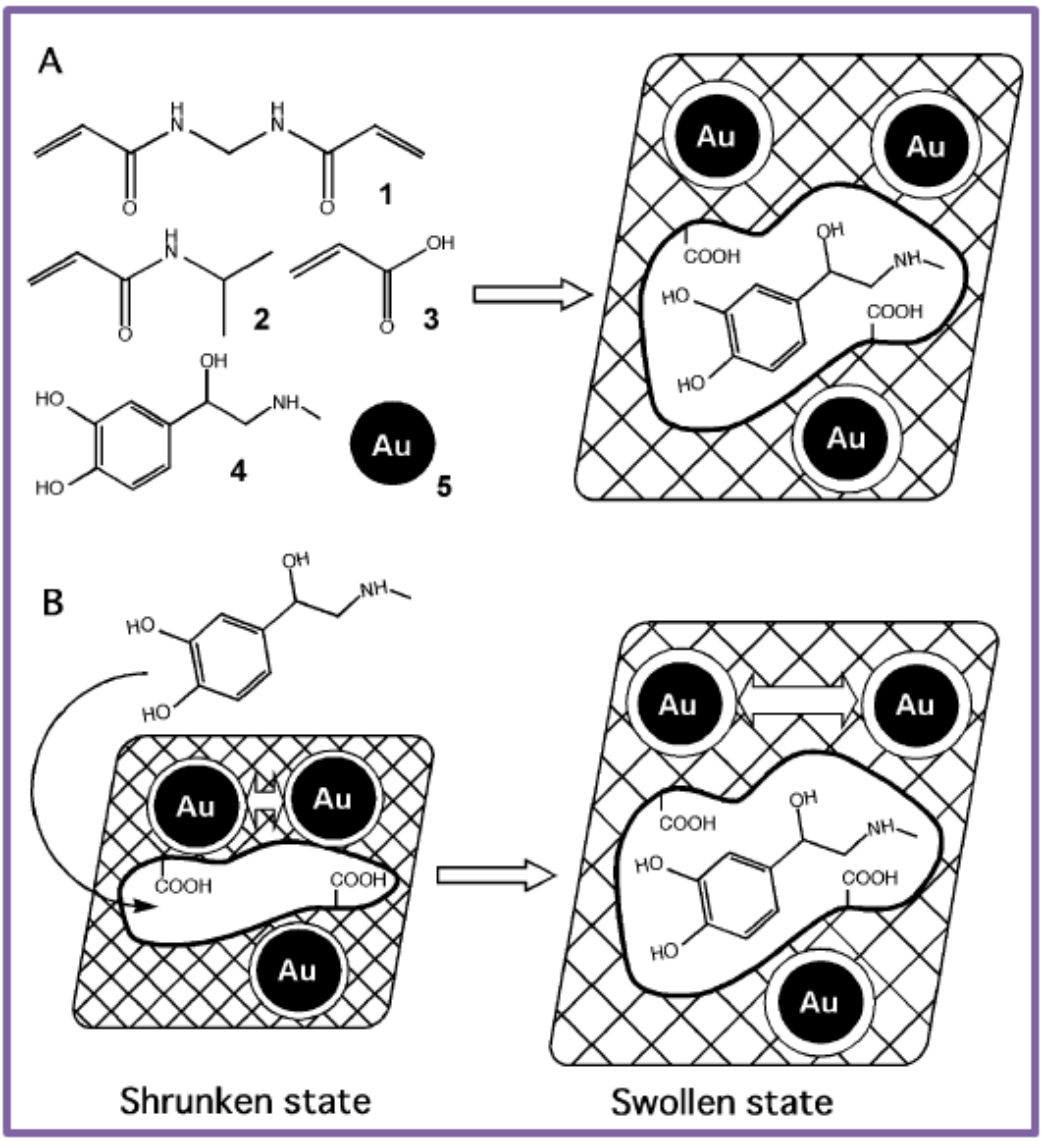

Figure 2.2.6: Schematic representation of the preparation of a MIP with immobilized AuNPs (A) and the detection of an analyte upon selective swelling of the imprinted polymer (B) [184].

The combination of MIPs and AuNPs is still worth pursuing for colorimetric sensing applications. However, interesting as they are, MIPs are not free of challenges. The drawbacks of MIPs are: low capacity and poor site accessibility leading to poor performance of MIP [122]. The challenges could be overcome to some extent by adopting a nanofabrication technique which could afford high surface area to volume ratio [127]. One such technique is electrospinning and is discussed in detail in section 2.3.

2.3 Electrospinning

2.3.0 Introduction

Electrospinning is a simple and yet low cost effective technique for fabricating ultrafine fibres with diameters ranging from several nm to several hundred nm using a high voltage power supply [185]. There are two approaches for electrospinning, viz. needle and needleless based. A basic needle electrospinning set–up consists of a high voltage power supply, collector, and a needle nozzle (**Fig. 2.3.1**). During the electrospinning process, the high voltage power supply provides electrostatic field to charge the surface of a polymer solution droplet and thus to induce the ejection of liquid jet through a spinneret.

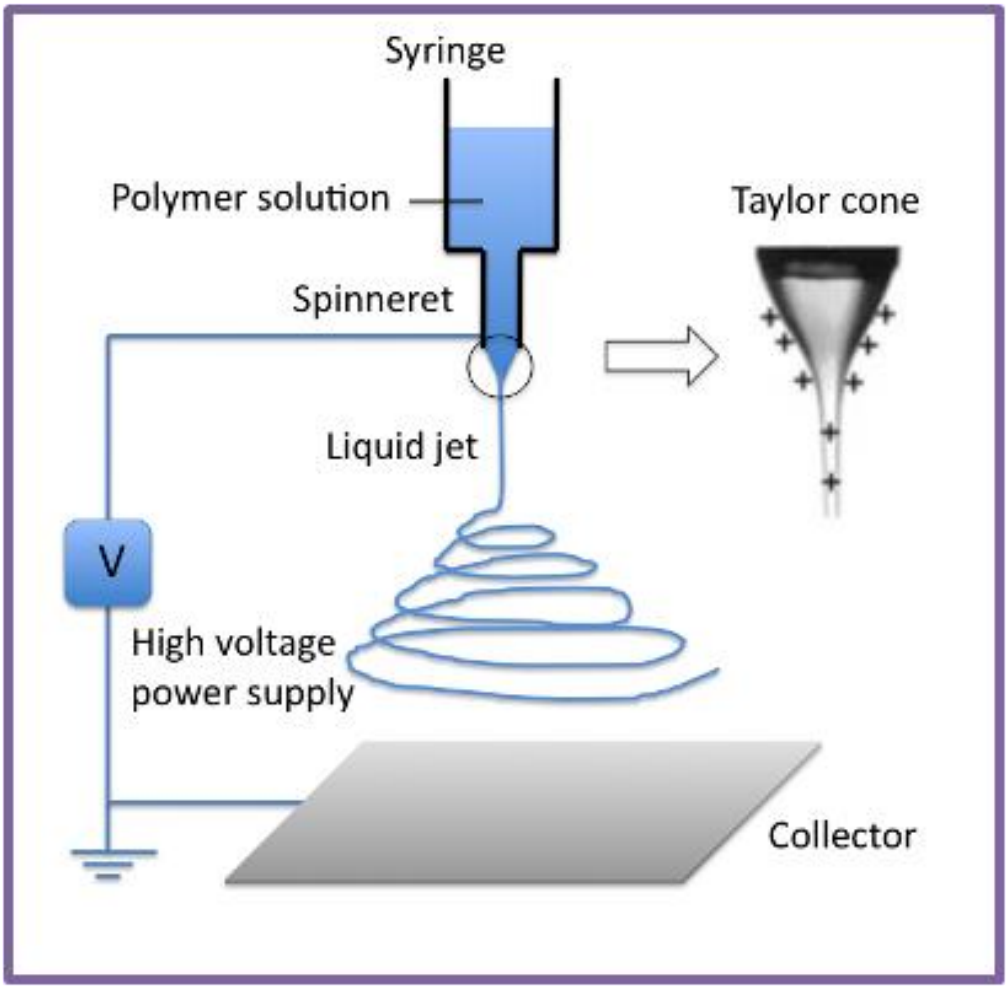

Figure 2.3.1: A schematic representation of a typical electrospinning set–up [186].

Ideally, the power is applied between needle and a collector; both are electrically conducting (with opposite charges) separated at an optimum distance between the two. When the charged species in the polymer solution interact with the external electric field, the pendant droplet deforms into a conical structure called a Taylor cone thereby reaching a critical voltage. Once the repulsive electrostatic force overcomes the surface tension of the droplet, a fine charged jet of the polymer solution is ejected from the tip of the Taylor cone. The fast evaporating solvent will cause the polymer jet to solidify to ultrafine fibres while travelling to the collector on which they are collected [185, 187, 188].

Although simple and versatile, the needle electrospinning is not widely applied in industrial scale the main reason being its low productivity (typically less than 0.3 g/h) [189, 190]. The straightforward way to improve the productivity is to employ a set–up known as 'multi–needle electrospinning" by increasing the number of needles [191, 192]. However, the limitation of the multi–needle electrospinning are that it require a large working space to avoid interferences between adjacent solution jets and cleaning systems are needed for an individual needle nozzle to ensure that clogging of the solution doesn't happen during the nanofibre forming process [190].

Nowadays, needleless electrospinning set–ups have been developed for large scale nanofibre production from a compact space. In needleless electrospinning, nanofibres are electrospun directly from an open liquid surface resulting in simultaneous formation of numerous jets from the needless fibre generator [190, 193]. Rotating spinnerets including as balls, coils, cylinders and cones are normally utilized in this approach (**Fig. 2.3.2**) [194, 195]. The main disadvantage of the needleless electrospinning strategy is the complexity of the electrospinning set–up. This thesis employed the needle based electrospinning approach.

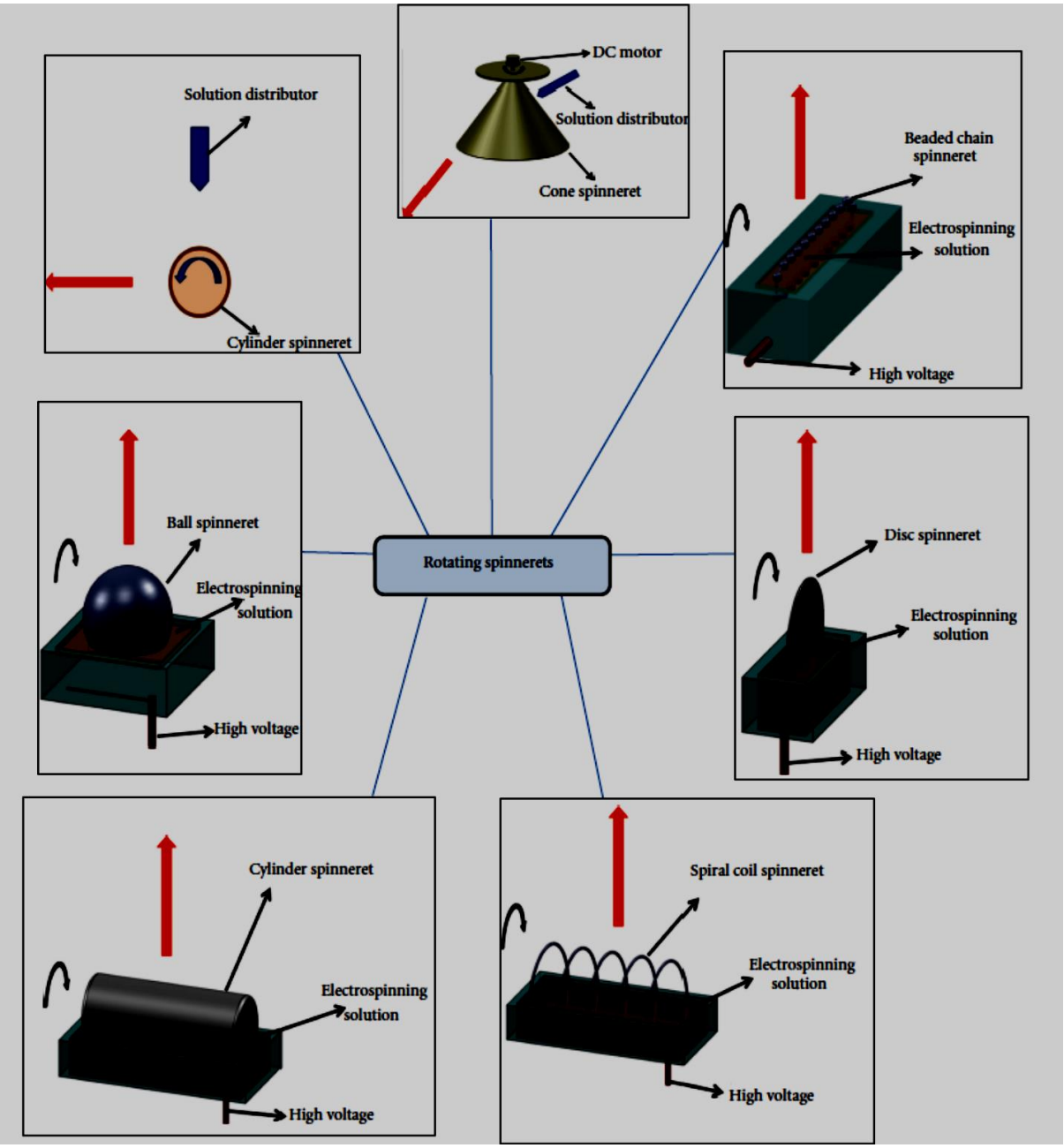

Figure 2.3.2: Schematic summery of rotating spinnerets used in needleless electrospinning (electrospinning direction along the red arrow) [190].

The morphology, structure and property of the fibrous mats can be controlled by adjusting the properties of the polymer solution and process parameters such as the flow-rate, solvents, solution viscosities, applied voltage, humidity, temperature [196-198]. The factors that affect the electrospinning process have been explored and reported extensively [199-203]. Fibres and the non-woven webs generated through the electrospinning process have outstanding properties, which include high porosity, large surface area to volume ratio and excellent pore interconnectivity [185, 204]. Due to these remarkable characteristics, electrospun fibres have

been applied in various areas such as sensors [205, 206], filtration [207, 208], dye–sensitized solar cells [209], tissue engineering [210]. For a desired application, electrospun fibres are normally combined with other materials. The materials include but are not limited to metal nanoparticless (e.g. AgNPs and AuNPs) and recognition elements (e.g. MIPs).

2.3.1 Metal nanoparticle/electrospun nanofibre composites

Preparation of metal nanoparticles dispersed in polymer fibres has recently become the subject of intense study because the metal/polymer nanocomposite can achieve the combined distinctive characteristics of metal nanoparticles and polymer nanofibres. Electrospun fibres are known to immobilize metal nanoparticless without changing their properties. AgNPs embedded in electrospun fibres have been intensely studied due to their potential applications in biomedical research [211-214]. On the other hand, there are a number of reports about AuNPs/electrospun composites [215-217]. These types of composites can be achieved by electrospinning AuNPs containing solutions. In most of the circumstances, the AuNPs have to be synthesized first and then dispersed in the polymer solution prior to electrospinning. For example, Kim *et al*. [218] synthesized one-dimensional arrays of AuNPs on polyethylene oxide nanofibres with most of the AuNPs wrapped within the fibres. Another method for synthesizing AuNPs−containing electrospun nanofibres involves electrospinning of a mixture of the gold salt and polymer solution followed by chemical reduction or physical treatment [219]. For instance, Liu *et al.* [220] prepared *in situ* AuNPs on polyacrylonitrile nanofibres for sensing applications by first dissolving the reducing agent 4-(dimethylamino)benzaldehyde (DMABA) in a N,N–dimethylformamide (DMF) solution of polyacrylonitrile (PAN). Electrospinning of the polymer solution yielded DMABA/PAN nanofibres that were subsequently exposed to a $HAuCl_4$ solution. Recently, a facile *in situ* strategy for immobilizing AuNPs into electrospun polyethyleneimine/polyvinyl alcohol nanofibre for catalytic applications was reported [221]. The authors also demonstrated that the AuNPs–containing nanofibres displayed an excellent catalytic activity and reusability for the transformation of 4−nitrophenol to 4−aminophenol. Due to the remarkable properties of AuNPs/electrospun nanofibres, preparation of the composites for various applications is expected to be the focus of study by many researchers. An example of a scheme for a procedure that could be used to synthesize metal nanopartcle/ electrospun nanofibre composite is shown in **Fig. 2.3.1.**

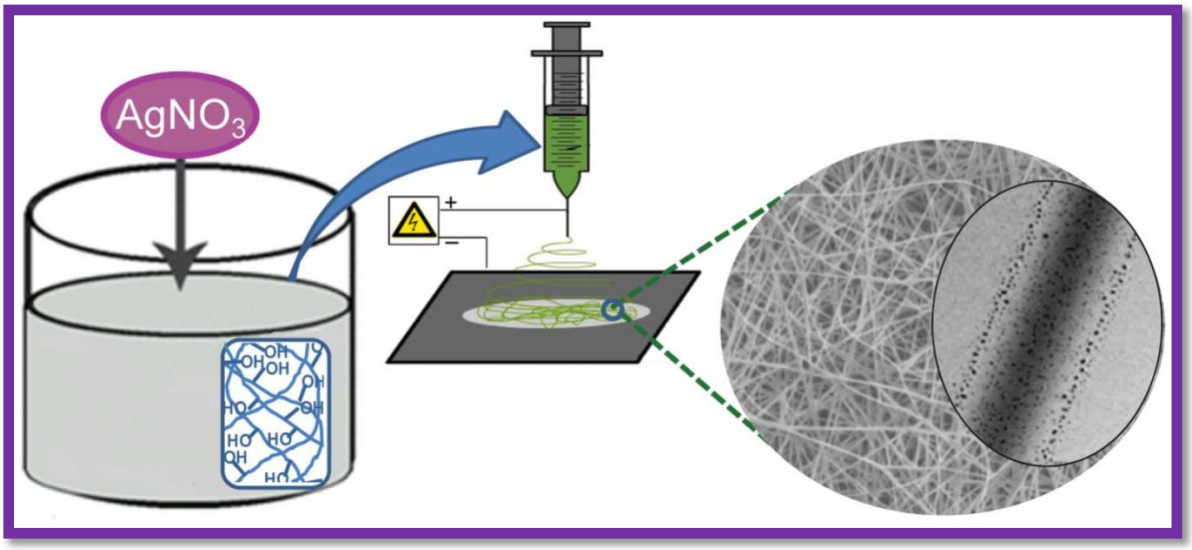

Figure 2.3.1: Schematic diagram for the preparation of polymer nanofibres containing silver nanoparticles by the electrospinning technique [222].

2.3.2 MIP/electrospun nanofibre composites

The electrospinning technique can be employed to overcome some of the challenges faced by traditional MIP particles thereby providing large surface area, and making more binding sites on the surface of the nanofibre (since the nanofibre is one–dimensional), thus improve the performance of the MIPs. There are two well–known strategies for producing MIP/electrospun nanofibre composites that have been reported. In one approach, a spinnable polymer is mixed with all the MIP reagents and electrospun under optimum conditions. An example of this technique was demonstrated by Chronakis *et al*. [188]. The second approach involves blending a suspension of already made MIP particles with a spinnable polymer solution, the mixture is stirred to form a homogenous solution which is then electrospun [122]. The MIP particles can be readily encapsulated, and the composite materials that is obtained will display well-controlled distribution of macro or nano particles along the fibrous structure [129]. Chronakis *et al*. [223] utilized this approach to fabricate a composite MIP/nanofibre for the analysis of theophylline and 17β–estradiol. Depending on the size and method of synthesis of the MIP particles, scanning electron microscopy (SEM) characterization may show no difference between the electrospun fibres with the non–imprinted polymers (NIPs) and MIPs or any evidence of particles inside the nanofibres more especially if the embedded particles are too small (**Fig. 2.3.2.1**). On the other hand, for bigger

particles encapsulated within very thin nanofibres the morphology will be rough revealing some of the particles on the surface (**Fig. 2.3.2.2**).

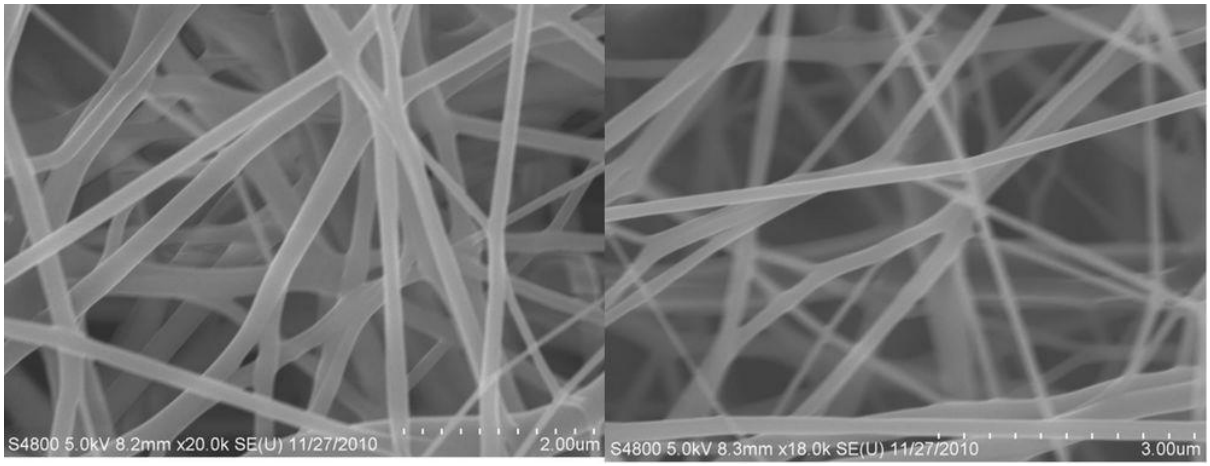

Figure 2.3.2.1: SEM images of electrospun molecularly imprinted microsphere (left) and non-imprinted microspheres (right) [224].

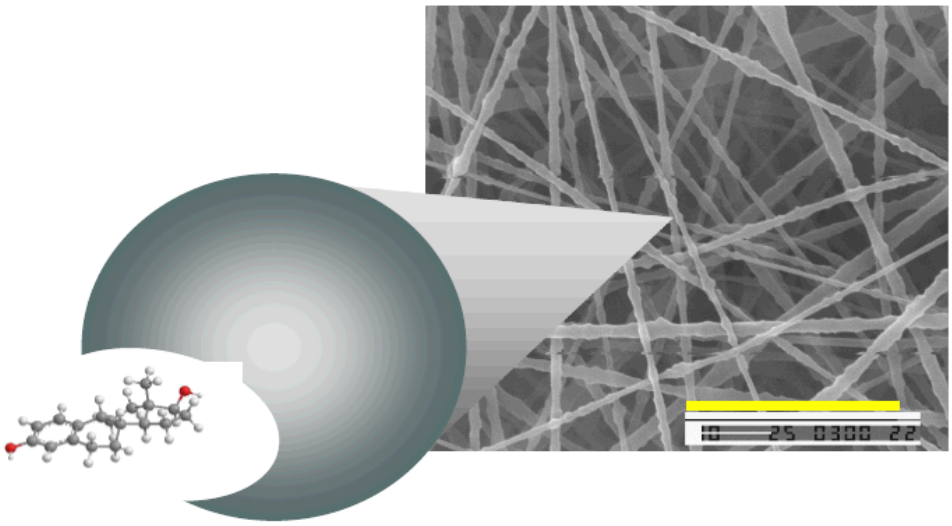

Figure 2.3.2.2: SEM image of electrospun nanofibre composite membrane containing molecularly imprinted nanoparticles [225].

2.3.3 Composite MIP/AuNP/electrospun nanofibres

As already shown in the previous sections (**2.3.1** and **2.3.2**), there are many reports on composite AuNPs/electrospun fibres and MIPs/electrospun fibres. But few or none have

combined the outstanding properties of MIPs, AuNPs and electrospun fibres. This thesis will discuss the investigations conducted on the applicability of the combined properties of these remarkable materials for sensing purposes. Herein the electrospun fibres are mainly utilized as solid support for both the AuNPs and the MIP particles.

Chapter 3: Experimental

3.1 Reagents and materials

Chemical name	**Purity/concentration**	**Supplier**
Gold (III) chloride hydrate($HAuCl_4 \bullet xH_2O$)	99.999 %	Sigma-Aldrich, USA
Sodium borohydride ($NaBH_4$)	98.0%	Sigma-Aldrich, USA
Sodium acetate tri–hydrate ($C_2H_9NaO_5$)	≥99.0%	Sigma-Aldrich, USA
Dopamine hydrochloride (DA, $C_8H_{11}NO_2 \bullet$ HCl)	99.95%	Sigma-Aldrich, USA
Uric acid (UA, $C_5H_4N_4O_3$)	99.0%	Sigma-Aldrich, USA
Ascorbic acid (AA, $C_6H_8O_6$)	99.0%	Sigma-Aldrich, USA
Nylon-6 (N6, $C_6H_{11}NO)n$)	1,084 g mL^{-1} at 25 °C	Sigma-Aldrich, USA
Methacrylic acid (MAA)	98.0%	Sigma-Aldrich, USA
Ethylene glycol dimethacrylate (EGDMA)	98.0%	Sigma-Aldrich, USA
Methanol (CH_3OH)	Analytical grade	Merck Chemicals, South Africa

Azobis(isobutyronitrile) (AIBN)	98.0%, refrigerated at 4°C	Sigma-Aldrich, South Africa
(-)-epinephrine (EPI, 4,5-β-trihydroxy-*N*-methylphenethylamine)	MW: 183.20 g mol^{-1}, stored at 2–8 °C	Sigma-Aldrich, China
(-)-norepinephrine (NORE, 4,5-β-trihydroxy phenethylamine	≥98%, crystalline	Sigma-Aldrich, USA
Catechol (CAT, 3,4-dihydroxy-L-phenylalanine)	MW: 197.19 $gmol^{-1}$	Sigma-Aldrich, China
Tri-sodium citrate dihydrate ($Na_3C_6H_5O_7$)	≥99.0%	Sigma-Aldrich, USA
3-mercaptopropionic acid ($C_3H_6O_2S$)	≥99.0%	Sigma-Aldrich, USA
Mercaptosuccinic acid ($C_4H_6O_4S$)	97.0%	Sigma-Aldrich, USA
DL-Tyrosine ($C_9H_{11}NO_3$)	99.0%	Sigma-Aldrich, Japan
Acetic acid (CH_3CO_2H)	99.5%	B & M Scientific CC, South Africa
Hydrochloric acid (HCl)	32.0%	B & M Scientific CC, South Africa
Nitric acid (HNO_3)	55.0%	B & M Scientific CC, South Africa
Formic acid (HCO_2H)	85.0%	Minema, South Africa

Sodium dihydrogen phosphate (NaH_2PO_4)		May & Baker, Dagenham, England
Sodium hydroxide (NaOH)		Merck Chemicals (Pty) Ltd, South Africa
(+) Glucose Anhydrous ($C_6H_{12}O_6$)		Merck Chemicals (Pty) Ltd, South Africa
β-Cyclodextrin	≥97.0%	Sigma-Aldrich, USA

The whole blood samples were purchased from Seronorm (Billingstad, Norway) and was kept in a freezer (bellow -4 °C). All chemicals were of analytical grade and used as received. All the glassware and magnetic stirrer bar used were washed with freshly prepared aqua regia (1:3 HNO_3: HCl) and rinsed thoroughly with water before use.

Ultrapure water obtained from a Millipore RiOS™ 16 and Milli–Q Academic® A10 system (Milford, MA, USA) was used throughout the study.

3.2 Instrumentation

3.2.1 UV-vis spectroscopy

Absorbance measurements were performed using a Lambda 25 Perkin–Elmer UV spectrophotometer in 1 cm quarts cuvettes (Santa Clara, CA, USA).

3.2.2 Transmission electron microscopy

For the aqueous studies, the morphologies of the AuNPs were characterized using either The FEI Tecnai F20 which is a 200 kV field emission gun (FEG) high resolution Cryo–TEM (HRTEM) or a Zeiss Libra® 120 Plus energy filter transmission electron microscope (Germany) with a megaview iTEM camera.

3.2.3 Scanning electron microscopy

Samples were prepared for high resolution electron microscopy by carbon coating them using a Blazer's "Sputtering device" prior analysis. The analysis was conducted using JOEL JSM-700IF high resolution SEM. Elemental analysis of samples using energy dispersive spectroscopy (EDS) was determined by using the same procedure as for SEM analysis, except that no sample surface coating was needed.

3.2.4 Standard test sieves and Fourier transform infrared (FTIR) spectroscopy

After grinding the MIP/NIP monoliths, Standard Test sieves by Retsch GmbH & Co., (Haan,Germany) combined with sedimentation were employed to collect polymer particles of anaverage size of ≤ 45 μm by screen analysis. A Perkin–Elmer 100 spectrum FTIR spectrophotometer (4000–650 cm^{-1}) was used to confirm the removal of the template (DA) and the generation of recognition sites (Santa Clara, CA, USA). Photographs of the electrospun fibres before and after analytes were taken with a Samsung ES30 camera with 12.2 mega pixels (China).

3.2.5 X–ray photoelectron spectroscopy (XPS)

X–ray spectroscopy (XPS) measurements were conducted with a Kratos Axis Ultra X–ray Photoelectron Spectrometer equipped with a monochromatic Al source Kα source (1486.6 eV) to generate the X–rays. The base pressure of the system was below 3×10^{-9} torr. XPS survey scans were recorded using a 75 W, a hybrid lens acquisition in slot mode at 160 eV pass energy and 500 ms dwell time. XPS data analysis was performed with Kratos Version 2 program.

3.2.6 ImageJ

The Gel analysis method was used. The image of the nanofibres (probe) that had been exposed to DA was first converted to grey scale by converting the image type to 8–bit. The rectangular selection was used and the arrow keys were utilized to move the box drawn on the first nanofibre (0 M DA) to all other fibres (5×10^{-6} – 5×10^{-2} M) to ensure that the area selected from each nanofibre is the same. The version of ImageJ that was used is ImageJ 1.42q on a Windows 7 64–bit install.

3.3 Experimental procedures

3.3.1 Synthesis of the colloidal AuNPs probe

The un–functionalized gold nanoparticles (UF–AuNPs) were prepared by dissolving 39 mg of $HAuCl_4 \bullet xH_2O$ in 10 mL of water. $NaBH_4$ (0.3 mg) was added in solid form under vigorous stirring. The solution was constantly stirred for 30 min at room temperature.

Tri–sodium citrate dihydrate (TSC), 3–mercaptopropionic acid (3–MCA) and mercaptosuccinic acid (MSA) stabilized AuNPs were prepared following the procedure for the synthesis of UF–AuNPs. The stabilizing agents were added before the addition of $NaBH_4$. The ratio of the $HAuCl_4 \bullet xH_2O$ to stabilizing agent was 12:1.

3.3.1.1 Evaluation of the four AuNP solutions (UF-AuNPs, TSC, MCA and MSA stabilized AuNPs) as colorimetric probe

Approximately 100 µL of the four AuNP solutions was reacted with 5 mL of AA, UA (2.1×10^{-4}M) and DA (1.9×10^{-4} M) separately. The standard solutions were prepared in water. Absorbance spectra were recorded over a range of 400 – 700 nm.

3.3.1.2 Evaluation of the contribution of the gold salt ($HAuCl_4 \bullet xH_2O$)

The gold salt solution was prepared by dissolving 39 mg of $HAuCl_4 \bullet xH_2O$ in 10 mL of water. 50 µL of the salt solution was reacted with 5 mL of various concentrations (0, 5×10^{-5},

5 x10^{-4}, 5 x10^{-3} and 5 x10^{-2}M) of DA. Absorbance spectra were recorded over the range of 270 – 700 nm. Photographs of the solutions were taken.

3.3.1.3 Detection of DA employing the UF-AuNPs

Various concentrations of DA (0.005 mM – 2.5 M) were selected randomly and prepared in water. 100 µL of the AuNPs solution was added to 5 mL of the DA solutions. The solutions that resulted from the reaction of the UF–AuNPs and the DA were transferred to a 1 cm path-length quarts cuvette to record the absorption spectra over the wavelength range of 270 – 700 nm.

3.3.1.4 Selectivity studies

AA and UA (each 0.125 M), DA (0.05 M) and mixtures of AA, UA and DA were prepared. Then the procedure in section **3.3.1.3** (addition of AuNPs) was followed to investigate the selectivity of the probe towards DA.

3.3.1.5 Optimization of pH

For the pH studies, two types of buffer solutions (acetate and phosphate) were used to adjust the pH of the solutions. The acetate buffer was prepared by mixing 10 mM of sodium acetate tri-hydrate and 10 mM acetic acid, and this was used for pH 2 – 6, whilst the phosphate buffer prepared by mixing 10 mM sodium dihydrogen phosphate and 10 mM of sodium hydroxide was used for pH 7 – 11. DA (5 µM) was used as a representative for the study and the profile of the absorbance ratio (A_{388}/A_{308}) was plotted against pH.

3.3.1.6 Detection of DA under controlled conditions

Firstly, 1 mL of the buffer solution (phosphate buffer pH 8) was added to 50 µL of the UF–AuNPs. Then 4 mL of various concentrations of DA solutions (5 nM – 50 mM) were added to the mixture. The solutions were incubated at room temperature (25 ± 2 °C) for 2 min before the absorbance was measured at 308 and 388 nm.

3.3.1.7 Colorimetric detection of DA in whole blood sample

The sample was diluted 100 times with phosphate buffer (pH 8) before analysis, and no other pre–treatment was required. Particularly, 3 mL of 5 µM and 50 µM DA was added to 2 mL of the sample solution and subsequently, 50 µL of the UF–AuNPs was added. Absorption spectra were recorded after incubation at room temperature as before, for 2 min.

3.3.2 Preparation of MIPs and NIPs

MIP particles were prepared using a protocol published by Luliński and co-workers [226]. Briefly, the template dopamine hydrochloride (0.33 mmol), MAA (monomer) (2.64 mmol, 0.224 mL), EDGMA (cross-linker) (20 mmol, 3.768 mL) and AIBN (initiator) (0.396 mmol) were mixed with a solution of methanol (3.67 mL) and water (0.53 mL). The mixture was stirred then purged with nitrogen for 15 min, and polymerized by heating at 60 °C for 24 h. The procedure for NIPs was the same as for MIPs, but with the exclusion of the template.

3.3.2.1 Template removal

After polymerization, the template was removed from the polymer complex firstly by Soxhlet extraction for 24 h with methanol – water (80 mL, 1:1 v/v). The polymer monolith was then ground and manually sieved. For optimal removal of the template a stationary extraction method was used, where the MIP particles were washed using a solvent mixture of 80% methanol and 20% acetic acid (v/v) (5 x extractions: shaking time 10 min each), the particles were then dried in oven at atmospheric pressure and at a temperature of 50 °C.

3.3.2.2 Preparation of the MIP/AuNPs/electrospun N6 nanofibre composite (MIP + AuNPs + N6)

The prepared MIP or NIP particles (0.5 g) were suspended in a mixture of formic acid and acetic acid (1:1). Then N6 was added to make a 16wt% solution. The mixture was stirred over night for complete dissolution of the polymer. Approximately 0.115 mmol of

$HAuCl_4 \bullet xH_2O$ was dissolved in the polymer solution and vigorously stirred for 15 min at room temperature. The resulting solution was yellow in colour. On addition of 0.00793 mmol of $NaBH_4$ (reducing agent), the solution turned black for a few seconds then wine red. After stirring for 2 min the solution gradually became purple.

3.3.2.3 Electrospinning

The purple solution was electrospun at an optimal voltage of 25 kV (other voltages used are 15 kV and 20 kV) and a flow rate of 0.5 ml/h controlled using a syringe pump. The continuous N6 fibres were collected on a stationary collector covered with an aluminium foil. The distance from the tip of the spinneret to the collector was 10 cm.

3.3.2.4 Colorimetric analysis of the fibres

Three solutions were prepared in ultrapure water, each containing AA (2.1×10^{-4} M), UA (2.1×10^{-4} M) and DA (1.9×10^{-4} M). Then portions of the composite MIP (NIP) + UF–AuNPs + N6 nanofibre mats were cut and dipped in 2 mL of these solutions and colour changes were monitored with the naked eye.

3.3.3 Preparation of the AuNPs/electrospun N6 nanofibre and the N6/$HAuCl_4$ nanofibre composites

The procedures in **3.3.2.2** and **3.3.2.3** were followed to fabricate the UF–AuNPs/ electrospun N6 nanofibre composite (UF–AuNPs + N6) except for that the MIPs were excluded. Employing the same procedures, TSC–AuNPs; 3–MCA–AuNPs and MSA–AuNPs/ electrospun N6 nanofibre composites were synthesized. The fibre mats were evaluated as solid state colorimetric probes by introducing them to 2 mL of AA, UA (both 2.1×10^{-4} M) and DA (1.9×10^{-4} M).

Before electrospinning, the polymer solutions were evaluated as liquid state colorimetric probes by reacting approximately 100 µL of the polymer solutions with 5 mL of AA, UA (2.1

x 10^{-4}M) and DA (1.8 x 10^{-4} M) in formic acid. Absorbance spectra were recorded over a range of 400 –700 nm.

The $HAuCl_4$ + N6 nanofibres was prepared by mixing already dissolved N6 as per in **3.3.2.2**. About 0.115 mmol of $HAuCl_4 \bullet xH_2O$ was then added to the polymer solution and vigorously stirred at room temperature until the salt dissolved completely. The colour of the composite solution was yellow and resulted into a white coloured nanofibre mat after electrospinning under the conditions explained in section **3.3.2.3** with a distance between the tip of the spinneret and the collector set at 12 cm. Parts of the as prepared nanofibre was put in various concentrations of AA (5 x 10^{-7} – 5 x 10^{-2} M) and DA (5 x 10^{-8} – 5 x 10^{-2} M) and photographs were taken.

3.3.3.1 Analysis of the UF–AuNPs + N6 nanofibres using TEM

The morphologies of the UF–AuNPs + N6 composite collected on carbon–coated copper grids were observed on a transmission electron microscopy (TEM). The analyte was introduced by spiking a small amount of 5 x10^{-5} M DA on the fibres that were already on the copper grid. The sample was allowed to dry and then analysed.

3.3.3.2 Detection of DA employing the AuNPs + N6nanofibres at pH 7.4

Portions of the UF–AuNPs + N6 nanofibre mat were cut and introduced to 2 mL of the interfering species (AA, UA, EPI, NORE and CAT, 50 µM and 5 µM DA. Photographs of the fibres were taken within 5 min.

3.3.3.3 Solid state colorimetric detection of DA in whole blood sample

Parts of the UF–AuNPs + N6 nanofibre mat were dipped to 2 mL of the untreated blood sample before and after spiking 5 µM and 50 µM DA. After 5 min, the fibres were removed from the samples and washed with water until there was no blood coming out of them. The fibres were also put in approximately 5 mL of water in centrifuge tubes then centrifuged for 5 min at 2000 rpm to remove any excess blood, and then photographs were taken.

3.3.4 Optimization of the reagents for the preparation of the UF−AuNPs + N6 probe

N6 was first dissolved then the gold salt was added at the required quantity in terms of the concentration ratios of 1:1, 1:3, 3:1, 1:5 and 5:1 (gold salt: $NaBH_4$). For each a slight change in colour from a clear solution to a pale yellow was observed. $NaBH_4$ was then added for the reduction of the gold ions in quantities representative of the given ratios. A colour change to purple was observed. The intensity of the purple colour increased with an increase in $NaBH_4$ concentration. The solution mixtures were electrospun under optimal conditions (see section **3.3.2.3**).

3.3.4.1Introduction to Analytes

Several concentrations of DA (5×10^{-7}, 5×10^{-6}, 5×10^{-5}, 5×10^{-4}, 5×10^{-3}, and 5×10^{-2} M) were prepared. Each solution of DA (2 mL) was put into vials. The different probes were cut into small pieces and introduced into these solutions to detect DA based on colour change of the probes. For each probe 2 mL of Millipore water was placed into a vial to be used as the reference of the experiment. This step was repeated for AA.

Stock solutions of epinephrine, norepinephrine, glucose anhydrous and tyrosine were prepared, each at a concentration of 5×10^{-6} M. The probes used to test these analytes were the ones fabricated using 5:1 and 1:5 concentration ratios of gold salt: $NaBH_4$. Colour change was monitored with a naked eye and images taken.

3.3.5 Optimization and preparation of the β–cyclodextrin–AuNPs + N6 nanofibre composite probe

Two methods namely the *in situ* and *ex situ* were employed to fabricate the composite probes. Firstly, it was necessary to investigate the order of addition of the reagents. For this investigation, two procedures were followed. The first procedure involved dissolving N6 (1.08 g) first followed by addition of β–cyclodextrin (β–CD) (1.08 g) which was also allowed to dissolve and the solution was electrospun. The second procedure involved dissolving of β–

CD first in a 1:1 mixture of acetic acid and formic acid (in 5 mL) then the addition of N6 followed by electrospinning.

3.3.5.1 *In situ* method

The second procedure was adopted for the *in situ* synthesis of the β–CD–AuNPs + N6 composite probe. Briefly, after the dissolution of the N6 on the same protocol, gold salt (39 mg) was added to the mixture and the solution was stirred until the salt dissolve. $NaBH_4$ (approximately 0.3 mg) was introduced to the solution for the reduction of the gold ions. All the prepared solutions were electrospun under the conditions in section **3.3.2.3**.

3.3.5.2 *Ex situ* method

Preparation of the β–cyclodextrin stabilized AuNPs

For the successful preparation of the nanoparticles, β–CD (0.0396 g) was dissolved in 5 mL deionized water and stirred for 15 min to form a clear solution of β–CD. Thereafter, 40 µL of the gold salt solution, $HAuCl_4$ (15 mM) was added with further stirring until solution was homogenous. It was followed by addition of 50 µl of NaOH (1 M), which activated the reduction capacity of the β–CD solution. The solution obtained was heated at 60 °C in a waterbath for 20 min, and a purple coloured solution was observed confirming the complete formation of nanoparticles. The nanoparticles obtained were further purified by dilution and centrifugation with deionized water.

For the *ex situ* method, N6 was dissolved following the above mentioned procedure. Pre–synthesized β–CD stabilized AuNPs (β–CD–AuNPs) were then added to the polymer solution, stirred for 15 min then the mixture was electrospun.

Pieces of the nanofibre with the *in situ* prepared β–CD–AuNPs were introduced to 5×10^{-6} M of EPI, NORE, CAT, DA, UA and AA. Images of the nanofibres were taken after 10 and 20 min exposure to the analytes.

Chapter 4: Results and discussions

4.1 Preliminary evaluation of the AuNPs as colorimetric probe

The un–functionalized gold nanoparticles (UF–AuNPs) (**Fig. 4.1A**) were green in colour and were stable against aggregation for more than 3 months (stored in a cupboard or in the refrigerator at 4 °C in the dark). The stability was attributed to excess $AuCl_4^-$ and $AuCl_2^-$ ions that were bound to the surface of the gold nanoparticles in the solution during the reduction of $AuCl_4^-$ [227]. The UF–AuNPs solution showed no absorption peak in the range 400–700 nm, and no significant change was observed either on the absorption spectrum or colour in a solution of UA. Conversely, when the nanoparticles were added to AA and DA a bright pink and orange colour were observed for the two analytes, respectively.

Other nanoparticles were prepared using stabilizers (tri–sodium citrate, 3–mercaptopropionic acid and mercaptosuccinic acid) to find the ones that will be suitable for our studies.

The tri–sodium citrate stabilized AuNPs (TSC–AuNPs) (**Fig. 4.1B**) solution was pale yellow in colour. When the solution was introduced to UA, the colour and spectrum remained similar to that of the control (the control was made of 100 µL of the nanoparticle solution and 5 mL of water). However, colour and spectral change were observed when the TSC–AuNPs were added to DA and AA. The DA + TSC–AuNPs solution was purple with a broad peak around 550 nm whilst the AA + TSC–AuNPs solution was reddish–purple and the absorption maxima was at 520 nm. Although the TSC–AuNPs showed potential for the detection of both AA and DA, the nanoparticles were stable for less than a week and the colours were too faint.

The 3–mercaptopropionic capped AuNPs (3–MCA–AuNPs) (**Fig. 4.1C**) was white in colour and showed no response in any of the analytes. The solution seemed homogenous for few hours after that two layers were observed, this was ascribed to the known tendency of short chain alkanethiolates to form disordered structures. A clear solution on top and a cloudy or precipitate formed at the bottom of the vial in which they were kept (not shown). Hence the nanoparticles could not be used for further studies.

In contrast to the other three AuNP solutions that were prepared, the mercaptosuccinic acid capped AuNPs solution (MSA–AuNPs) (**Fig. 4.1D**) had the typical colour (wine–red) and absorption peak for AuNPs around 500 nm. However, no colour change or significant spectral shifts were observed when the nanoparticles were introduced to the analytes.

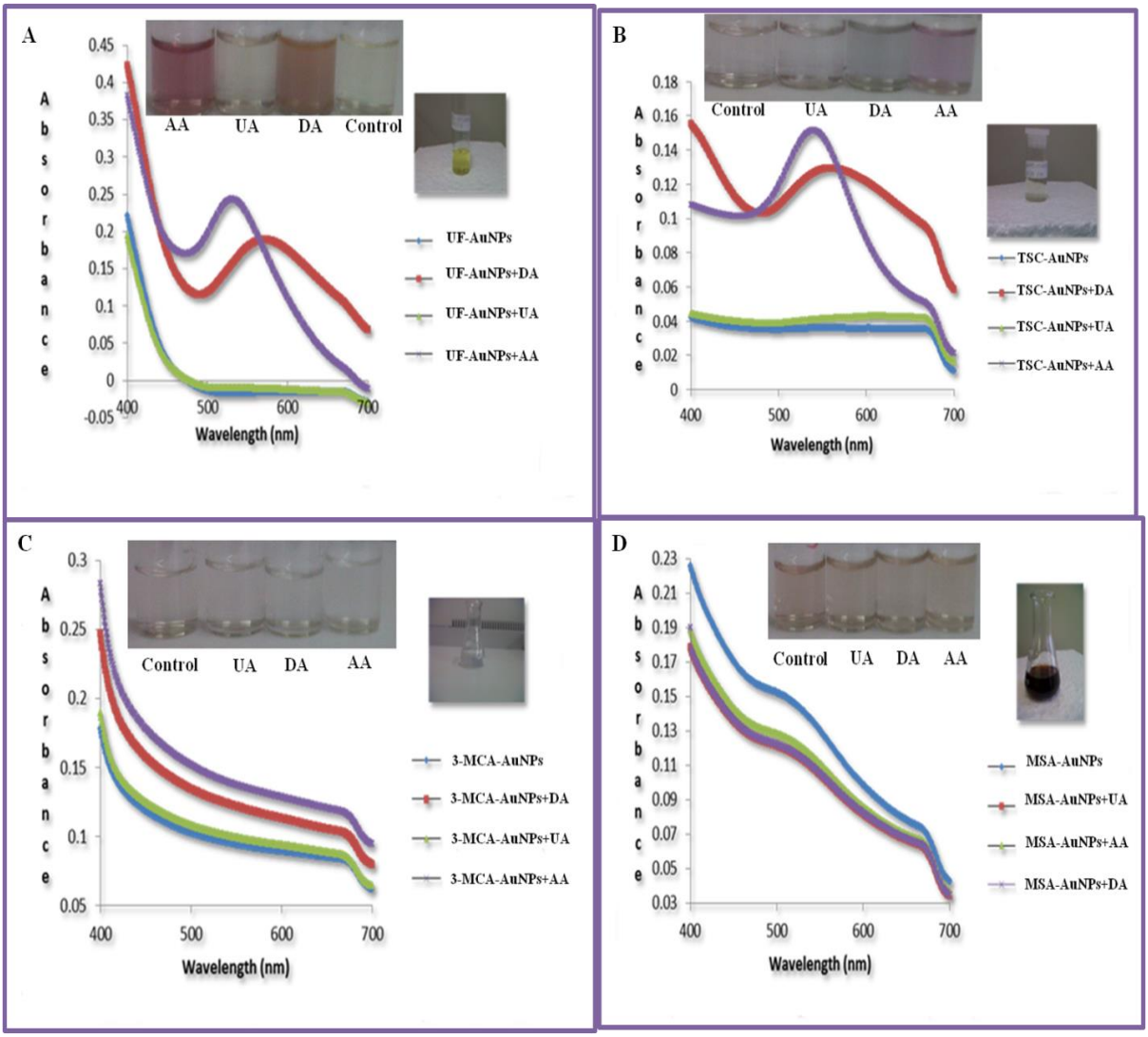

Figure 4.1: Photographs and absorbance spectra of (A)- UF–AuNPs, (B)- TSC–AuNPs, (C)- 3–MCA–AuNPs and (D)- MSA–AuNPs in AA, UA and DA.

The contribution of the $HAuCl_4^-$ in the probe was investigated in order to find out if it was necessary to reduce the gold salt or use it as it was for the detection of DA. To achieve this, a solution of the gold salt was prepared and added to various concentrations of DA. The results are shown in **Fig. 4.2**. Different colours were observed instead of increasing intensity of the same colour with increasing concentration of DA. The pink colour of the 5 $x10^{-5}$ M DA was

also observed in AA (**Fig. 4.1A),** presenting a potential for interference hence it was concluded that in order for the probe to be selective to DA, the gold salt had to be reduced to form the green AuNPs. Based on these results, the UF–AuNPs were chosen as the liquid state colorimetric probe and for further analysis.

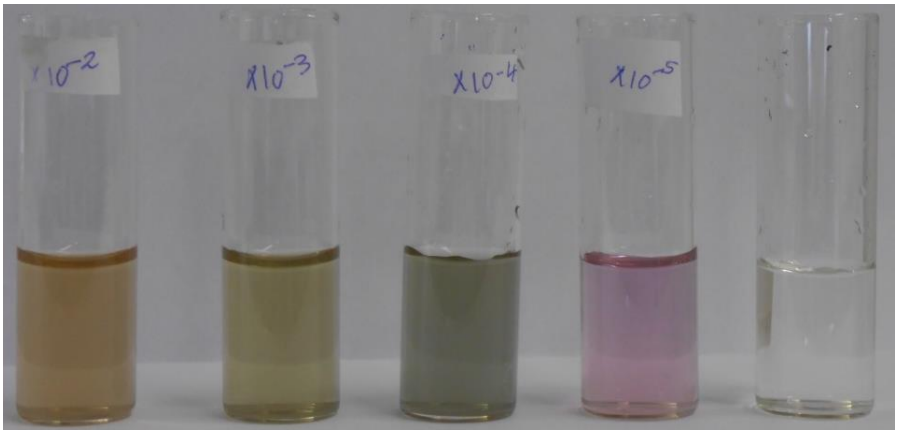

Figure 4.2: A photograph showing colours that were obtained when 5 x10^{-5}, 5 x10^{-4}, 5 x10^{-3}, 5 x10^{-2} M DA were mixed with 50 µL of the gold salt solution.

4.1.1 Visual and spectroscopic characteristics of dopamine

Fig. 4.1.1A shows the colours of the solutions of different concentrations of DA that resulted from reacting with 100 µL of the AuNPs. The 0 M solution (pale green) was used as a control. Colour changes from pale green to pale orange (0.5 mM), orange (5 mM), dark orange (0.05 M), wine–red (0.5 and 1 M) and brown (2.5 M) were observed immediately on addition of different concentrations of DA. The series of photographs and corresponding absorption spectra are shown in **Fig. 4.1.1A** and **Fig. 4.1.1B**, respectively. Additional DA concentrations of 1.25 mM, 2.50 mM, 12.5 mM, 25.0 mM, 0.125 M, 0.250 M and 0.625 M were also prepared in order to better evaluate the subtle spectroscopic changes **Fig. 4.1.1B.** The absorption band of the gold salt exhibited a maximum at 294 nm as shown in **Fig. 4.1.1B, a1.**

$AuCl_4^-$ ions have been reported to exhibit a strong absorption band at 220 nm with a shoulder at 290 nm due to charge transfer between gold and the chloro ligands [228]. After reduction with $NaBH_4$, but before addition of the analyte (DA), the absorption band had shifted to 308 nm (**Fig. 4.1.1B, a**). The band at 308 nm confirmed that nanoparticles were

formed despite the fact that the borohydride that was added could not reduce all the $AuCl_4^-$ ions. A progressive decrease in absorbance at 308 nm with increasing concentration of DA was observed, especially at very low DA concentrations of 0.005 mM and 0.05 mM (**Fig. 4.1.1B, a-c**). The spectral shifts were not sufficient to allow visual detection of DA, but may be developed in a spectrophotometric method. On addition of significant amounts of DA (1.25 mM, 2.5 mM, 0.0125 M and 0.025 M) an absorption maximum at 388 nm was observed (**Fig. 4.1.1B, d-g**). A second band at 500 nm was observed for higher DA concentrations of 0.125, 0.25, 0.625, 1 and 2.5 M (**Fig. 4.1.1B, h-j**). DA is known to act as a good reducing agent in certain circumstances [229]. When the green AuNPs were mixed with the different concentrations of DA, more and more of the remaining $AuCl_4^-$ and $AuCl_2^-$ ions were reduced to Au^0 nanoparticles, thus resulting in a decrease in intensity of the initial band at 308 nm. The newly formed nanoparticles attached themselves onto the existing nanoparticles to form bigger nanoparticles or aggregate particles resulting in colour changes and shifts in the absorption spectra from lower to higher wavelengths. A similar process is common in the deliberate synthesis of shaped nanoparticles from small "seed" nanoparticles [230].

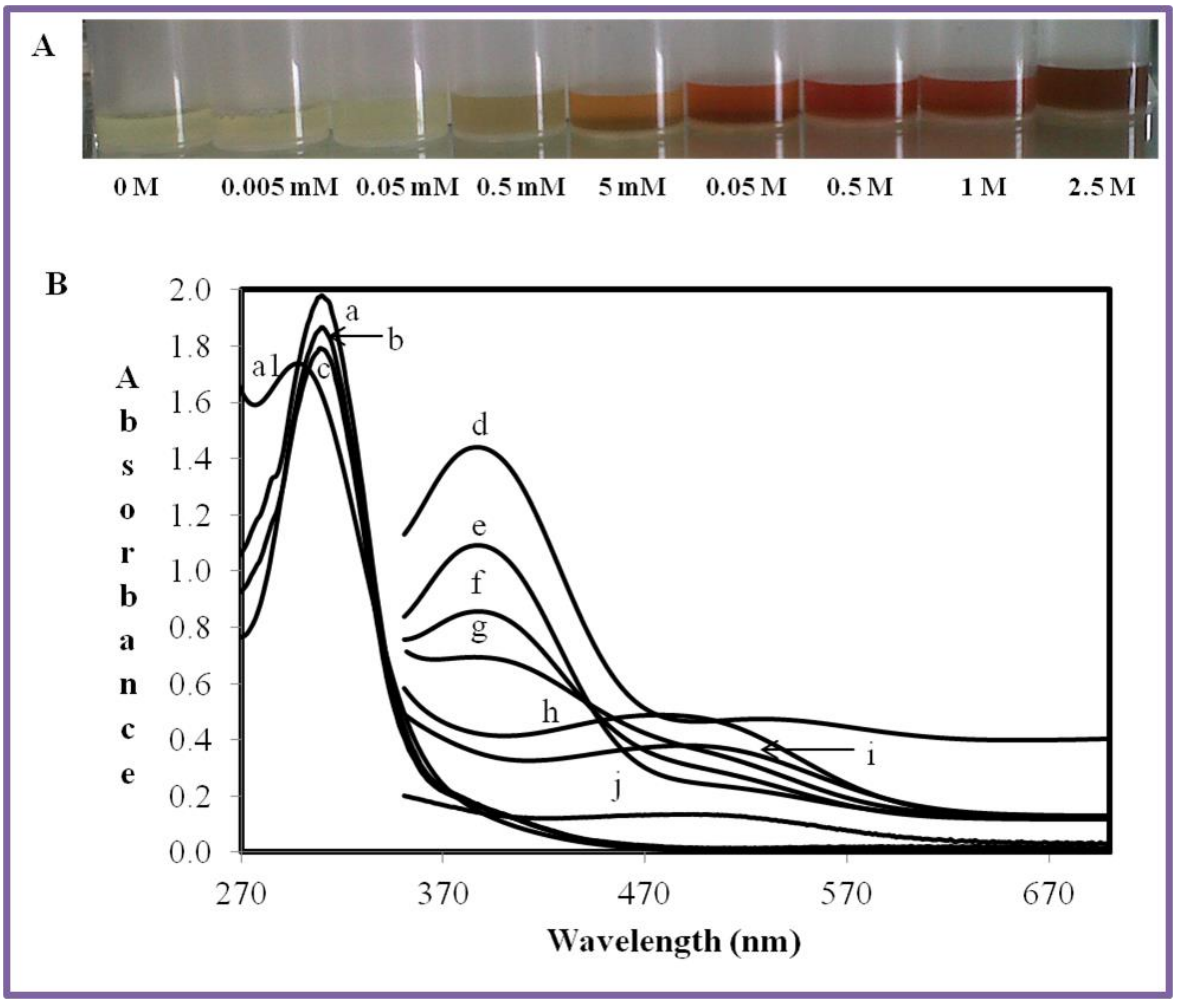

Figure 4.1.1: (A) Photograph showing colour changes of solutions of different concentrations of DA reacted with 100 µl of the UF–AuNPs, (B) Absorbance spectra of: a1- Au salt before $NaBH_4$, AuNPs in a- 0 M, b- 0.005 mM, c- 0.05 mM, d- 1.25 mM, e- 2.5 mM, f- 0.0125 M, g- 0.025 M, h- 0.125 M, i- 0.625 M, j- 2.5 M

4.1.2 HRTEM characterization of the UF−AuNPs

To further understand how the spectral features of the probe were related to particle size and shape, transmission electron microscopy (TEM) studies were conducted. The morphologies of the AuNPs (**Fig. 4.1.2**) were in agreement with the UV–visible spectroscopy results as they showed growth in the size of the nanoparticles and that aggregates were formed. The synthesized nanoparticles were initially well dispersed, roughly spherical in shape and their average diameter was estimated to be 10 nm (**Fig. 4.1.2a**). The TEM images confirmed growth and aggregation of the AuNPs in the presence of DA (**Fig. 4.1.2, b-f**). Interestingly, TEM also revealed the generation of different shapes of the AuNPs for different concentrations of DA. Again the observations were consistent with a "seed" approach to

AuNP synthesis [230].

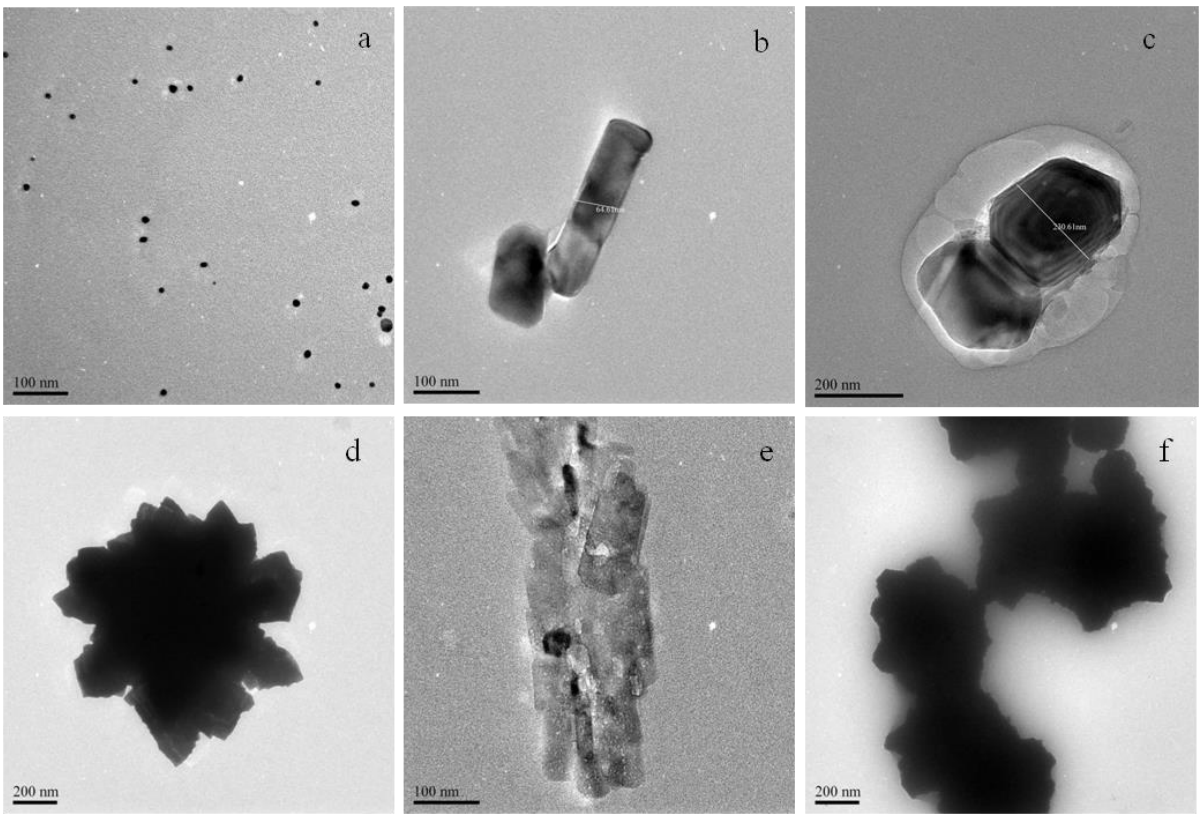

Figure 4.1.2: HRTEM of the UF–AuNPs in various DA concentrations. a–c shows growth in the size of the NPs from 0 M (a) average diameter of 10.12 nm, in 5 mM (b) with core size of 64.61 nm and in 0.05 M (c) with core size of 230.61 nm, d–e shows aggregates of NPs formed in 0.05 mM, 1 M and 2.5 M respectively.

4.1.3 Selectivity

The selectivity of the UF–AuNPs for DA detection in the presence of interferences (ascorbic acid and uric acid) was investigated. The results shown in **Fig. 4.1.3.1** indicate that there was no colour change when the UF–AuNPs were introduced to a relatively high concentration of UA (**Fig. 4.1.3.1A, b**) and that there was also no significant spectral change for the solution (**Fig. 4.1.3.1B, b**). An orange colour was observed for DA (**Fig. 4.1.3.1A, c**) while the colour changed to purple in AA (**Fig. 4.1.3.1A, d**) with absorption maxima at 498 and 609 nm, respectively (**Fig 4.1.3.1B, c and d**). The response of AA to the nanoparticle probe was not surprising since it is known that AA and DA have similar chemical properties. In this case, both analytes have been used as reducing agents for nanoparticle synthesis [231, 232]. In this study, however, while it is plausible that AA like DA is reducing excess $AuCl_4^-$ and $AuCl_2^-$

ions, the resulting nanoparticles were different and presented a very different colour. Interestingly, a mixture of the three analytes resulted in an orange colour (**Fig 4.1.3.1A, e**) with absorption maxima at 490 nm (**Fig. 4.1.3.1B, e)** corresponding to that of DA yet the concentration of DA was much lower (almost one third of both AU and AA).

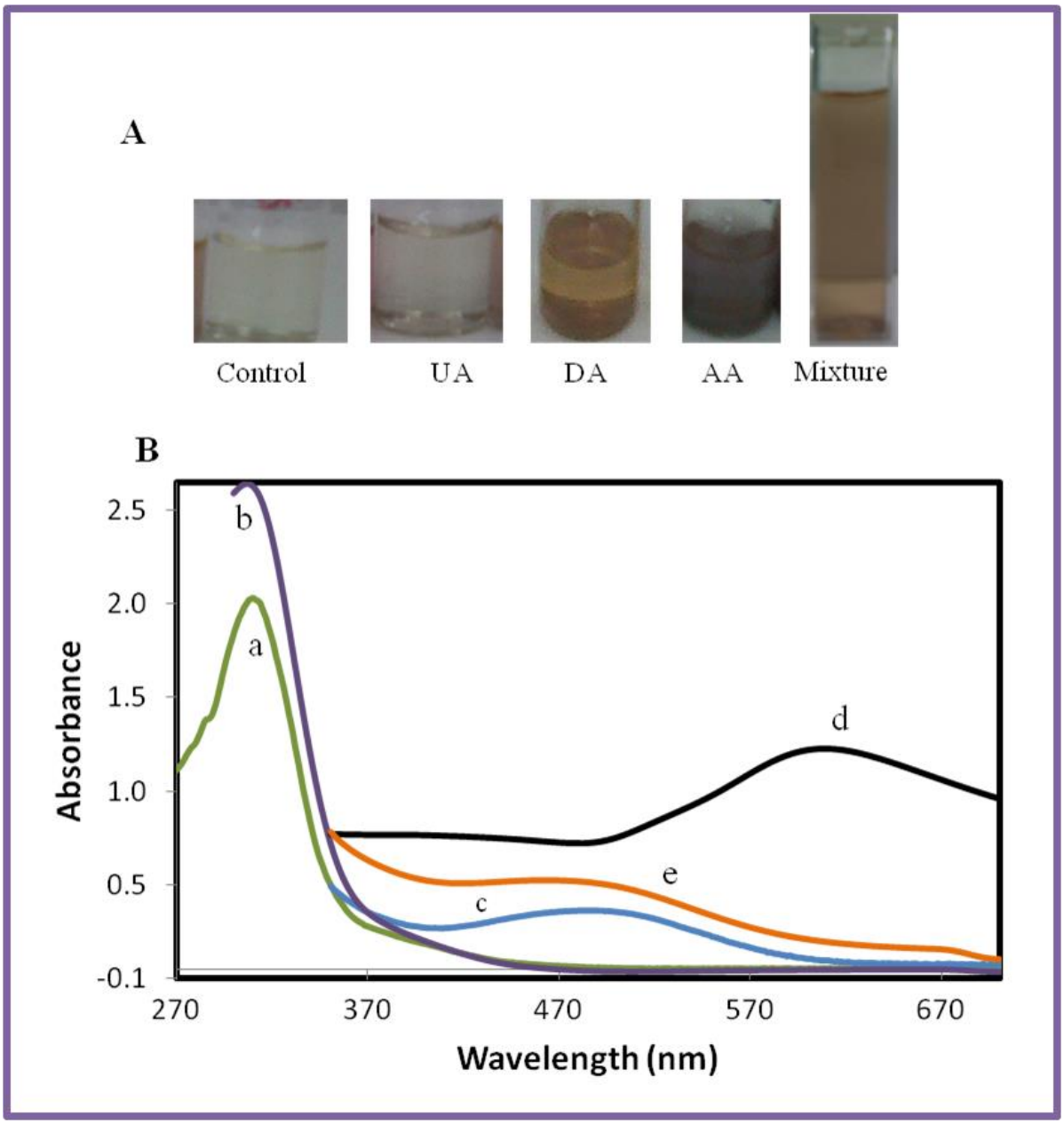

Figure 4.1.3.1: (A) shows the colours that resulted when the analytes reacted with the AuNPs. a- is a control, AuNPs in water, b- UA (0.125 M), c- DA (0.05 M), d-AA (0.125 M) and e mixture of the three analytes. (B) depicts the absorption spectra corresponding to (A).

Based on the results in **Fig. 4.1.3.1**, the UF–AuNPs probe could be used to detect AA in the

absence of the interfering species. AA was further investigated as a possible interfering species because of the observed colour change. Different concentrations of AA were prepared to investigate the extent to which the probe could detect AA. Colour changes were observed from light green to purple for 0.125 mM to 1 M AA (**Fig. 4.1.3.2A**). The absorption maxima for the nanoparticles in the presence of AA were between 553 and 613 nm (**Fig. 4.1.3.2B, c-g**) while the ones for the reduced particles alone was at 308 nm ((**Fig. 4.1.3.2B, a and b**).

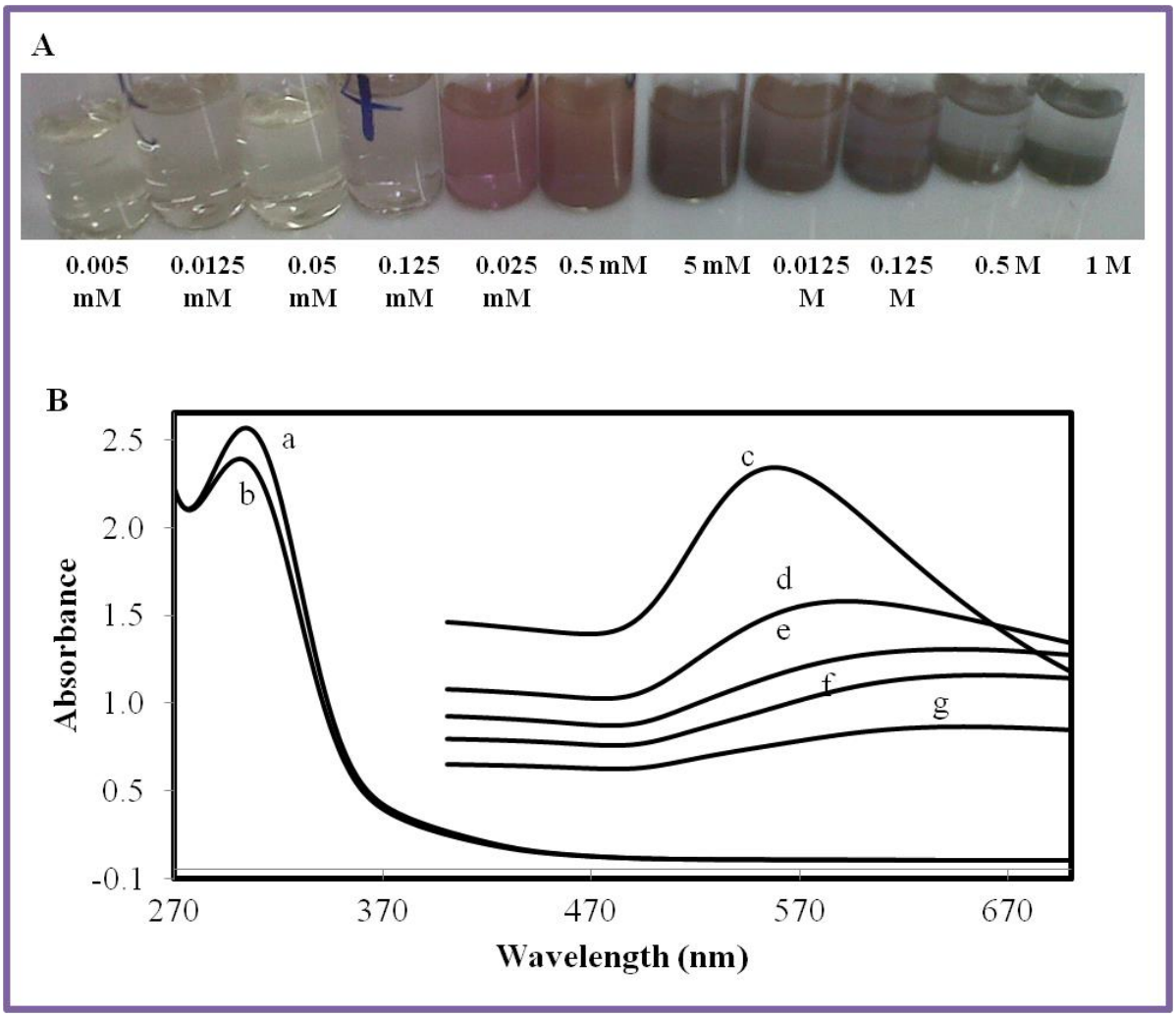

Figure 4.1.3.2: (A) shows the response of the probe to AA. (B) Depicts the absorption spectra of the UF–AuNPs in different concentrations of AA. a- 0.005 mM, b- 0.05 mM, c- 1.25 mM, d- 2.5 mM, e- 5 mM, f- 0.0125 M, g- 0.5 M

Next, concentrations of DA and AA were varied and mixed to investigate if the probe was selective to different concentrations of DA in the presence of AA. The results are shown in **Fig. 4.1.3.3**. An orange colour was observed on addition of the AuNPs to a solution of DA, even when AA concentration were 20 times greater or 50 times lower than that of DA (**Fig.**

4.1.3.3A, **b** and **c** respectively). The corresponding absorption spectra (λ_{max} around 500 nm) (**Fig. 4.1.3.3B**, **a** and **b**) were similar to those that were observed for DA in the absence of AA (**Fig. 4.1.1A**). When the concentration of AA was increased to 200 times greater than that of DA, a purple colour was observed (**Fig. 4.1.3.3A, a**) and the corresponding absorption spectra (λ_{max} around 605 nm) was similar to that observed for AA (**Fig. 4.1.3A**) in the absence of DA (**Fig. 4.1.3.3B, a**). It is clear that the probe could be used for detecting both AA and DA, separately, or for detecting DA in the presence of moderate concentrations of AA. In biological samples where concentrations of AA are higher than those of DA (usually 100 – 1000 times higher) the probe will only remain effective until the AA concentrations are 200 times greater than those of DA. When the concentrations of AA are above 200 more than those of DA, the high concentrations of AA would interfere with the detection of DA.

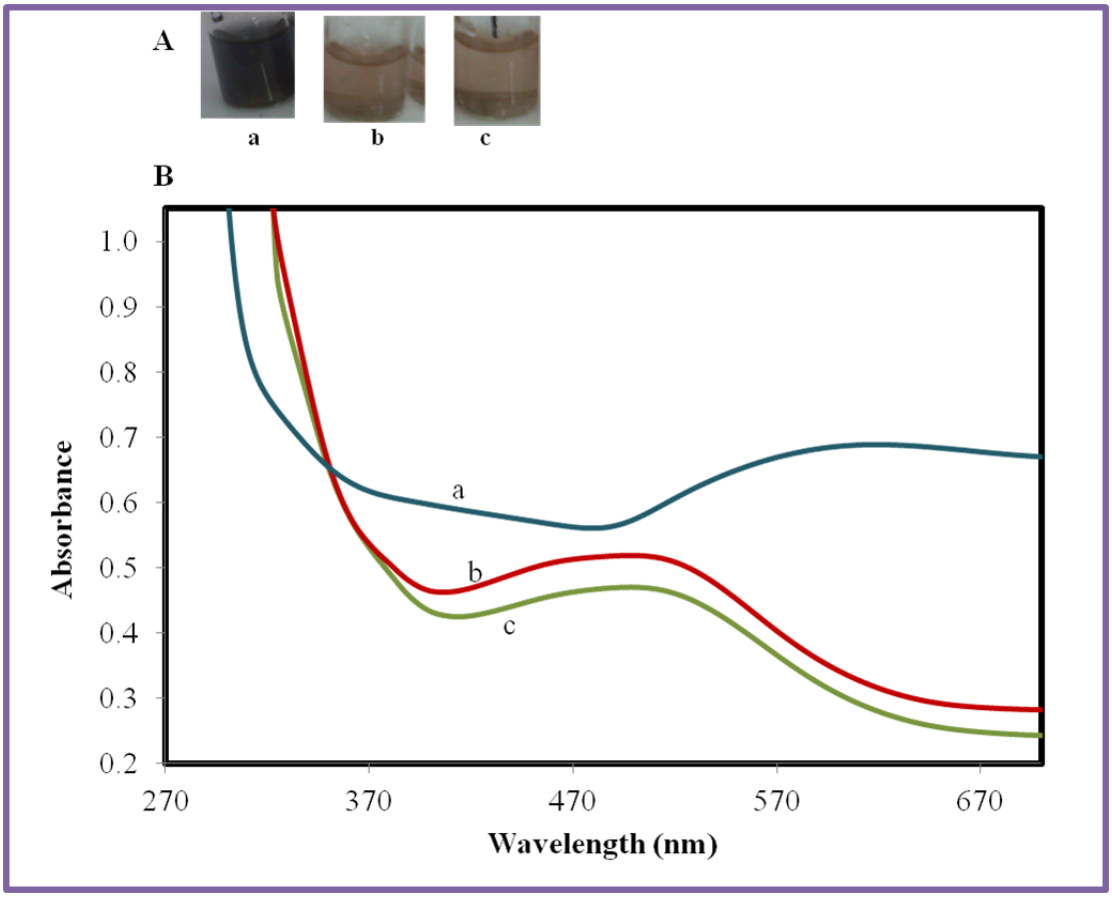

Figure 4.1.3.3: (A) Photograph showing the response of the probe to the mixtures of DA and AA concentrations. (B) Depicts the corresponding absorption spectra of the mixtures of a- 0.25 mM: 0.05 M, b- 1.25 mM: 0.025 and c- 2.5 M: 0.05 M (DA: AA).

4.1.4 Optimization of pH

DA is an organic base with a pKa of 8.9. The media pH can therefore affect the form of DA in aqueous solution and thus the reaction between DA and the AuNPs. Therefore, it is important to optimize the pH of the solution. We investigated the impact of pH in the range from 2 to 11 (**Fig. 4.1.4**) and the absorbance ratio of A_{388}/A_{308} were plotted against pH. It must be noted that DA absorbs at three wavelengths (308, 388 and 500 nm). The A_{388}/A_{308} ratio was chosen because most of the DA concentrations that were prepared absorbed at these two wavelengths. For this study, 5 µM DA was used as a representative. Lower absorbance ratios (A_{388}/A_{308}) were observed for pH < 7.4 and pH > 9. The highest absorbance ratio (A_{388}/A_{308}) was observed at pH = 8. For pH < 7.4, the lower ratio was probably due to the fact that DA is protonated and relatively stable at acidic and neutral pH; it can therefore not be used to reduce the excess $AuCl_4^-$ or $AuCl_2^-$ ions. In basic media (e.g. pH 8), DA becomes deprotonated [233], very unstable and easily oxidized; this results in the $AuCl_4^-$ or $AuCl_2^-$ ions being easily reduced to form nanoparticles, hence resulting in a higher absorbance ratio. At pH > 9 the AuNPs were not stable and tend to aggregate rapidly, resulting in a colour change before DA is introduced (not shown). Therefore pH 8 was chosen as the optimal media pH.

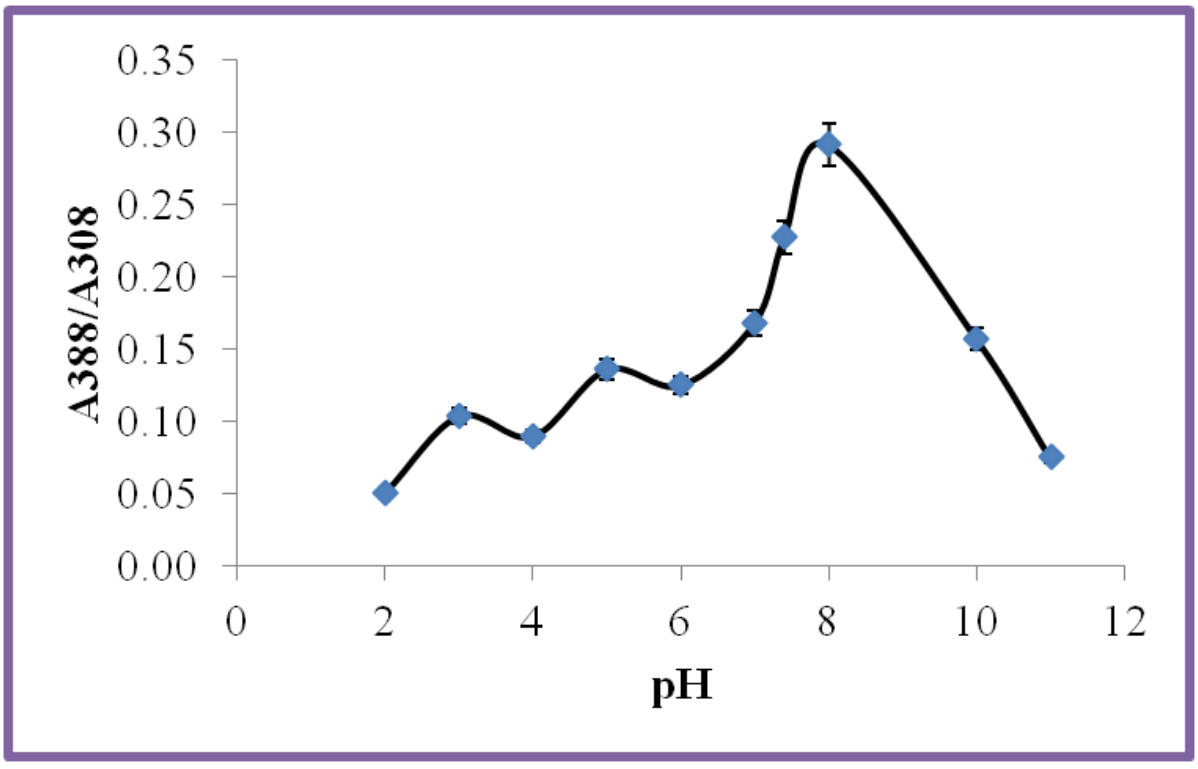

Figure 4.1.4: Effect of media pH on the absorbance ratio (A_{388}/A_{308}) of 5 µM DA.

4.1.5 Detection of DA under optimal conditions

Under optimal pH, colour changes were observed for solutions of DA as low as 5 nM (**Fig. 4.1.5.1A**). The control solution (0 M DA), was pale green but when DA was introduced the green colour first intensified with increasing concentration of DA (5 nM – 5 μM) and gradually changed to an orange colour (for higher concentrations of DA). As depicted in **Fig. 4.1.5.1B**, the absorbance ratio of A_{388}/A_{308} gradually increased upon addition of more DA. The mechanism that brings about the colour change is similar to the one observed previously under sub-optimal pH conditions, where the AuNPs were seen to become larger, changed morphology and aggregated on addition to increasingly more DA (**Fig. 4.1.5.2**). Good linearity was obtained over a range of 5.0 $x10^{-8}$ – 5.0 $x10^{-5}$ M and the detection limit was estimated to be 2.5 nM (3σ). The probe has better selectivity than other reported AuNP–based colorimetric probes for detecting DA [31, 93, 96, 97].

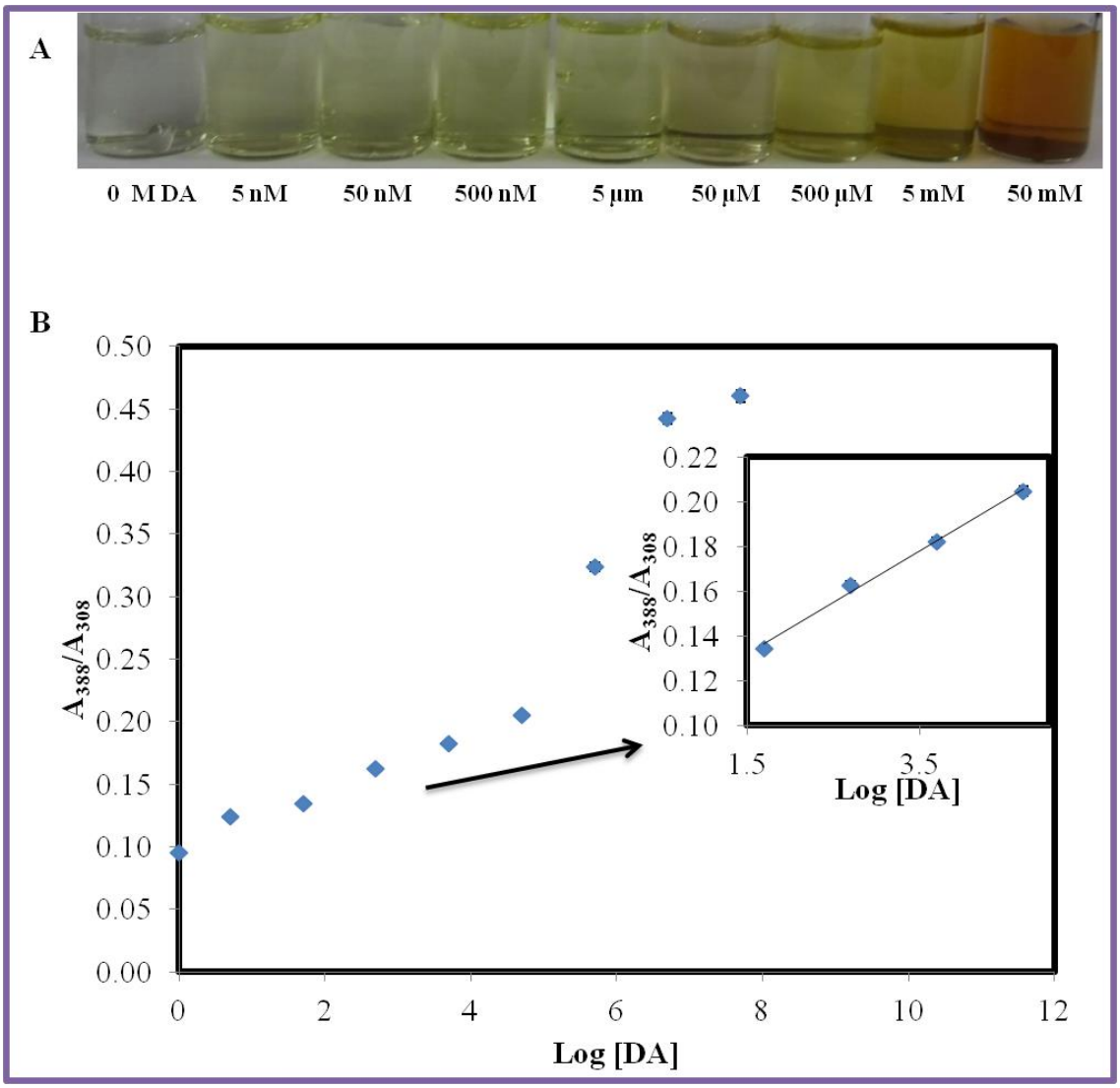

Figure 4.1.5.1: (A) photograph of the UF–AuNPs in the presence of different concentrations of DA at pH 8. (B) Plots of the absorbance ratio (A_{388}/A_{308}) versus logarithm of the concentrations of DA (0 M, 5 nM, 50 nM, 500 nM, 5 µM, 50 µM, 500 µM, 5 mM and 5 mM respectively).

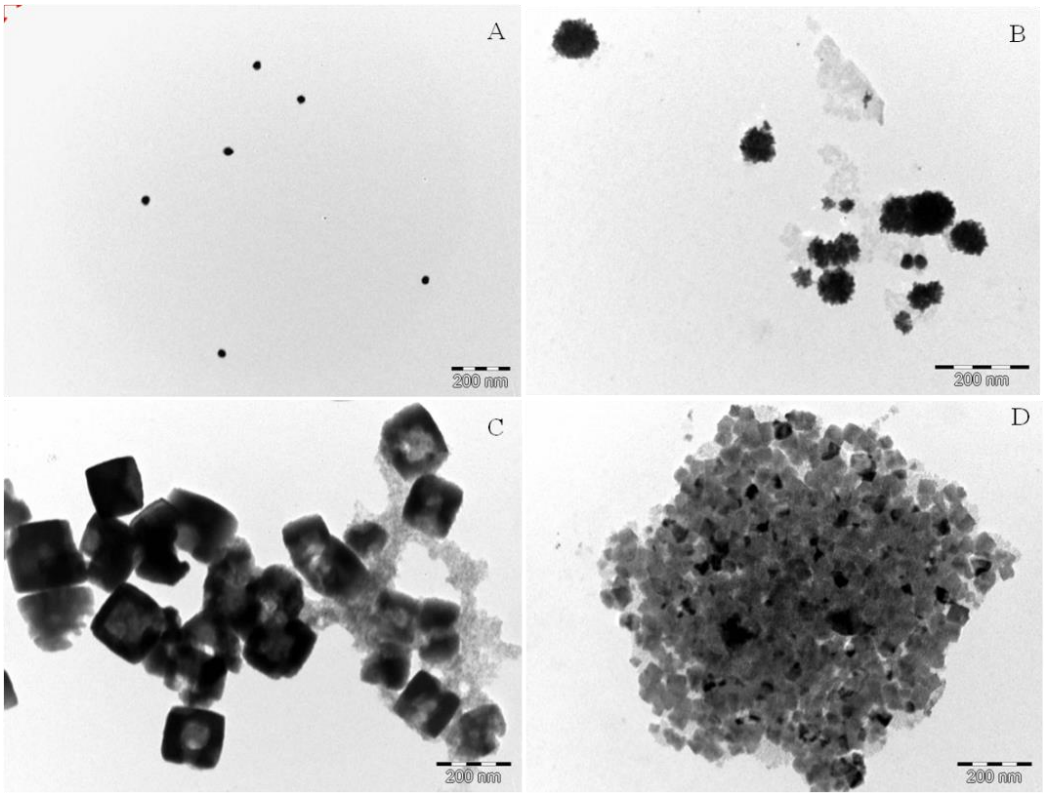

Figure 4.1.5.2: TEM images of the UF–AuNPs in the presence of DA. A–B shows growth in the size of the nanoparticles, in 5 nM (B) with core size of 18.37 nm and in 5 µM (C) with core side of 83.66 nm, C and D shows aggregates of NPs formed in 0.05 mM and 0.5 mM respectively.

4.1.6 Detection of dopamine in whole blood sample

The sensitivity and selectivity of the probe towards DA in a whole blood sample was also investigated (**Fig. 4.1.6)**. Before the addition of any AuNPs the blood sample was red in colour (**Fig. 4.1.6A, a**). When the AuNPs were added to the solutions, a colour change from red to green was observed; the green colour intensified after spiking the solutions with DA (**Fig. 4.1.6A, b–d**). The change of colour before spiking in **Fig. 4.1.6A, b**; was likely due to the presence of DA in blood. In **Fig. 4.1.6B**, (**a**) is the absorption spectra of the blood sample before the AuNPs were added. Apart from the main intense band at 406 nm, several small absorption bands (~280, 500, 538, 574 and 633 nm) were observed, which all disappeared in the presence of the AuNPs (**Fig. 4.1.6B, b–c**). The insert in **Fig. 4.1.6B** clearly shows the disappearance of the minor bands from the whole blood sample, which means that the probe was not sensitive to other interferences present in the whole blood. The additional peaks that were formed in the presence of the AuNPs around 308 and 389 nm, shown in the spectra of

Fig. 4.1.6b (whole blood + AuNPs), **Fig. 4.1.6**c (whole blood + AuNPs + 5 µM DA) and **Fig. 4.1.6**d (whole blood + AuNPs + 50 µM DA) corresponded to those that were observed for DA in the absence of whole blood. Another band was formed around 540 nm (**Fig. 4.1.6B, d**), which further confirmed the detection of DA (the increase of DA in the solution as before). The probe showed good selectivity and sensitivity for DA in a very complex matrix (whole blood), without any additional sample preparation.

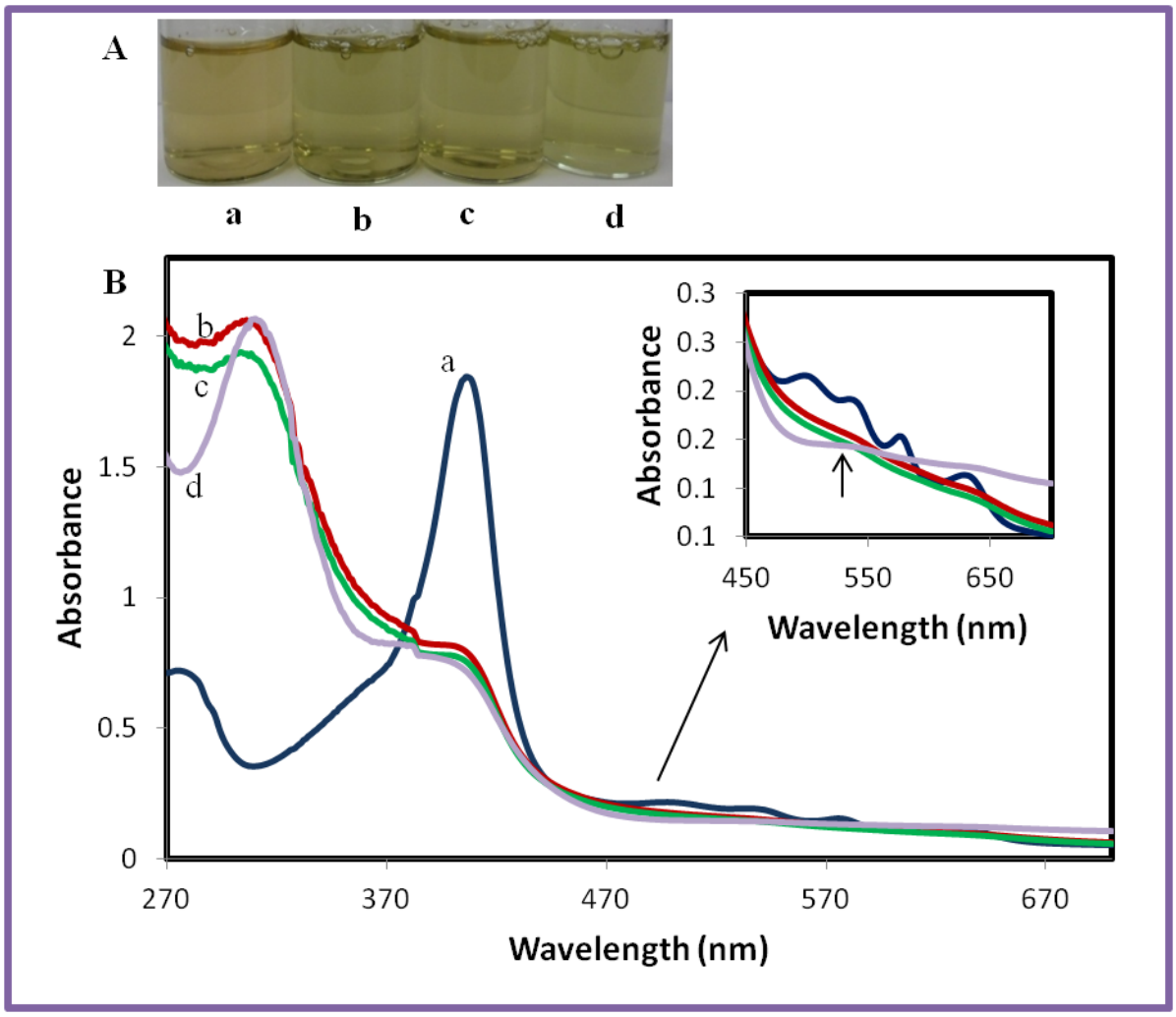

Figure 4.1.6: Detection of dopamine in whole blood. In (A), a- whole blood, b- whole blood + AuNPs, c- whole blood + AuNPs + 5 µM DA and d- whole blood + AuNPs + 50 µM DA. (B) depicts the absorption spectra that correspond to the solutions in (A).

In summary, a novel colorimetric probe for detecting DA in aqueous samples by utilizing UF–AuNPs was successfully developed. By taking advantage of good reducing properties, DA induced growth of UF–AuNPs and the subsequent change in the morphology of the nanoparticles resulted in a clear and observable colour change from pale green to orange then

brown. Spectral shifts were observed to accompany the colour changes signalling the formation of large particles or aggregates. Under non–optimized conditions, colour change was observed from 0.5 µM. In the mixture of DA and AA, the probe could detect DA, even when the concentrations of AA were up to 200 times higher than those of DA. At very high concentrations of AA (more than 200 times greater than DA), a deep purple colour was observed with absorption maxima around 605 nm, showing the interference of AA. Under optimized pH conditions, colour changes were observed already from 5 nM DA and the detection limit was improved to 2.5 nM from the previous 500 nM. The probe could selectively detect DA in whole blood sample without any sample preparation other than dilution. The practical simplicity of the probe proved that it would be very useful in the development of new AuNP-based probes as it is safe and reproducible (no toxic functionalization is required) and rapid, resulting in colour changes at room temperature within 2 minutes. The developed probe also gave some insight into the synthesis of various shaped AuNPs during the detection of DA, and this information is now being used to further develop sensitive probes with both free and immobilised nanoparticles in our lab.

Although the colloidal UF–AuNPs colorimetric probe showed good response towards the analyte of interest, there is still a challenge with liquid state probes. One striking challenge is the issue of portability and transportation. Hence, solid state probes that will address these challenges are in demand. In this thesis, solid state colorimetric probes in the form of a nanofibre were fabricated.

4.2 Solid state colorimetric probe

Nylon 6 (N6) was selected as the polymer matrix because it is biocompatible, biodegradable, low cost, has superior fibre forming ability, good mechanical strength, and strong chemical and thermal stabilities [234-236]. The mechanical strength of nylon makes it easy for the fibres to be cut into strips that would be used for the detection of the target analyte. Moreover, synthetic nylon membranes have a porous structure and are composed of microfrills that are interconnected forming a three–dimensional network [237]. Because of these remarkable morphological features, nylon fibres are ideal candidates to be used as supporting materials for metal nanoparticles, ligands or molecules that are used to provide selectivity when the fibres are employed as a sensor material.

Since in liquid state colour change was observed for AA, the solid state probe had been designed such that there will be no response from the interfering substances. In order to achieve such a goal, the suitability of MIPs for the selective detection of DA was investigated and the results are discussed in section **4.2.1.**

4.2.1 Evaluation of the MIP + UF–AuNPs + N6 nanofibre composite as a selective colorimetric probe for detecting DA

4.2.1.1 FTIR characterization of MIPs

The successful synthesis of the DA–MIP was confirmed with the aid of FTIR spectroscopy (**Fig.4.2.1.1**). The OH stretching band at 3402 cm^{-1}, the C=C band at 1630 cm^{-1} and the C–H bending band at 746 cm^{-1} all indicated to the presence of DA in the unwashed MIP, which diminished significantly from the spectra of the washed MIPs. These characteristic bands do not appear in the spectrum of the NIP since it does not contain DA.

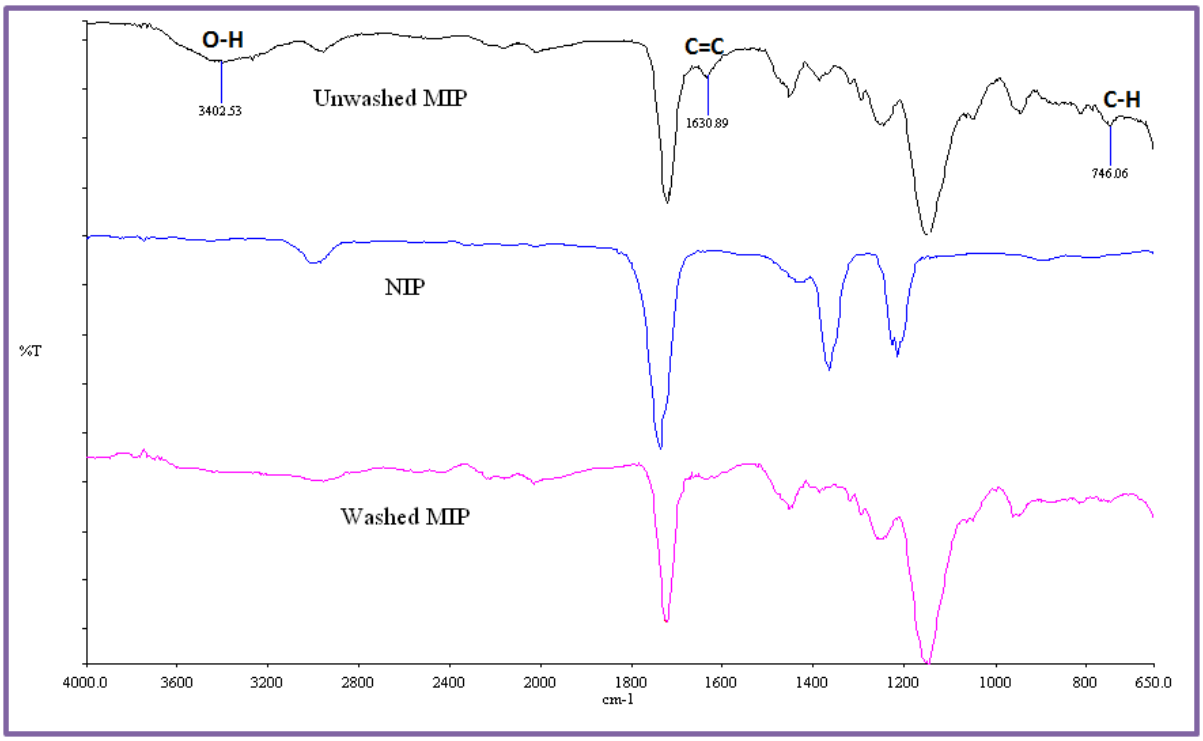

Figure 4.2.1.1: FTIR spectra of the unwashed MIP, NIP and washed MIP.

4.2.1.2 HRSEM characterization of the MIP particles

The morphology of the imprinted polymers determined by SEM displayed irregular shaped particles (**Fig. 4.2.1.2**), typical of these polymers [238].

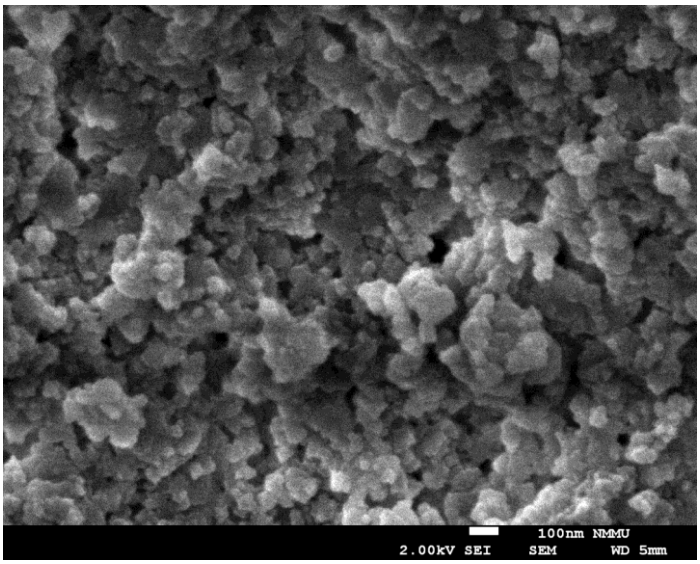

Figure 4.2.1.2: HRSEM image of the DA−MIP

4.2.1.3 TEM and UV/vis spectroscopy characterization of the polymer solution before electrospinning

The TEM image (**Fig. 4.2.1.3A**) showed that most of the AuNPs were mono-dispersed while only a few were aggregated. The TEM analysis was in agreement with the UV spectrum (**Fig. 4.2.1.3B**) with absorbance intensities at 530 and 640 nm, which are typical of dispersed and aggregated AuNPs, respectively.

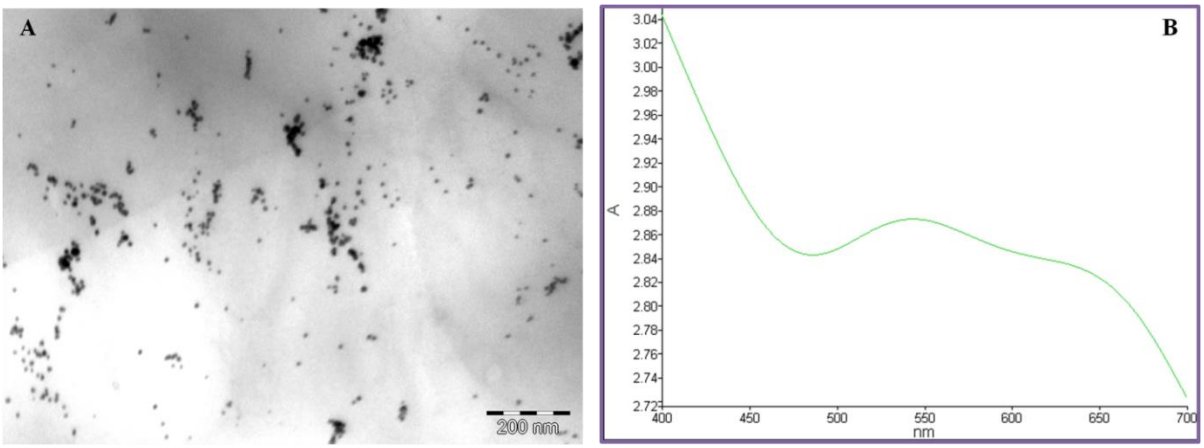

Figure 4.2.1.3: (A) TEM image and UV/vis spectrum (B) of the MIP + UF–AuNPs + N6 solution.

The UF–AuNPs were synthesized following the *in situ* reduction method, where gold salt was reduced with $NaBH_4$. Thereafter, electrospinning resulted in encapsulation of the UF–AuNPs and MIP particles within electrospun N6 nanofibres.

4.2.1.4 Colorimetric evaluation of the MIP + UF–AuNPs + N6 nanofibre

For the preliminary studies, ascorbic acid (AA) and uric acid (UA) were chosen as the interfering species since they are known to coexist with DA in real samples and are normally present at higher concentrations than DA [1].

In the presence of DA, a colour change from purple to navy blue/black was observed with or without the MIPs whilst they remained unchanged in both AA and UA solutions (**Fig. 4.2.1.4**). The fibres labelled "control" are the original fibre mats in water (without any of the analytes).

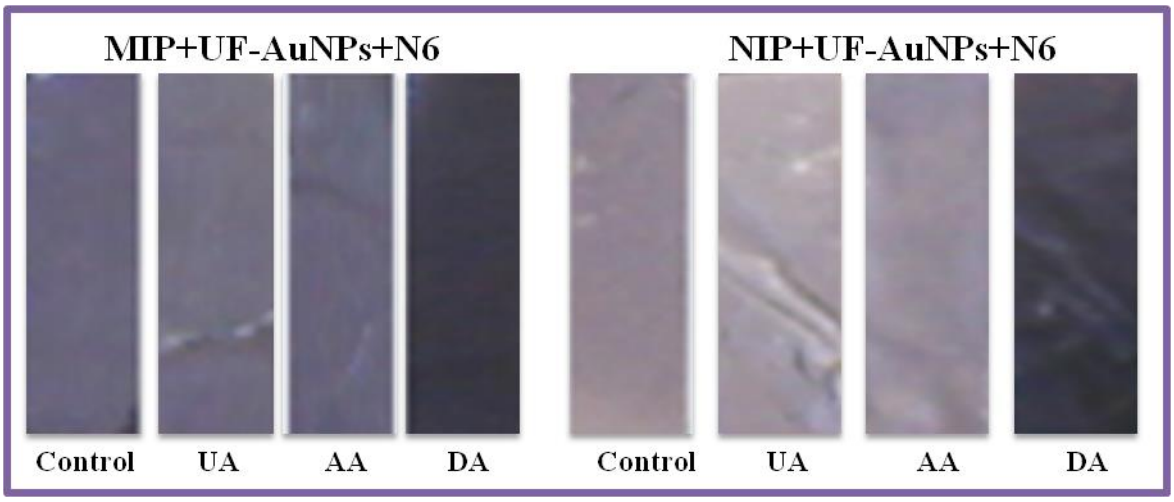

Figure 4.2.1.4: Colorimetric response of the MIPs/NIPs +UF–AuNPs + N6nanofibres.

4.2.1.5 HRSEM characterization of the fibres

The morphological changes of the nanofibres caused by introducing DA were evaluated using HRSEM. SEM images of the nanofibres with NIP and MIP particles before and after DA are shown in **Fig. 4.2.1.5**. Significant differences were observed on the nanofibres. The NIP + UF–AuNPs + N6 nanofibres (**Fig. 4.2.1.5A**) were smooth and very few nanoparticles were visibly embedded in the nanofibres. In the presence of DA (NIP + UF–AuNPs + N6 + DA) many more particles were observed on the surface of the nanofibres (**Fig. 4.2.1.5B**). Compared to the NIP fibres, the MIP fibres showed an even greater number of nanoparticles on the surface. Some particles were present even before addition of DA (**Fig. 4.2.1.5C**). This may be due to the DA molecules that remain after incomplete removal of template DA during the washing of the MIP. The excess DA molecules interact with the UF–AuNPs in the polymer solution and result in the formation of aggregates that are too large to be embedded within the nanofibre material. The presence of DA on the imprinted polymers could be the reason why the MIP + UF–AuNPs + N6 fibres in **Fig. 4.2.1.4** were purple even before they were dipped in DA. An increase in the number of particles and size of aggregates on the nanofibres was observed in the presence of DA (**Fig. 4.2.1.5D**).

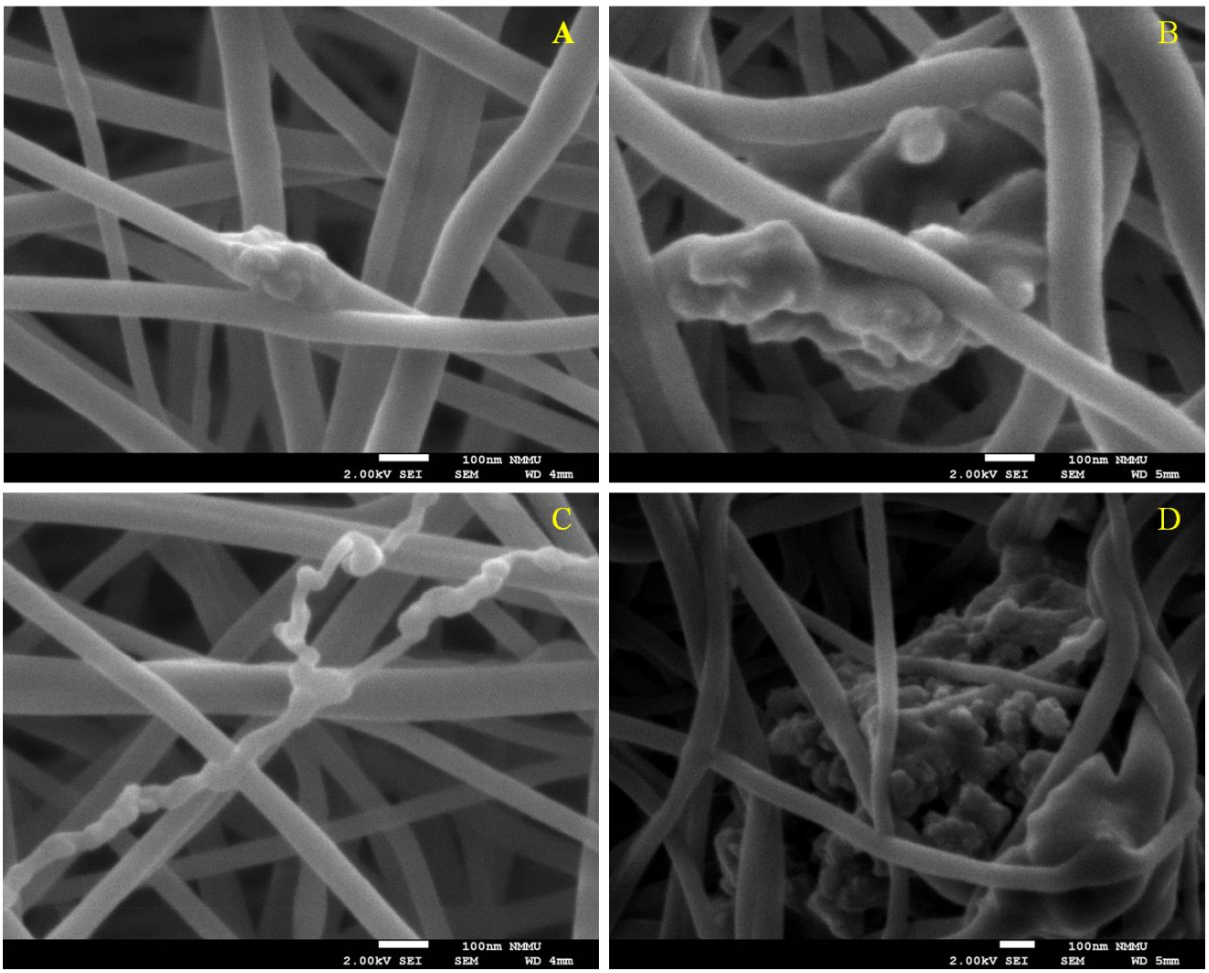

Figure 4.2.1.5: HRSEM of A- NIPs+UF-AuNPs+N6, B- NIPs+UF-AuNPs+N6+DA, C- MIPs+UF-AuNPs+N6 and D- MIPs+UF-AuNPs+ N6 +DA.

4.2.1.6: Energy–dispersive spectroscopy (EDS) analysis

Energy-dispersive spectroscopy (EDS) analysis of the fibres was conducted to profile the elemental composition of the particle aggregates that were observed on the surface of the HRSEM. All the EDS spectra confirmed the presence of AuNPs (**Fig. 4.2.1.6**). The inserts in **Fig. 4.2.1.6A – D** are the EDS quantitative analysis. Along with the Au peak, Na and Cl peaks were observed on the spectra of the NIPs + UF–AuNPs + N6 fibres (**Fig. 4.2.1.6A**). The source of the Na may be the $NaBH_4$ that was used to reduce the $AuCl_4^-$ in the polymer solution. The Cl could be from the $AuCl_4^-$ or $AuCl_2^-$ that could have remained after reducing with the $NaBH_4$. The decrease in the Cl atoms and the increase of the Au atoms from 51.02 – 27.07% and 7.96 – 66.88% respectively observed in **Fig. 4.2.1.6B** indicates that $AuCl_4^-$or $AuCl_2^-$are almost completely reduced possibly caused by the presence of the analyte. The

same thread was observed for the MIP fibres (**Fig. 4.2.1.6C and D**), where Cl decreased from 52.49 – 12.57% and Au increased from 11.09 – 82.10%.

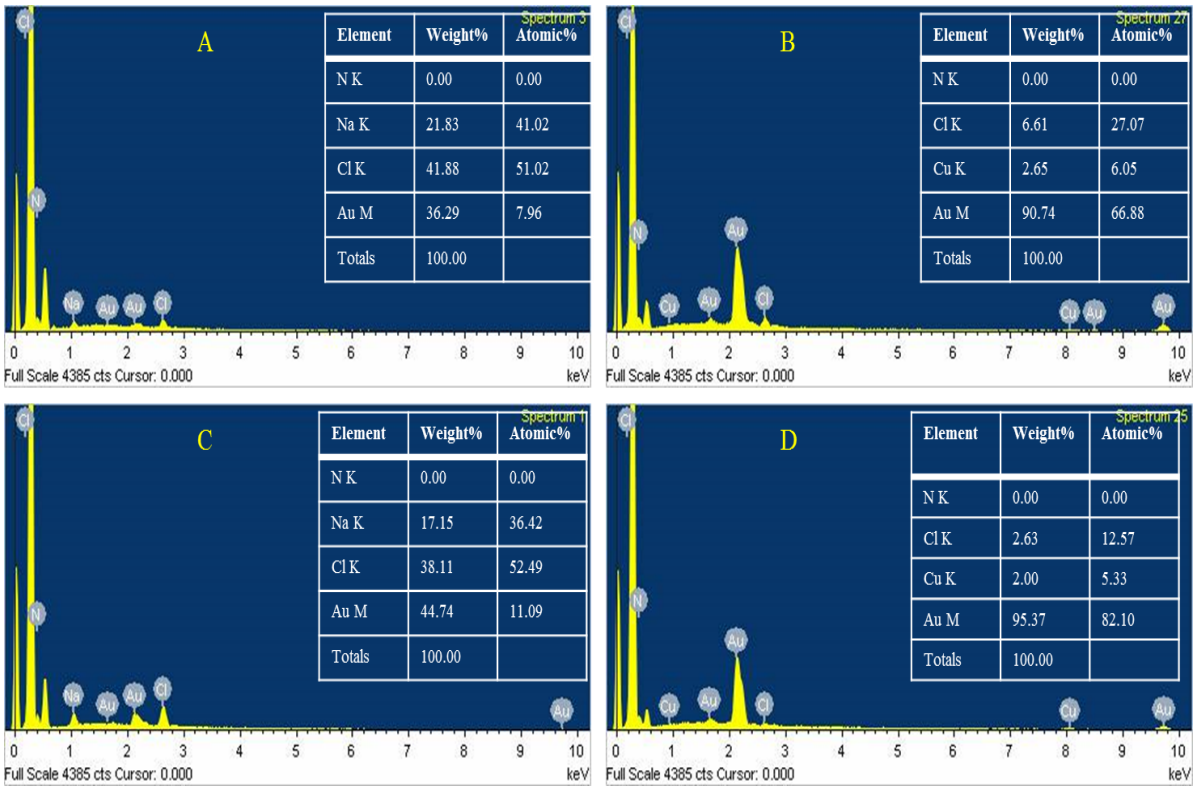

Figure 4.2.1.5: EDS images of A- N6+ UF–AuNPs + NIPs, B- N6+ UF–AuNPs + NIPs + DA, C- N6 + AuNPs + MIPs and D- N6 + UF–AuNPs + MIPs + DA

Briefly, the purpose of this part of the study has been to investigate if a composite of electrospun MIPs and AuNPs could be applied for colorimetric detection of DA. As seen in the previous chapters, there are many reports on combination of AuNPs and electrospun nanofibres, AuNPs and MIPs for colorimetric detection and other applications. However, to the best of our knowledge there are no reports that exploited the outstanding properties of MIPs, AuNPs and electrospun nanofibres combined for the colorimetric detection of DA. The composite material prepared displayed good selectivity towards DA giving a colour change from purple to navy blue/black and it was not responsive to interfering compounds (AA and UA). This research forms a foundation to study composites of the three materials for fabrication of colorimetric probes for various analytes and for other applications.

However, the fact that the NIP fibres were also responsive towards DA meant that the MIPs are not very significant in this case even though their presence within the fibres resulted in

more particles coming to the surface of the nanofibres. Ideally, NIPs are not supposed to be responsive towards DA since they do not possess the required DA imprint for recognition.

Since including the MIPs within the N6 fibre proved to be insignificant, a probe based on UF−AuNPs + N6 composite was developed. In order to investigate the significance of using UF−AuNPs, we investigated the effects of using stabilized AuNPs and the results are shown in section **4.2.2**.

4.2.2 AuNPs + N6 composite based colorimetric probe

The UF−AuNPs + N6 composite polymer solution was prepared following the procedure in section **3.3.3**. The polymer solution was first characterized by UV/vis spectroscopy and was evaluated as a liquid state colorimetric probe before electrospinning. Three other polymer solutions (TSC–AuNPs + N6, 3–MCA–AuNPs + N6, and MSA–AuNPs + N6) were prepared in order to investigate the merits of using UF-AuNPs as a probe. The original polymer solutions were then electrospun under the conditions explained in section **3.3.2.3** and then evaluated as solid state colorimetric probes.

4.2.2.1 UF−AuNPs + N6 composite

The UF–AuNPs + N6 solution was purple in colour and exhibited a broad peak around 550 nm. Upon addition of the polymer solution to AA and DA, two peaks were observed around 520 and 660 nm (**Fig. 4.2.2.1.1A, a and b**) which is typical of dispersed [239] and aggregated [240] AuNPs respectively. When AuNPs destabilizes, the original excitation peak decreases in intensity due to the decreasing of stable NPs, and often a secondary peak will form at higher wavelengths due to the formation of aggregates. That is, addition of AA or DA in the polymer solution induced aggregation of the UF–AuNPs and resulted in colour change from purple to blue (AA) and dark blue (DA) (**Fig. 4.2.2.1.1B**) and the formation of the new peak at 660 nm. No noticeable change in absorbance was observed upon addition of the polymer solution to UA (**Fig. 4.2.2.1.1A, c**) and the colour of the solution obtained was similar to that of the control (**Fig. 4.2.2.1.1B**).

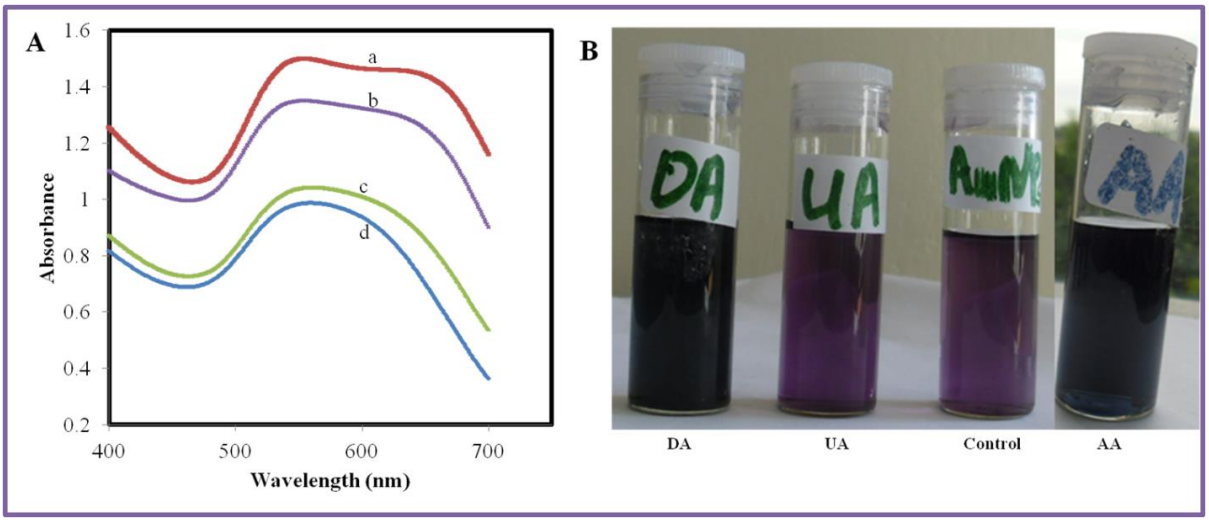

Figure 4.2.2.1.1: (A) Absorbance spectra of the UF−AuNPs + N6 solution in (a) DA, (b) AA, (c) UA and (d) the polymer solution (control). (B) Photograph showing the colour changes of the solutions in the three analyes.

The fibre mat that was obtained from electrospinning the UF−AuNPs + N6 composite was purple in colour (**Fig. 4.2.2.1.2**). Although AA seemed to have a potential to interfere with DA detection in the polymer solution (as it gave a colour that could not be easily be distinguished from that of DA), the nanofibres showed selectivity towards DA. The colour of the nanofibre in the presence of DA was navy blue to black and remained unchanged in both AA and UA.

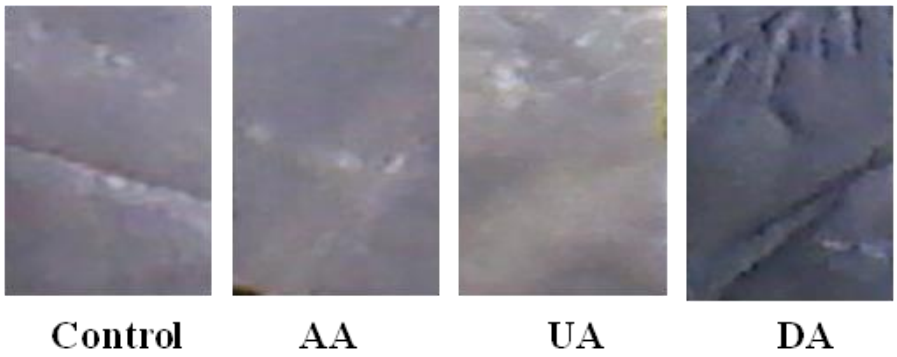

Figure 4.2.2.1.2: UF−AuNPs + N6 fibres in AA, UA and DA.

4.2.2.2 TSC–AuNPs + N6 composite

A purple polymer solution became light blue in AA and dark blue in the DA whilst in the presence of UA it remained unchanged (**Fig. 4.2.2.2.1A**). There was no significant difference in the spectra of the control (TSC–AuNPs + N6), DA and UA solutions (**Fig. 4.2.2.2.1B, a,c,d**). The absorption maxima of all the solutions were at 540 nm with the spectrum of the AA solution broader compared to that of UA and DA.

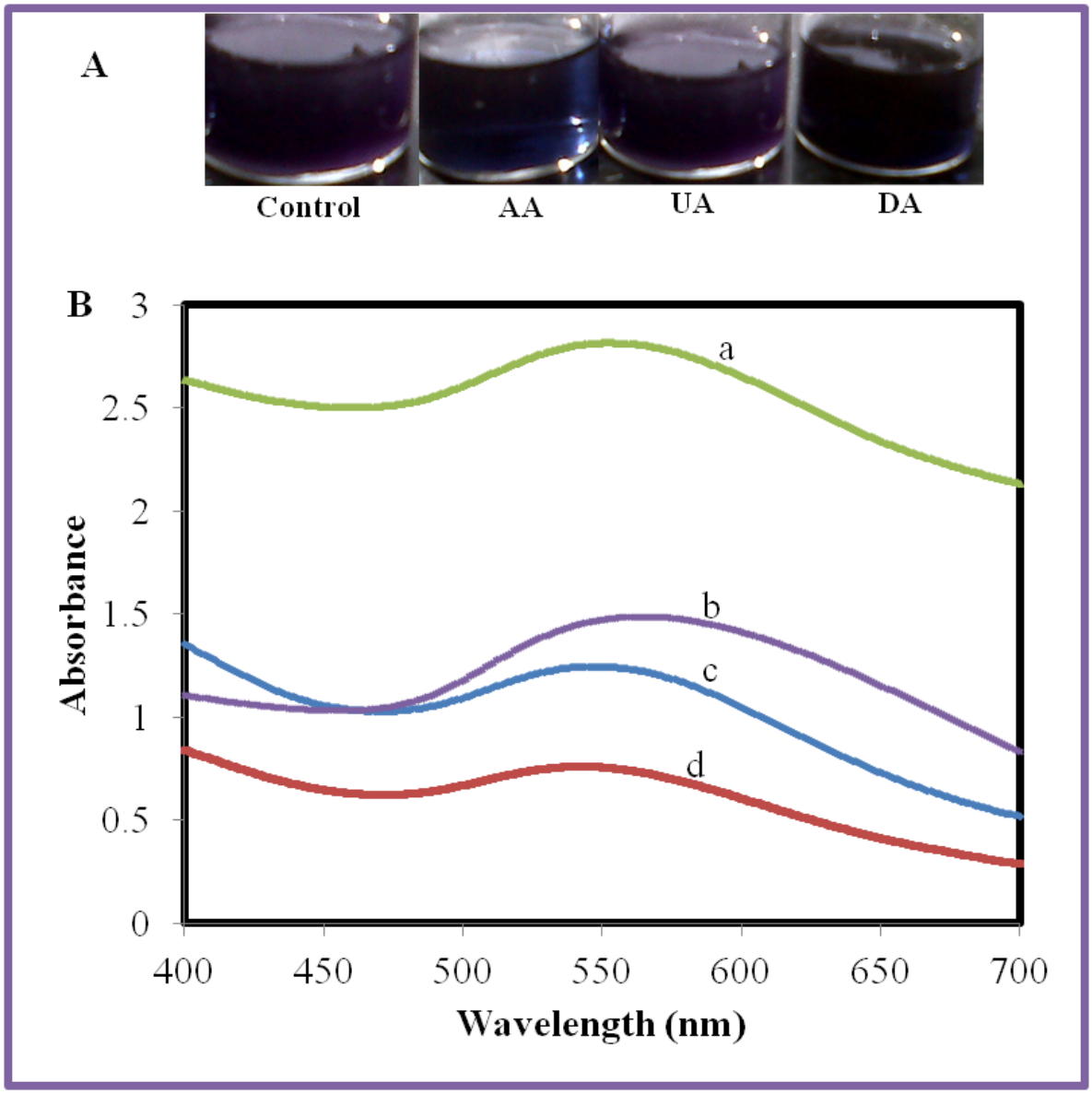

Figure 4.2.2.2.1: (A) photograph showing the response of the TSC–AuNPs + N6 in the analytes. (B) Absorbance spectra of the NPs in (a) UA, (b) AA, (c) control and (d) DA.

A purple coloured fibre mat was obtained from the TSC–AuNPs + N6 composite (**Fig. 4.2.2.2.2**). The fibres remained unchanged in UA. In AA the nanofibres became reddish and the one in DA became blue. However, the colour changes observed in the presence of both AA and DA were too faint that one may need to have a very good eye sight to perceive the change. Moreover, in the presence of DA leaching was observed as the solution also changed colour instead of the fibre only.

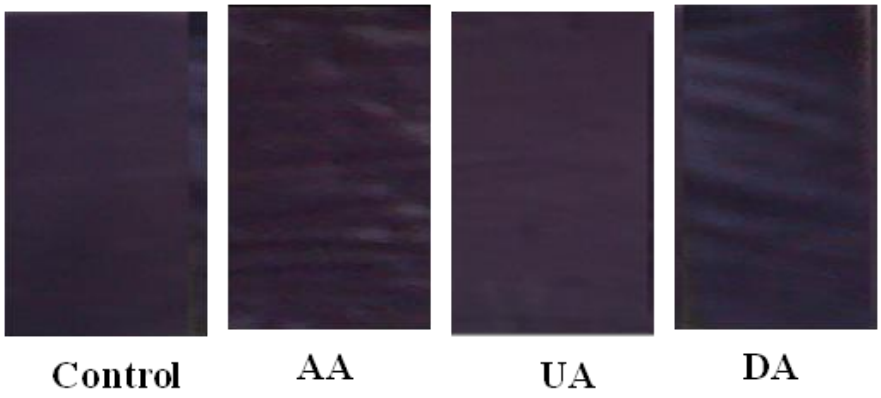

Figure 4.2.2.2.2: TSC–AuNPs + N6 fibres in AA, UA and DA.

4.2.2.3 (3–MCA–AuNPs + N6) composite

The white polymer solution (not shown) and the nanofibre mat obtained from the 3–MCA–AuNPs + N6 composite remained unchanged in all the analytes (**Fig. 4.2.2.3**).

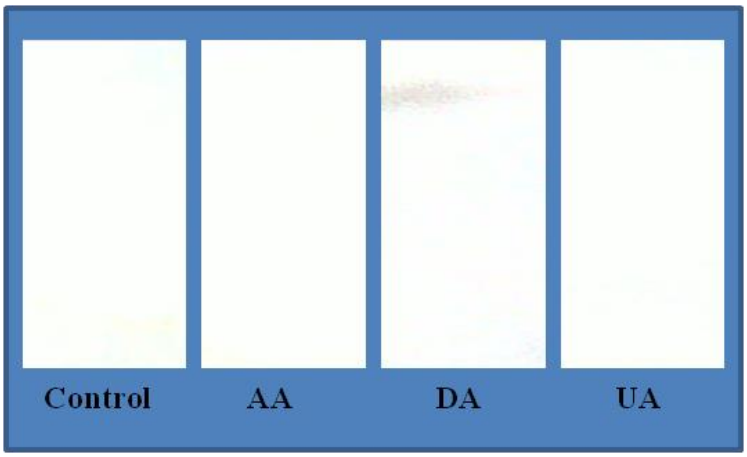

Figure 4.2.2.3: 3–MCA–AuNPs + N6 composite nanofibres

4.2.2.4 MSA–AuNPs+N6 composite

The brown colour of the MSA–AuNPs + N6 solution did not change when it was introduced into solutions of the three analytes (**Fig. 4.2.2.4B**) nor did the absorption spectra show any significant difference (**Fig. 4.2.2.4A**). All the solutions absorbed at 550 nm. The fibre mat obtained from electrospinning of the composite was brown and the analytes could not induce any colour change (**Fig. 4.2.2.4C**).

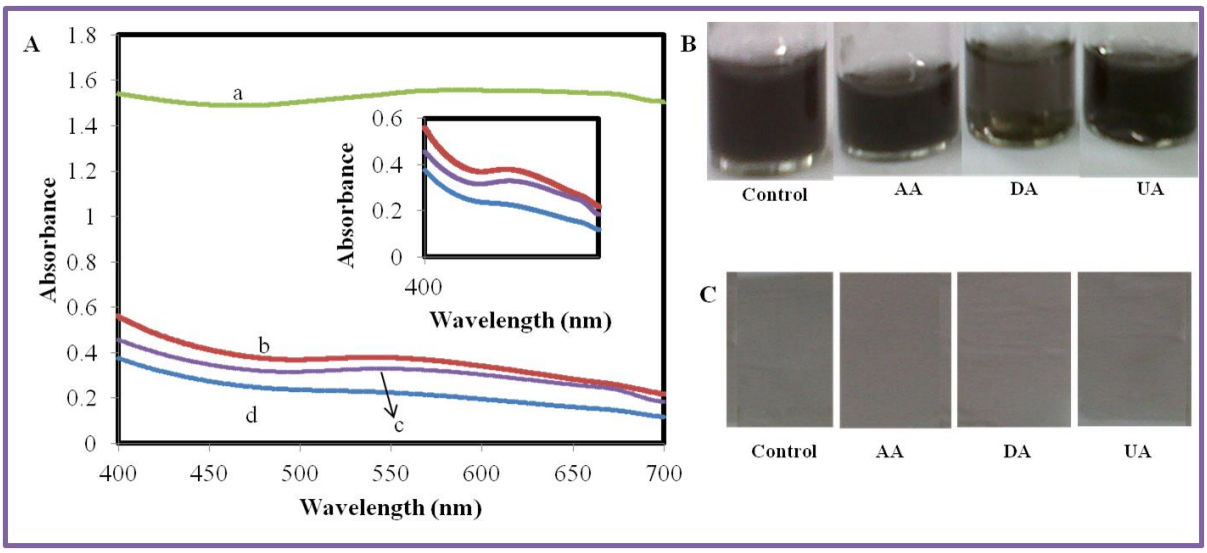

Figure 4.2.2.4: (A) UV/vis spectra of the MSA–AuNPs + N6 composite in (a) UA, (b) DA, (c) AA and (d) control. (B) and (C) shows the liquid and solid state colorimetric response of the composite in the presence of the analytes respectively.

In summary, only the UF–AuNPs + N6 composite showed good response towards DA. In the liquid state studies it was observed that DA could change the colour of the solution from purple to dark blue. However, AA showed similar results with the same colour and spectral changes but different intensities. It was noted however that in solid state (fibre), the developed method was insensitive to both UA and AA since the fibres in the two analytes remained purple but became navy blue to black in DA. No change was observed on the 3–MCA–AuNPs + N6 and MSA–AuNPs + N6 composites both in liquid and in solid state. It was assumed that since the nanoparticles were stabilized, the analyte did not have access to them and hence no change in absorbance and no colorimetric response. This is because the sulphur group forms a strong bond with the AuNPs and unless the analyte has functional groups that can interact with the other groups of the stabilizer thereby changing the environment of the nanoparticles, no effect would be observed. On the other hand, the citrate ion is easily displaceable by any species that has a strong affinity for AuNPs. That is why the TSC–AuNPs + N6 composite were responsive. However, due to the faint colour change by the TSC−AuNPs + N6 nanofibres and the superiority of the UF–AuNPs + N6 nanofibres in the detection of DA successive studies focused on the UF–AuNPs + N6 composite nanofibres. Moreover, the use of stabilizing agents proved to be unnecessary.

4.2.2.5 N6–Au salt nanofibre composite

Since DA can act as a reducing agent, it was important to investigate if it was necessary to add the $NaBH_4$ during the synthesis of a specific probe for DA. A probe that is based on N6 and the gold salt composite was prepared and evaluated for both AA and DA. The composite gold and N6 nanofibres displayed high sensitivity since it could change colour to as low as 5 $x10^{-8}$ M DA (**Fig. 4.2.2.5A**). However, the nanofibres were not selective towards DA because they also showed similar colour changes in the presence of AA (**Fig. 4.2.2.5B**). The white fibre mat became purple and the colour intensified with increasing concentration of the analytes. It was noted however that no matter how high the AA concentrations were, the nanofibres could not become navy blue/black as observed in the presence of DA. This was assumed to be due to the presence of the Au^{3+} ions, that could be reduced to Au^{1+} by the AA to give the purple colour and in more DA all the gold ions got reduced to Au^0. These outcomes proved the necessity of reducing the salt with a small quantity of $NaBH_4$.

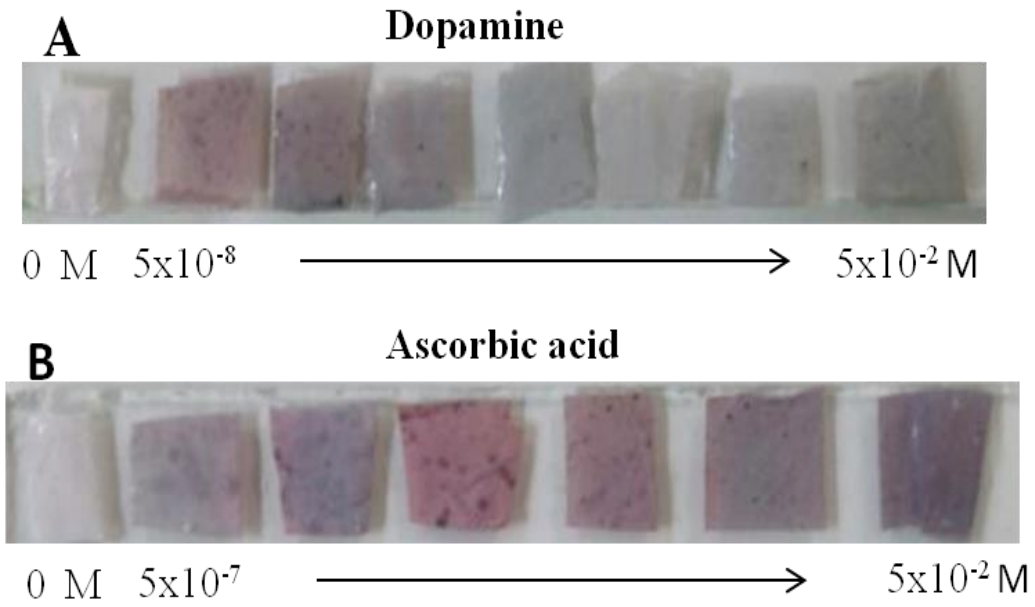

Figure 4.2.2.5: Au salt + N6 nanofibres in various concentrations of AA and DA.

4.3 Colorimetric detection of DA employing the UF–AuNPs + N6 composite nanofibers

The purple fibres were evaluated as probes by introducing strips of the nanofibre mat to various analytes. In aqueous solutions of DA (5 µM) a colour change from the purple to navy blue/black was observed (**Fig. 4.3**). However, when the same fibres were dipped in solutions (50 µM each) of other compounds that are known to interfere with DA detection such as uric acid (UA), ascorbic acid (AA), catechol (CAT), norepinephrine (NORE) and epinephrine (EPI) the nanofibre mats remained almost unchanged. No matter how high the concentrations of AA and UA were made, colour change was not observed. The concentration of the catecholamines in urine and blood samples of healthy subjects is normally lower than those for DA for example, in urine NORE is ~0.088–0.47 µmol/24 h and EPI is ~0.002–0.11 µM/24 h [241]. On the other hand, the concentrations of AA and UA are normally found to be higher than those of DA (1.48–4.43 mmol/24 h for UA [242] and AA is ~100–1000 times the concentration of DA [243]).

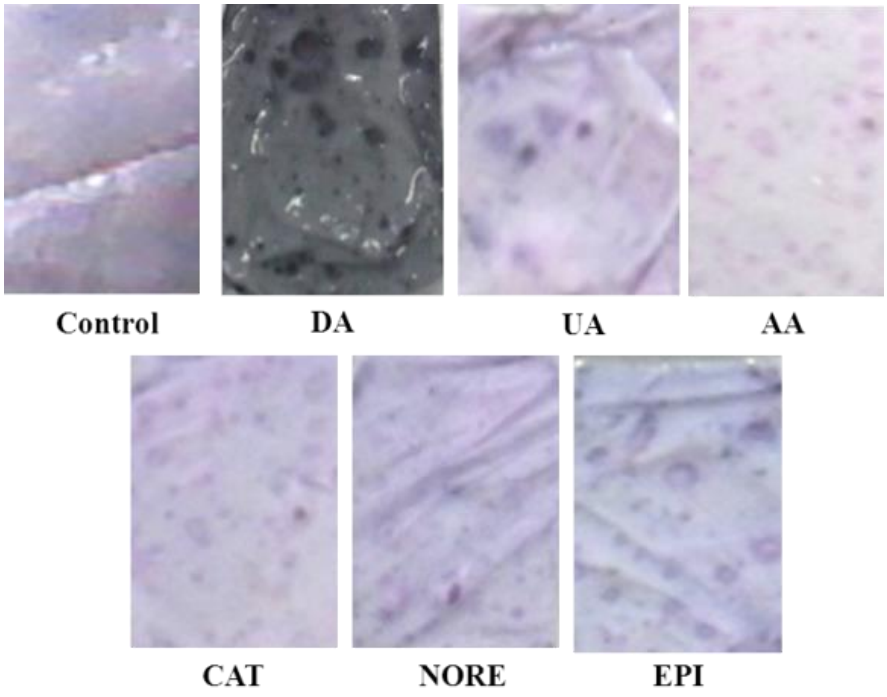

Figure 4.3: The UF−AuNPs + N6 composite nanofibres in DA (5 µM) and other interfering substances (50 µM) at pH 7.4.

4.3.1 High resolution scanning electron microscopy characterization

In order to evaluate the morphological variations of the AuNPs that resulted in the colour change that was observed in the presence of DA, the fibres were subjected to HRSEM analysis (**Fig. 4.3.1**). There was no significant difference between the fibres that were in the other analytes (AA and UA) and that of the control (**Fig 4.3.1 A&B**). The fibres in AA were used as a representative for the interfering substances. However, in the presence of DA, more AuNPs were observed on the surface of the nanofibres (**Fig. 4.3.1 C&D**).

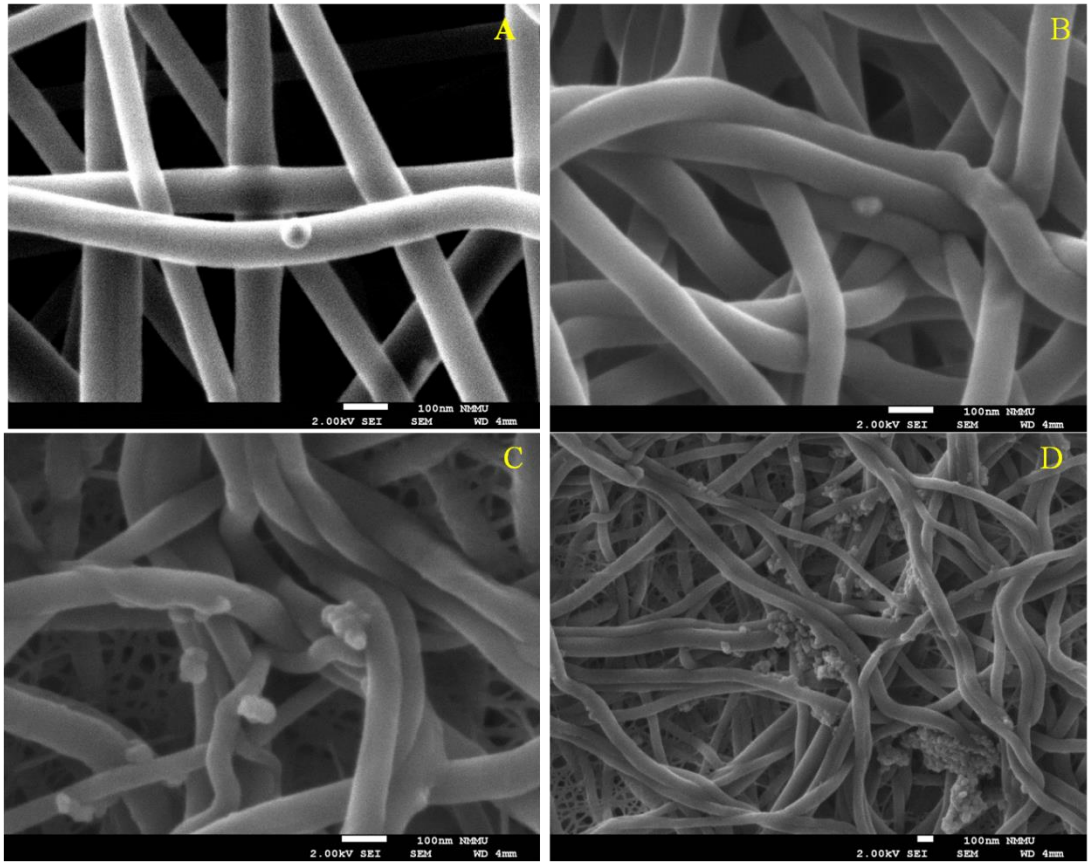

Figure 4.3.1: HRSEM image of (A) the UF–AuNPs + N6 composite nanofibre, (B) the fibres in AA and (C&D) in DA. C and D are the same just different magnifications.

4.3.2 Evaluation of the detection limit of the N6−AuNPs nanofibre composite probe

The fibres were next placed in contact with solutions containing various concentrations of DA to investigate the detection limit for this process (**Fig. 4.3.2**). The colour change was evident already from 5 x 10^{-7} M (the normal content of DA in healthy people is in the range of 1.3–2.6 μM [14]) displaying high sensitivity towards DA. The intensity of the colour increased with increasing concentrations of DA, and the development of the final colour was most rapid in DA concentrations over 5 x 10^{-7} M. The blinds in the laboratory were closed and lights switched of before capturing of the fibre image to exclude interference of light conditions of the ambient environment.

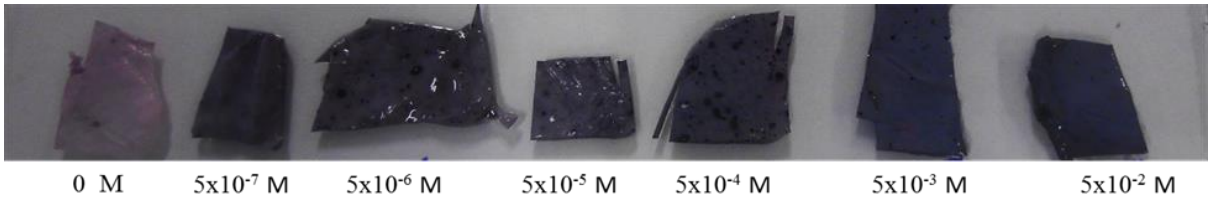

Figure 4.3.2: The UF–AuNPs + N6 composite in various concentrations of DA.

For quantification of DA using the solid state probe (nanofiber mat), open–source software ImageJ was used to assist in the analysis of the fibre colours (**Fig. 4.3.3**). It was observed that the intensity of the colour increased with the increase in concentration of DA in a linear fashion. The use of ImageJ can be a great alternative where the colour changes are not so clear or for visually impaired people.

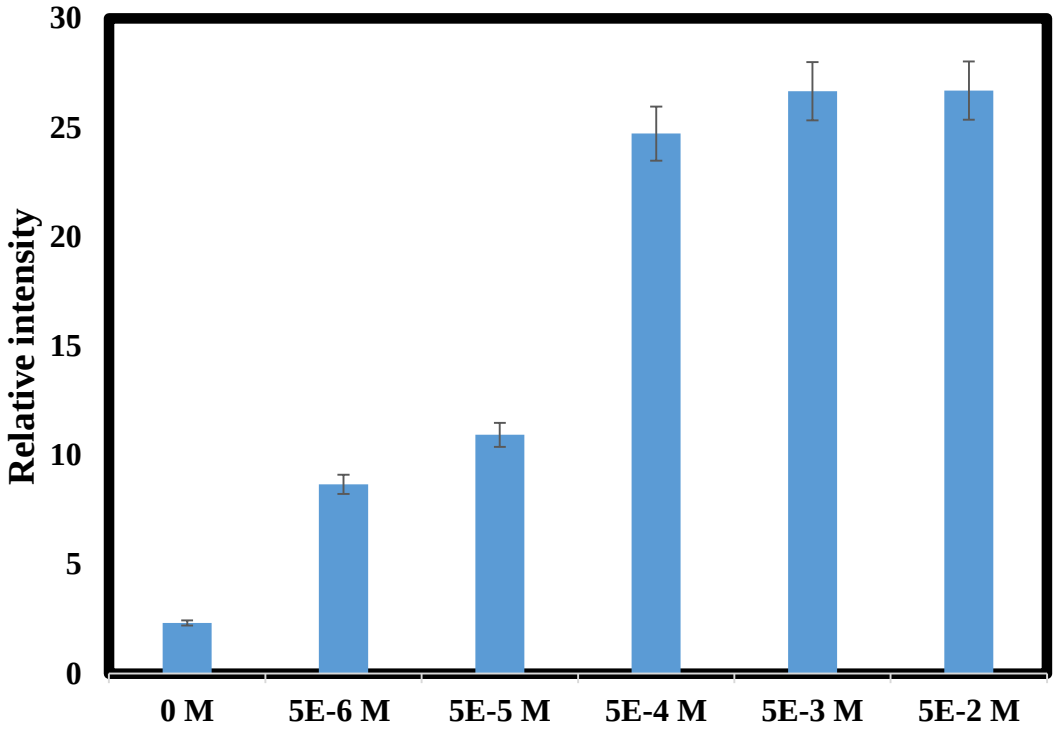

Figure 4.3.3: Bar graph showing the relationship between concentration of DA and relative intensities of the colour of the fibres in the various concentration of DA.

Having achieved the main objective of the research study which was to develop a simple, selective, sensitive and rapid solid state colorimetric probe for DA, it was then necessary to understand the mechanism associated with the probe. Some hypothesis about what could be the possible mechanisms of detection are stated on the next section.

4.4 Discussion of the possible detection mechanism

In this thesis, three mechanisms for the detection of DA by the N6 nanofibres incorporated with the UF−AuNPs are proposed. The first mechanism is based on the reduction of the gold ions that are presumably in the form of Au^{1+} to form Au^0 by the DA. The second mechanism is based on direct interaction between the AuNPs and DA or a combination of both reduction and interaction. The third mechanism is based on the change of the SPR of the gold on interaction with DA.

4.4.1 First proposition:

Assuming incomplete reduction of the gold salt, that is, if we assume that the reducing agent added did not reduce all the Au^{3+} to Au^0 but that the polymer solution consisted of both the Au^0 and Au^{1+} after reduction by $NaBH_4$; this would mean that the nanofibre is comprised of nanoparticles in the form of Au^{1+} (i.e. the surface of the AuNPs has Au^{1+}) and Au^0 that were encapsulated within the nanofibre during electrospinning. Due to the known tendency of the electron–rich oxygen and nitrogen atoms of polar amide groups to interact with positive metal ions, the Au^+ ions would be presumed to be bound to nylon macromolecules via electrostatic (i.e. ion-dipole) interactions [237]. For the ions that were already reduced to Au^0 nanoparticles, the chains of the N6 molecule on the surface of the AuNPs form intermolecular interactions with other chains and with the gold in the solution thereby stabilizing the AuNPs [214]. Upon exposure to the analyte that reduces the remaining Au^{1+} ions to Au^0 nanoparticles the purple nanofibre mat immediately changes colour to navy blue/black. This is consistent with the growth of the AuNPs through the N6 nanofibre. The presence of the gold nanoparticles in the form of Au^{1+} (if this is the case, the counter ion is likely to be Cl^- from the $HAuCl_4$) could explain the lack of response of the probe towards AA. The reason for the insensitivity of the probe towards AA could be due to the fact that AA is a weak reducing agent and could only reduce Au^{3+} to Au^{1+} ions. If the only ions available within the nanofibre are the Au^{1+}, a weak reducing agent can have no effect. Hence, no colour change was observed in the presence of AA.

How to prove if this is the actual mechanism?

Required to prove:

- The presence of Au^{+} ions by conducting Au4f XPS studies.
- Interaction between the gold atom and the N6 using FTIR.

4.4.2 Second proposition:

Suppose that the gold ions (Au^{3+}) were completely reduced to gold atoms. Then the nanoparticles could be stabilized by the nylon molecules that are on the surface of the particles. In addition, nylon is known to have an interconnective porous structure [244].This feature enables easy impregnating of the AuNPs into the nylon nanofibres through the pores. Exposing the probe to DA produces interactions that cause the AuNPs to move to the surface of the nanofibres owing to their high affinity to DA. The small clusters of particles that were embedded in the polymer matrix aggregate into large particles hence the movement to the surface. It is however possible that the Au^{1+} and DA can form complexes that give these colour changes.

How to prove if this is the actual mechanism?

Required to prove:

- Investigate the arrangement of the nanoparticles within the nanofibre to prove dispersion using TEM.
- Investigate any possible interaction between the functional groups of DA and the UF−AuNPs by conducting nitrogen 1s and oxygen 1s XPS analysis of the probe.

Proving the presence of the Au^{1+} ions would not necessarily mean that the second mechanism does not apply. It is possible that both mechanisms are responsible for the generation of the colour change and the movement of the nanoparticles to the surface of the fibres. It would be interesting to find out the reason for the high specificity of the probe towards DA; more especially the reason why norepinephrine (a catecholamine that is much more similar to DA) could not interfere with DA detection.

4.4.3 Third proposition:

A third possibility related to the second could be that the interaction with DA changes the SPR. Since the colour of AuNPs depends on the SPR, it stands to reason that anything on the surface would change the molar extinction at the surface. Perhaps for some reason, the extinction coefficient of the gold or more likely the DA changes, causing a change in the light absorbed and hence the colour. The change in the extinction coefficient might explain the selectivity since every substance has a different molar extinction coefficient. Such phenomena should be concentration dependent which supports our observations.

How to prove if this is the actual mechanism?

Required to prove:

- That the intensity of the colour changes with change in concentration of DA by looking at the quantitation of the colour and intensity using ImageJ.

4.5 Further characterization to determine the mechanism of detection that holds

To understand the mechanism of detection, i.e. to prove or disprove any of the suggested mechanisms further characterization was necessary.

4.5.1 Fourier transforms infrared characterization of the composite fibres

FTIR studies were conducted to investigate any possible interactions between the UF–AuNPs and the functional groups of N6 (**Fig. 4.5.1**). The FTIR spectrum of the N6 + UF–AuNPs (**Fig. 4.5.1a)** showed an increase in percentage transmittance while the intensity of all the peaks remained similar to that of the clean N6 nanofibres (**Fig. 4.5.1b**). The absorption bands at 3299 cm^{-1} for the clean N6 nanofibres shifted to 3301 cm^{-1}, while the band at 1639 cm^{-1} shifted to 1642 cm^{-1} and the band at 690 cm^{-1} shifted to 698 cm^{-1} in the case of the N6 + UF–AuNPs nanofibres. When the N6+UF–AuNPs composite nanofibres were introduced to DA, a decrease in percentage transmittance was observed and the intensity of all the peaks

increased significantly (**Fig. 4.5.1c**). In addition to these changes, the peak at 3301 cm^{-1} of the N6 + UF–AuNPs fibres shifted to 3299 cm^{-1}, whereas the peak at 1642 cm^{-1} moved to 1638 cm^{-1} and the peak at 698 cm^{-1} shifted to 687 cm^{-1}. The shifting of wave numbers from lower to higher numbers has been associated with the presence of interactions between functional groups of polymers and nanoparticles [245-247].

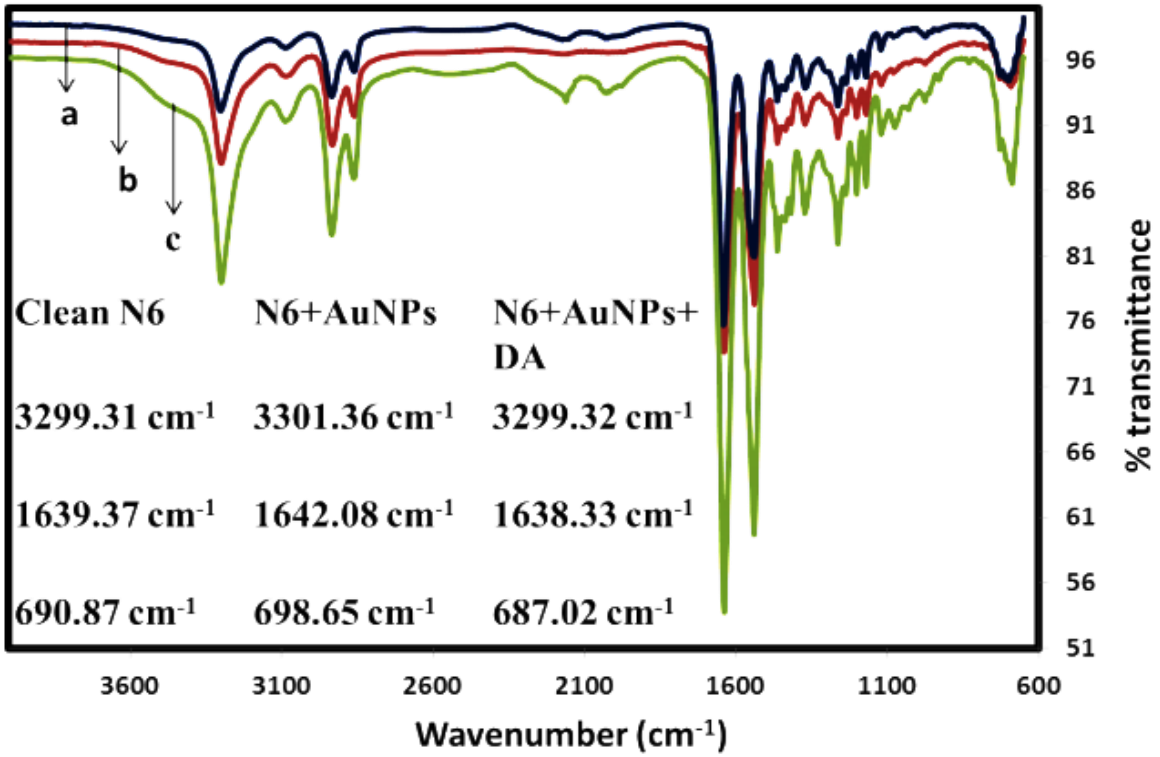

Figure 4.5.1: FTIR spectra of (A) N6 and AuNPs, (B) clean N6 and (C) N6 and AuNPs fibres in DA.

In this case, since the major shifts are observed at 1639 cm^{-1} and 690 cm^{-1} the results implies the existence of molecular interaction between the amide (I) and amide (V) groups of N6 [236] respectively and the AuNPs in the N6 + UF−AuNPs nanofibre composite. These data showed that the AuNPs were stabilized by the functional groups of N6. The shoulder around 3483 cm^{-1} was assigned to the free NH [248]. Since the bond formed by the interaction between the amide (I) and amide (V) of N6 and the AuNPs are not strong, they can be broken easily. Owing to the strong affinity of DA for AuNPs, putting the nanofibres in a solution with DA result in the breaking of those bonds and the AuNPs become free to interact with DA to form aggregates that can no longer be embedded by the nanofibres. Hence, the shifting of bands from higher to lower wave numbers was assumed to be indicative of broken interactions between the AuNPs and the N6.

In order to evaluate the morphological changes before and after DA, transmission electron microscopy analysis was conducted.

4.5.2 Characterization using TEM

The TEM results showed that before introduction of DA, the AuNPs were spherically shaped and well dispersed within the nanofibre matrix (**Fig. 4.5.2.1**). The dispersion further confirmed stabilization of the AuNPs by the functional groups of N6. The average diameter of the AuNPs was estimated to be 8 nm.

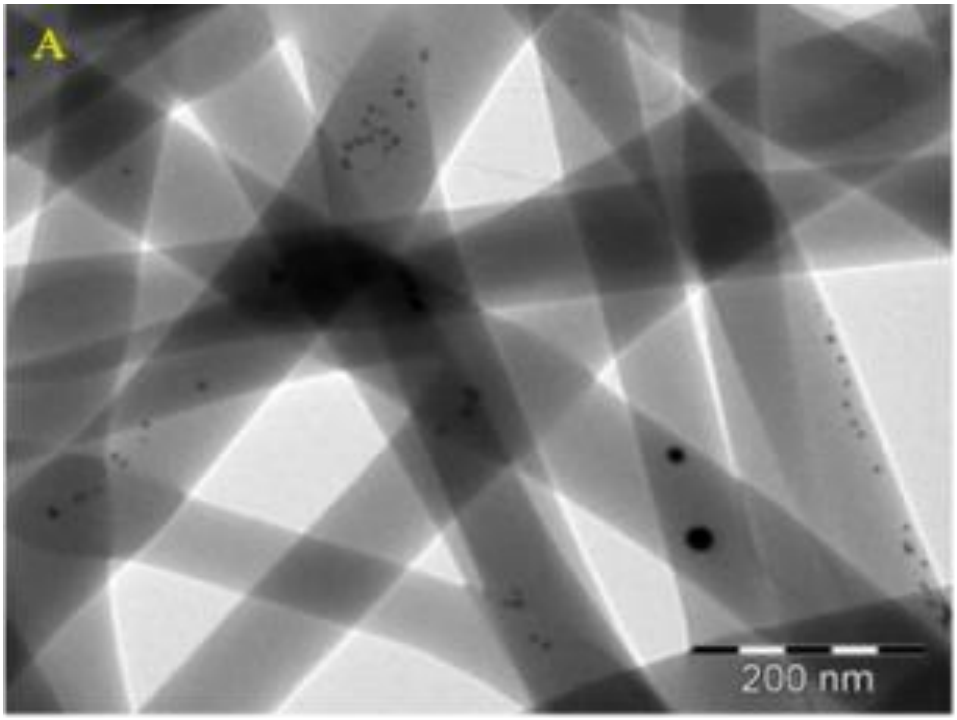

Figure 4.5.2.1: TEM images of the N6 + AuNPs composite nanofibres before DA.

The TEM image of the fibres that have been put to DA confirmed the formation of aggregates (**Fig.4.5.2.2C**) which was also in agreement with the HRSEM results. N6 nanofibres have pores that are interconnected, such a morphology enables DA to penetrate the nanofibre and interact with the embedded AuNPs. The interactions causes change in the shape of the nanoparticles from the spherical to hexagonal and star shapes, growth and formation of aggregates that can no longer be impregnated by the nanofibres hence they diffuse to the surface (**Fig.4.5.2.2A & B**). The change is especially evident from **Fig.4.5.2.2B and D**, which are images of the same nanofibre taken at difference magnifications.

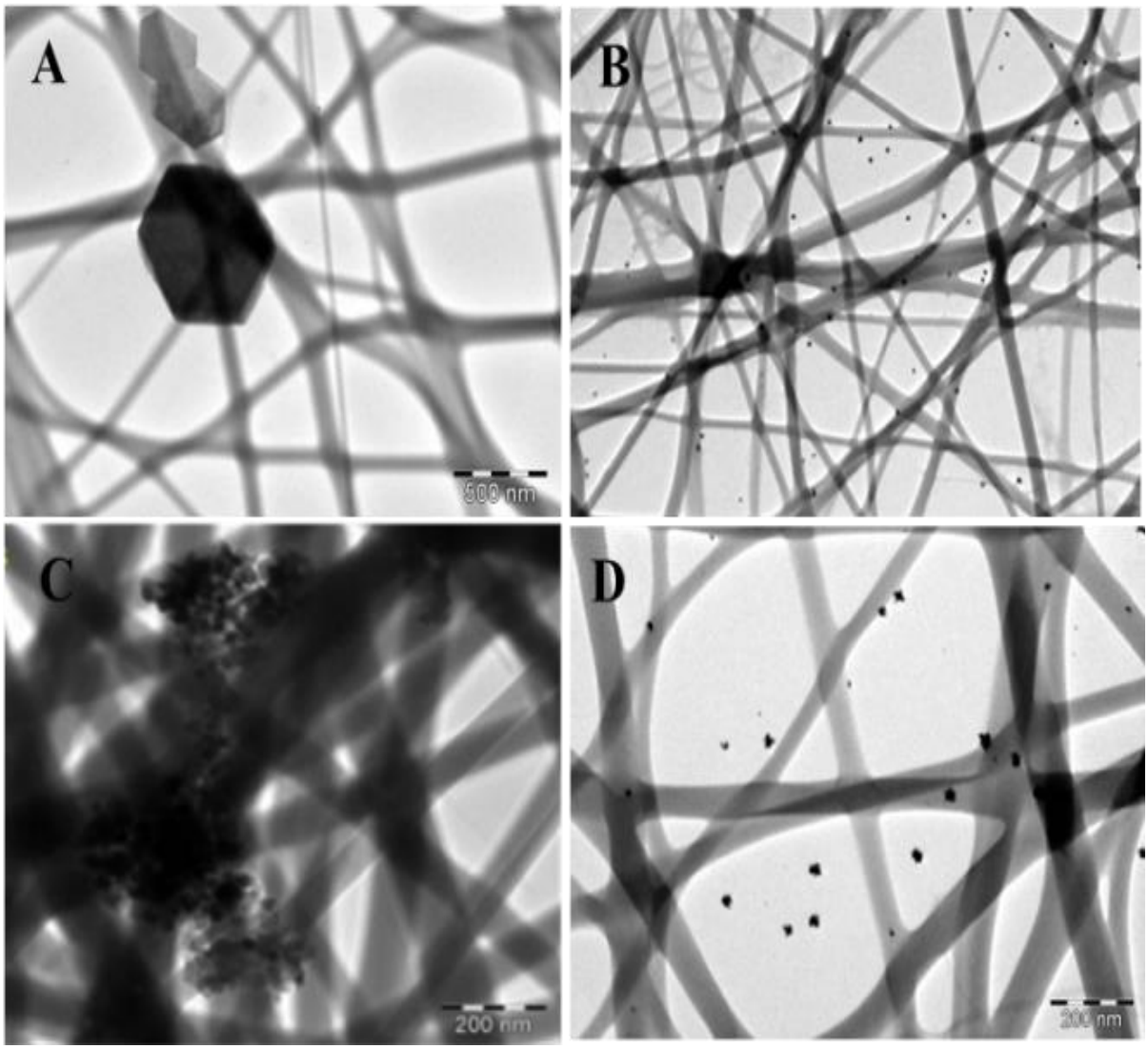

Figure 4.5.2.2: TEM images of the N6+AuNPs composite nanofibres after DA.

4.5.3 X-ray photoelectron spectroscopy (XPS) characterization

The Au4f XPS spectrum of the probe before introduction to DA (**Fig. 4.5.3A**) showed two peaks at 82.7 eV and 86.3 eV. The two peaks shifted slightly to 81.7 eV and 85.4 eV in the presence of DA (**Fig. 4.5.3B**). The latter peak around 86.3 eV has been assigned to Au^{3+} species, while the peak at 82.7 eV has been attributed to Au^{0}. Since there was an excess of gold salt used, a plausible mechanism for the formation of nanoparticles on the surface of the fibres that would be responsible for the colour change is further reduction of gold cations. This is possible since DA is a reducing agent, but unlikely in this case since we would have expected a third peak around 86.3 eV or even a small shoulder after introducing the probe to

DA. The third peak together with a significant change to the peak at 85.4 eV would have meant that in the presence of DA excess Au^{3+} ions was reduced to Au^{0} or Au^{1+}.

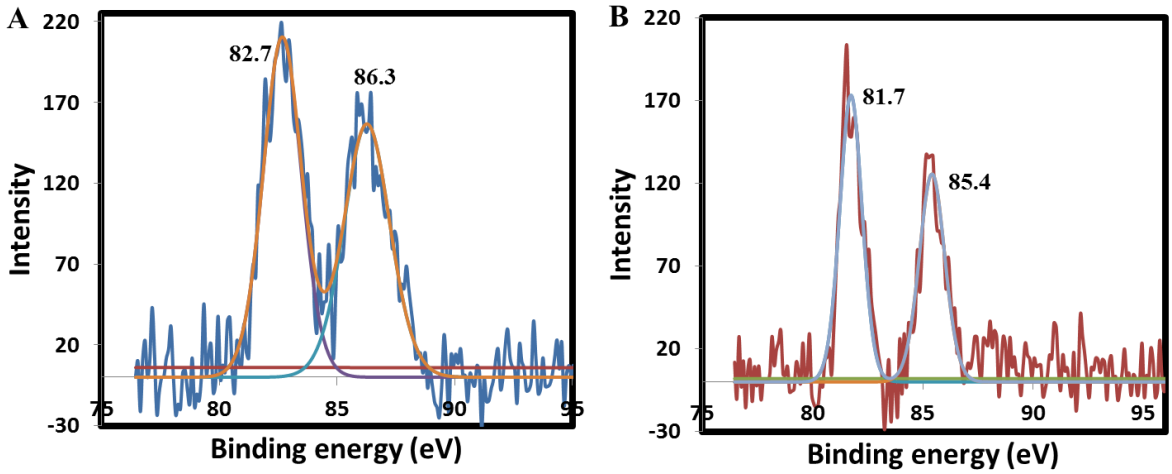

Figure 4.5.3: Au 4f XPS spectra of the UF–AuNPs + N6 composite fibres before (A) and after (B) DA.

These results implied that the mechanism of detection is based on a direct interaction of the UF−AuNPs and DA, resulting in an unexpected aggregation of nanoparticles near the surface of the nanofibers. In this case it should result in a change in the interaction of functional groups with the surface of the nanoparticles, which we sought to investigate by XPS analysis of nitrogen and oxygen.

From the XPS analysis for the binding energy of nitrogen (**Fig. 4.5.4**) it is evident that the relative contributions of all the binding modes that make up the main peak are approximately the same. It is feasible that there is only a very slight decrease of the contribution from the 400 eV peak after exposure to DA. The observation suggests that there was no change in the binding mode with respect to nitrogen. Since the binding energy of different compounds vary and overlap quite a bit, one should expect that any significant variation would be reflected in a large change in the nitrogen binding energy. In our case, this is not seen which fits well with other data and our suggestion that the N6 nanofibre backbone stabilises the nanoparticles.

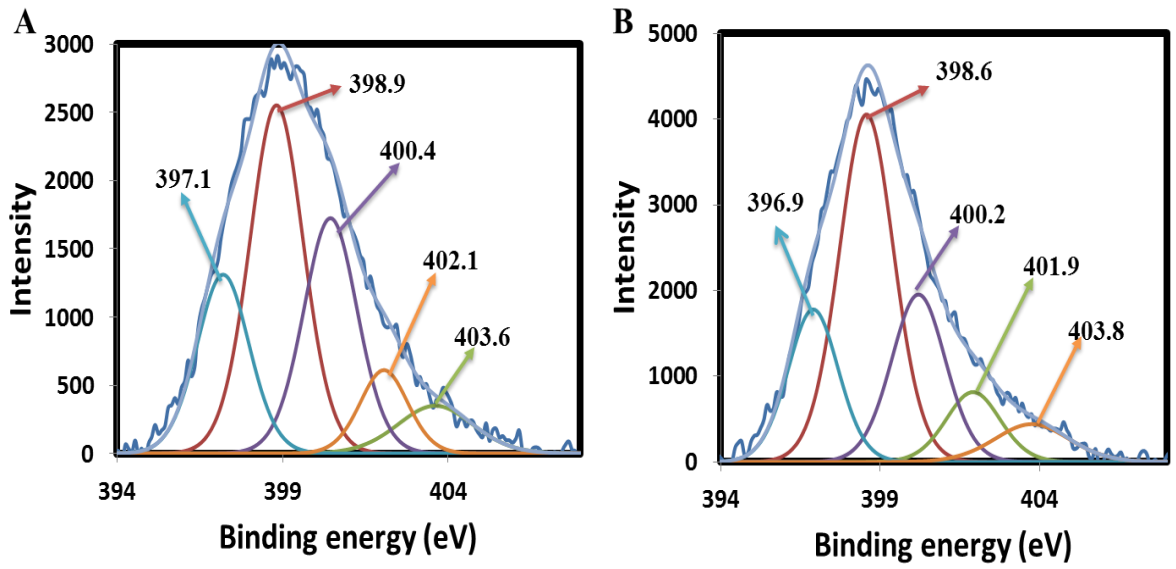

Figure 4.5.4: XPS high resolution N 1s spectra of the UF–AuNPs + N6 composite fibres before (A) and after (B) DA

The oxygen binding energy, on the other hand, showed quite a significant shift to favour the 531.0 eV contribution over the others (**Fig. 4.5.5**). The binding energy at 529.4 eV shifted to 529.0, 532.7 to 533.0, 534.6 to 535.3 and 536.7 to 538.0 eV after DA. This signifies that there is one specific binding mode of oxygen that changes significantly after exposure to DA. According to Beamson and Briggs, the 531.0 eV peak is likely to be that of a carbonyl. Since DA does not have a carbonyl this binding mode could be that of the ortho diphenol moiety (or its easily oxidised dicarbonyl or ortho-quinone form), or could reflect a different binding mode with the polymer backbone.

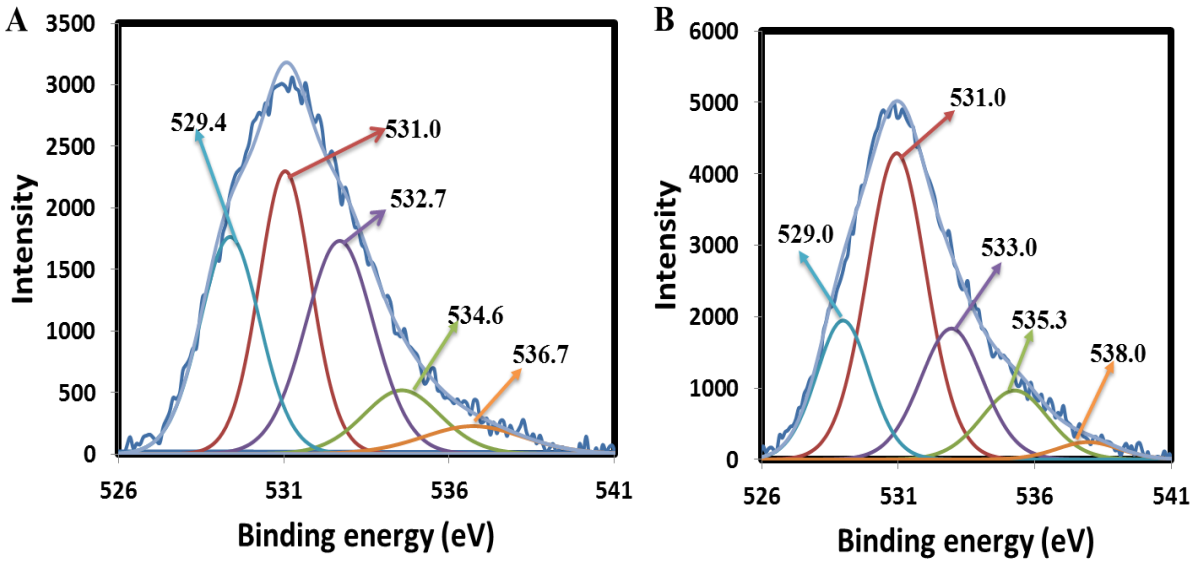

Figure 4.5.5: XPS high resolution O 1s spectra of the UF–AuNPs + N6 composite fibres before (A) and after (B) DA

The interaction of the AuNPs with quinone carbonyl justifies the reasoning that there could be no colour change in the other compounds more especially in epinephrine and norepinephrine. The two catecholamines form unstable protonated species that easily oxidize to form quinone derivatives at acidic pH [249, 250]. Since the solutions were alkaline (pH 7.4), we do not expect epinephrine and norepinephrine to induce any colour change.

After understanding the mechanism of action, we went further and applied the probe in a real sample. The results are shown in the next section.

4.6. Detection of DA in the whole blood sample.

The results in **Fig. 4.6.** showed that the fibres changed colour from purple to black even before spiking with DA. The colour intensified with the addition of DA. The assumption made in solution studies about the presence of DA in the blood sample was also drawn in this case. Of course, this would have to be experimentally proven.

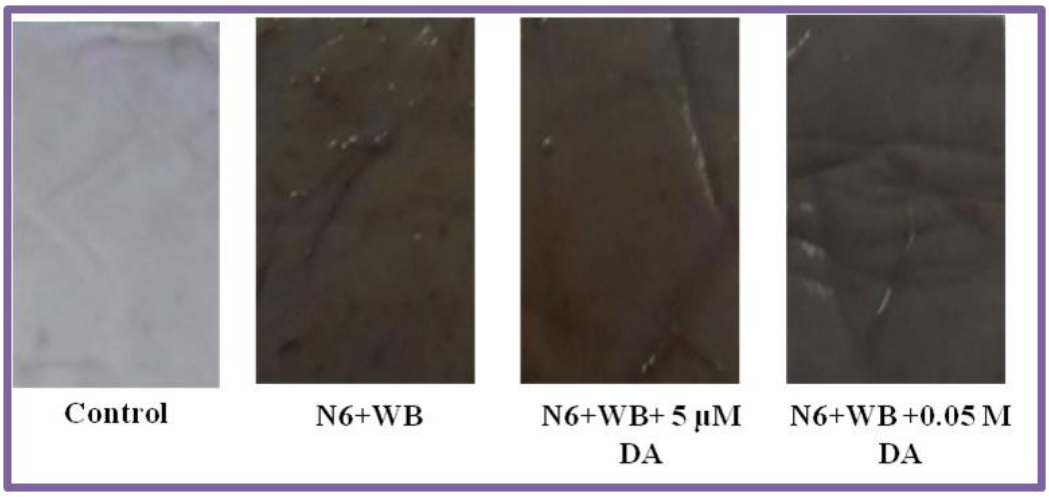

Figure 4.6: Colorimetric response of the UF–AuNPs + N6 composite nanofibre in the whole blood sample

In conclusion, a solid state colorimetric probe based on UF–AuNPs + N6 composite nanofibre was successfully synthesized. The merit of the probe for DA was evaluated by testing it against other catecholamines. Very impressive results were obtained; the probe was insensitive to the other analytes but was only responsive towards DA at pH 7.4. AuNPs were observed on the surface of the fibres and the colour of the fibres was black in DA. The probe was successfully applied in a whole blood sample.

4.7 Preliminary results on prospective work

Detection and determination of biological analytes in the human body is essential since that may help during the diagnosis and treatment of various diseases. Given that most of the currently used methods involve the use of facilities that are only available to the elite, on continuation of the studies done in this thesis our future research will focus on developing cost–effective point of care diagnostic colorimetric probes for various analytes. Amongst other routes, the future work will make use of the methods realized in this thesis such as the use of the UF–AuNPs and also introduction of other compounds to enhance the selectivity and sensitivity of the chosen analyte or group of analytes. Even though the feasibility of the potential probes may first be studied in solution, our main focus will be to fabricate solid state probes. For our initial investigations to form a foundation of the imminent work, we report here in two strategies one using the UF–AuNPs in N6 fibres (section **6.7.1**) and also the use of *β*–cyclodextrin (*β*–CD) (section **6.7.2**) to enhance selectivity of selected analytes.

4.7.1 Detection of analytes based on their strength

Since we already suggested that one of the possible mechanisms of detection by the probes developed in this thesis is the reduction of excess gold ions that remained during the reduction of the gold salt, we now investigate the possibility of detecting analytes based on their reducing strength. In this case, we particularly, expect the fibres that have less quantities of $NaBH_4$compared to the gold salt to be responsive to both the weak and stronger reducing compounds. This is due to the presence of excess gold ions (Au^{3+} form) caused by incomplete reduction of the tetrachloroaurate in the polymer solution. On the other hand, the fibres with similar or slightly higher $NaBH_4$ are expected to be selective to compounds that have a stronger reducing power because the ions that could be remaining are likely to be in the form of Au^{1+}. Weak reducing agents such as AA can only reduce Au^{3+} to Au^{1+} after that only the stronger reducing agents can have an effect/reduce the ions to Au atoms. A particular analyte amongst the stronger reducing compounds can be selectively detected based on pH.

For the preliminary investigations, DA was chosen as a stronger reducing compound while AA was a representative for mild reducing compounds. Other compounds that were analysed are: EPI, NORE, glucose and tyrosine. The results of the experiments explained in sections **3.3.4** and **3.3.4.1.** are shown next.

The colour of the 1:1 (gold salt: $NaBH_4$) polymer solution was a dark shade of purple (insert in **Fig. 4.7.1A**) and exhibited an SPR peak at 543 nm. The fibres obtained from this solution did not change colour in DA nor in AA (**Fig. 4.7.1B I and II).** This observation was assumed to be due to the complete reduction of the gold ions hence the analytes could not have any effect on the nanoparticles.

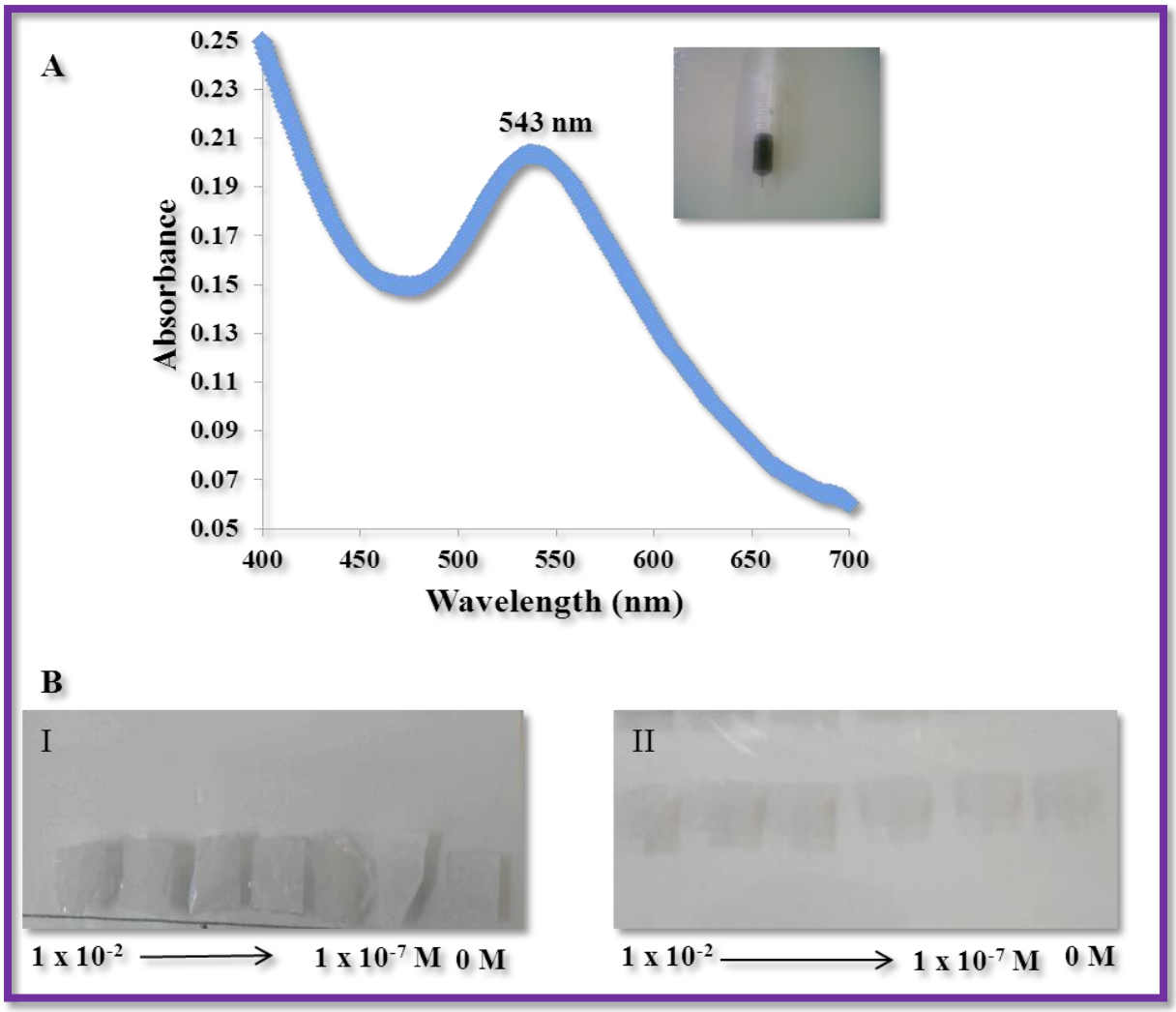

Figure 4.7.1: (A) The UV spectrum and photograph of the 1:1 polymer solution and the corresponding images of the nanofibres in DA and AA (B I and II).

The insert in **Fig. 4.7.2a** displays the polymer solution that resulted from the 1:3 mixture. It was wine–red in colour and the SPR peak was observed at 541 nm. No colorimetric response was noted in the presence of both DA and AA (**Fig. 4.7.2b I and II**).

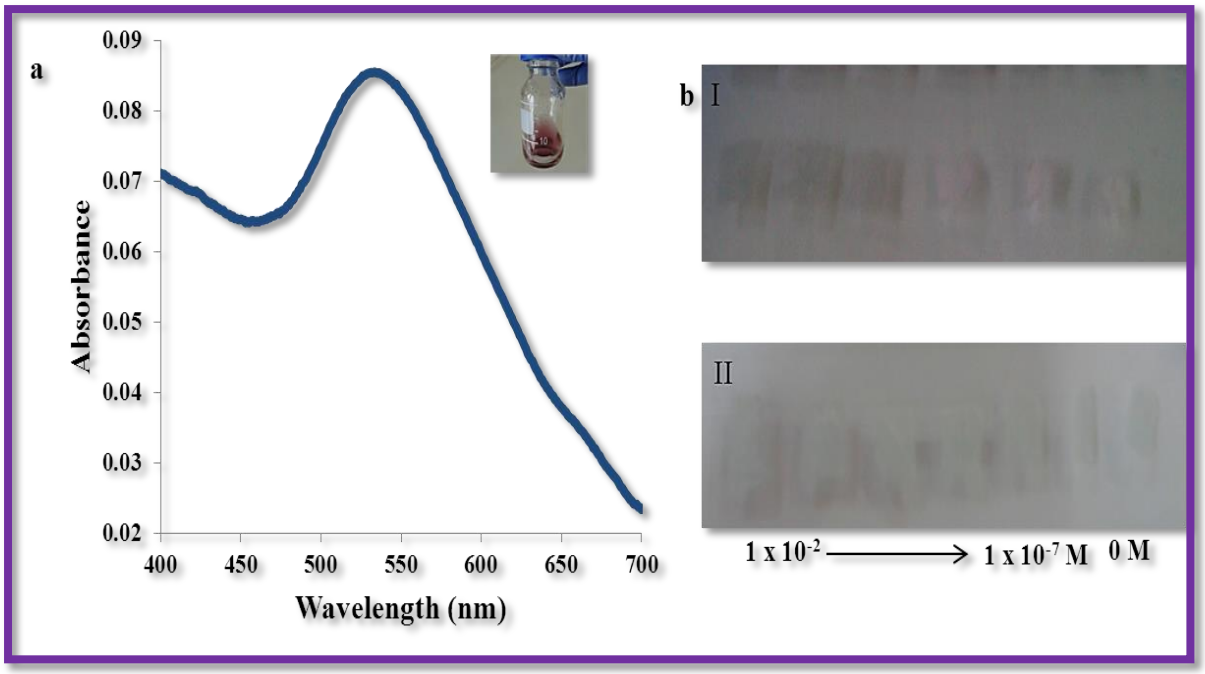

Figure 4.7.2: (a) The UV spectrum and photograph of the 1:3 polymer solution and the corresponding images of the nanofibres in DA and AA (b I and II) respectively.

A wine–red polymer solution was obtained for the 3:1 mixture with an SPR peak at 542 nm confirming the success of AuNPs synthesis (**Fig. 4.7.3a**). The resulting nanofibre also did not change colour in the analytes (**Fig. 4.7.3b I and II**).

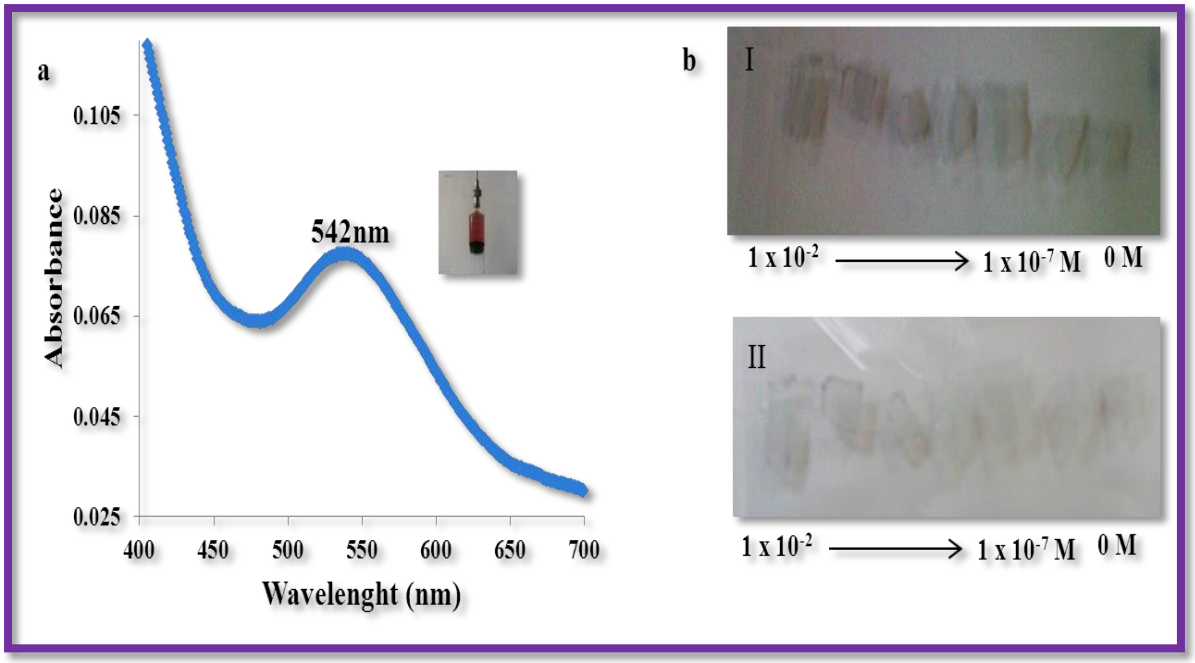

Figure 4.7.3: (a) The UV spectrum and photograph of the 3:1 polymer solution and the corresponding images of the nanofibres in DA and AA (b I and II) respectively.

The 5:1 composite polymer solution had a wine–red colour and an SPR peak at 550 nm (**Fig. 4.7.4a**). In the presence of DA, the fibres changed colour from white to blue. The colour change was observed from 5 x 10^{-5} M to higher concentrations of DA (**Fig. 4.7.4b I**). This trend was also observed in AA showing a colour change from white to purple then navy blue for higher concentration (1 x 10^{-2} M) (**Fig. 4.7.4b II**).

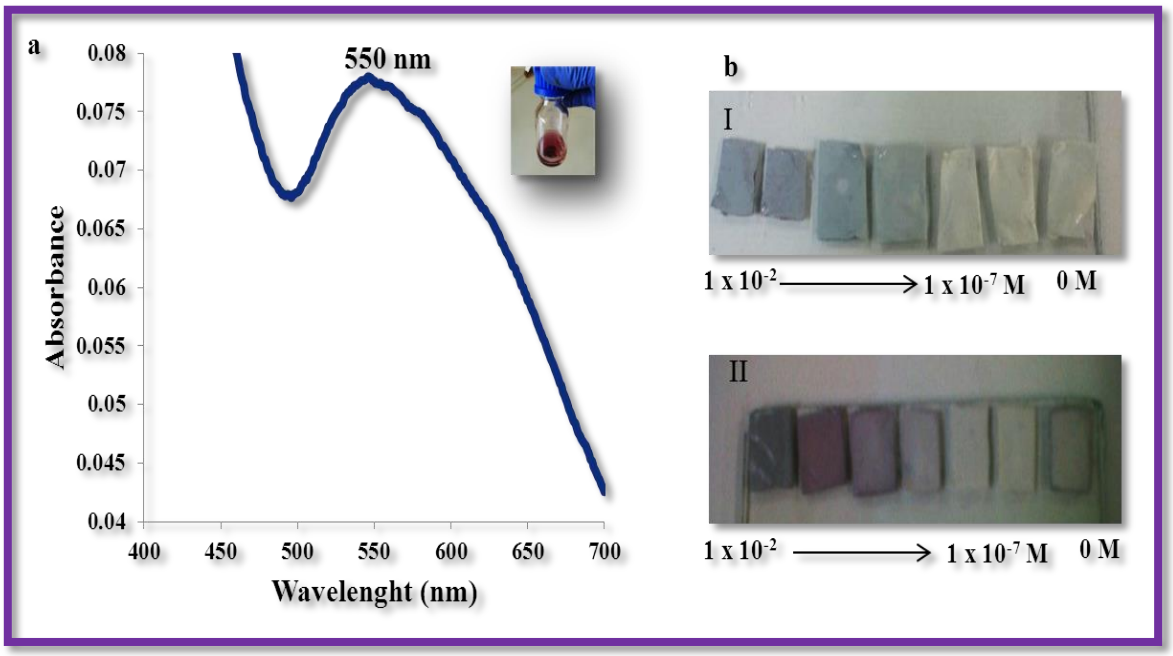

Figure 4.7.4: (a) The UV spectrum and photograph of the 5:1 polymer solution and the corresponding images of the nanofibres in DA and AA (b I and II respectively).

Fig. 4.7.5a depicts the 1:5 polymer solution; it was purple in colour and had an SPR peak at 542 nm. Visible colour change of the nanofibres placed in DA from 5 × 10^{-5} to 5 × 10^{-2} M was observed (**Fig. 4.7.5b I**). Conversely, no significant colour change was observed on the nanofibres that were placed in AA (**Fig. 4.7.5b II**).

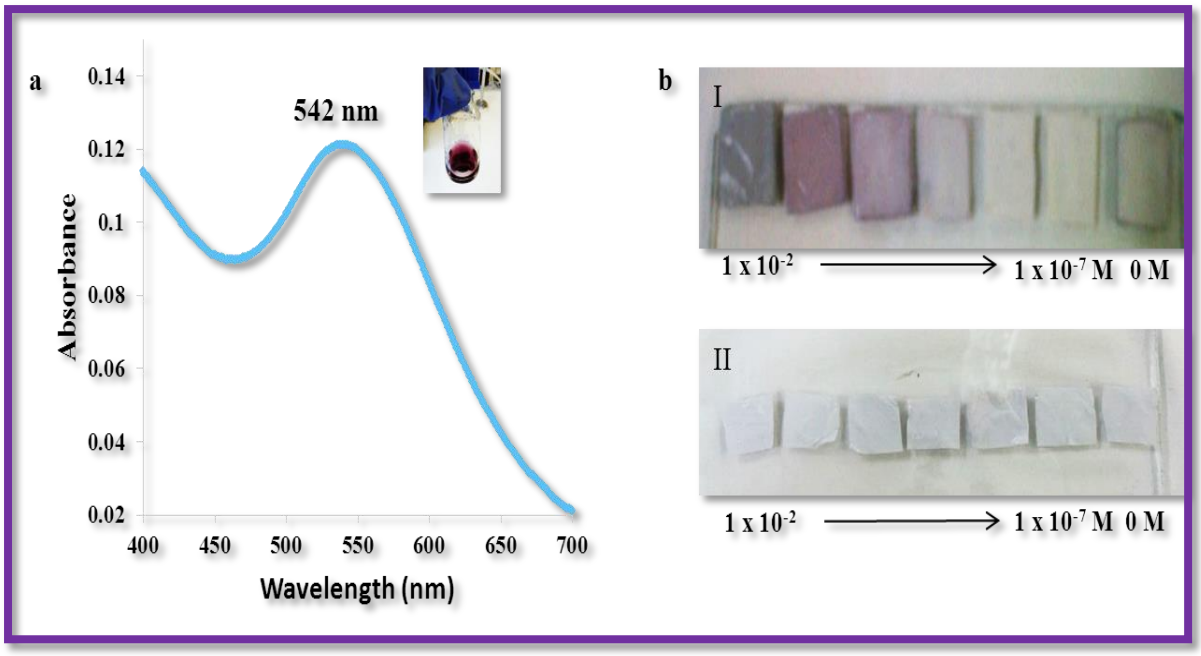

Figure 4.7.5: (a) The UV spectrum and photograph of the 1:5 polymer solution and the corresponding images of the nanofibres in DA and AA (b I and II) respectively.

Due to the visible colour change of probes 5:1 and 1:5, they were selected for further studies. These nanofibres were evaluated for their potential to detect other reducing compounds. The analytes tested were each at a concentration of 5×10^{-6} M. The images were captured at 10 min intervals.

The 5:1 composite nanofibres did not change colour in all the analytes after 10 min (**Fig. 4.7.6 I**). However, after 20 min a slight colour change to navy was observed for EPI and NORE (**Fig. 4.7.6. II**). The 1:5 composite exhibited no colour change even after 20 min (**Fig. 4.7.7**).

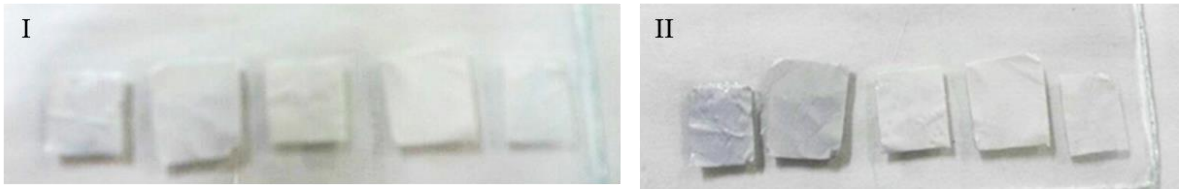

Figure 4.7.6: Shows the 5:1 probe placed in (from left to right) epinephrine, norepinephrine, glucose, tyrosine and the reference. (I) after 10 min and (II) after 20 min.

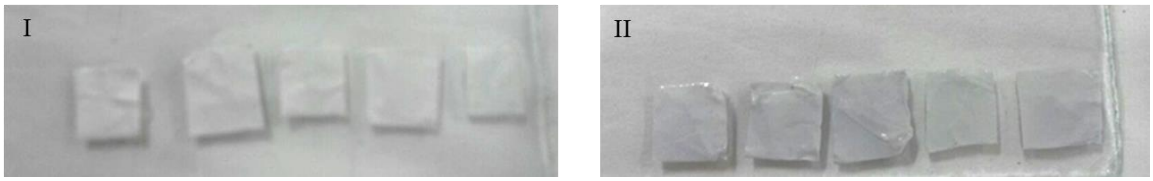

Figure 4.7.7: Shows the 1:5 probe placed in (from left to right) epinephrine, norepinephrine, glucose, tyrosine and the reference. (I) after 10 min and (II) after 20 min.

In summary, the concentration ratios of gold salt to $NaBH_4$ affected the effectiveness of the probes. The probe with more $NaBH_4$ than gold salt showed good selectivity towards the stronger reducing agent (DA). The probe with less $NaBH_4$ than gold salt showed a colour change for the weaker reducing analyte (AA) meaning that further reduction could occur after reduction with $NaBH_4$. Briefly, the outcome of this part of study showed that correct concentration ratio combination of the $HAuCl_4$ and the $NaBH_4$ can produce novel colorimetric probes for the reducing compounds.

4.8 *β*–CD–AuNPs + N6 composite nanofibre probe

As an alternative for achieving selectivity of an individual or a collection of analytes, here in we have investigated the use of cyclodextrin. This compound was chosen because it is well known for its distinct configuration that enables it to form host–guest interactions, resulting in inclusion complexes. In comparison to other forms of cyclodextrin, *β*–CD is commonly used because it is readily available, and its cavity size is good enough to host a wide range of guest molecules. Moreover, *β*–CD has been applied to design electrochemical and spectrophotometric sensors that are selective to DA and for simultaneous quantification of DA and serotonin [251, 252]. However, there is still a need for a simple colorimetric probe that will overcome the challenges of the currently used methods in the complex biological fluids such as urine, blood/serum and cerebral fluid. Outcomes of our initial attempts to seek a solution to this crucial issue are presented in the following section.

4.8.1 *Ex–situ* prepared *β*–CD–AuNPs + N6 nanofibre probe

When the *ex−situ* prepared gold nanoparticles were introduced to a solution of N6, it turned purple. The solution was electrospun both on a copper grid (for the TEM analysis) and on the

aluminium foil. Molecular interaction between the three materials was evaluated using FTIR spectroscopy (**Fig. 4.8.1**) which revealed that there was no significant difference between the spectra of the clean N6 (**red**) and that of CD–AuNPs + N6 (**blue**). The characteristic peaks of *β*–CD were also not seen on the spectrum of the *β*–CD –AuNPs + N6 composite nanofibre. The absence of the *β*–CD implied that there was no physical interaction between the *β*–CD –AuNPs and the N6. Interestingly, the spectrum of the *β*–CD + N6 composite revealed a shift in some of the peaks of N6 and new peaks that are characteristic of CD (**green**). The frequencies of β–cyclodextrin were observed at 1155 cm^{-1} and 1028 cm^{-1} which corresponds to the stretching vibration of C–C and bending vibration of O–H [253] respectively. The absorption band at 862 cm^{-1} belongs to the deformation vibrations of C–H bonds and the pulsation vibration in glucopyranose cycle [254].

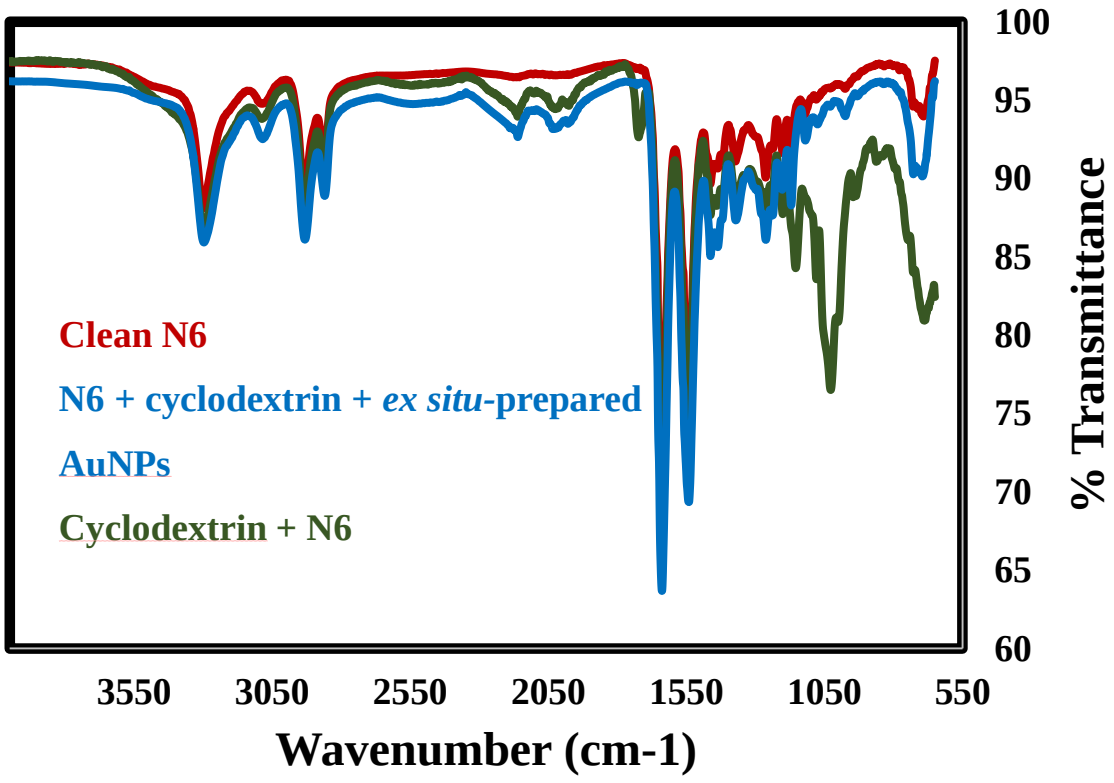

Figure 4.8.1: FTIR characterization of clean N6, N6 + CD + *ex situ* prepared AuNPs and CD + N6 nanofibres.

When the fibres were introduced in AA, DA, EPI, NORE and UA their colour remained unchanged. TEM observations (**Fig. 4.8.2**) showed that the *β*–CD –AuNPs coated the nanofibre instead of being encapsulated within the nanofibre composite. **Fig. 4.8.2A and B**

are images of the same nanofibre taken at different magnification. This observation was thought to be the reason for the lack of response by all the analytes.

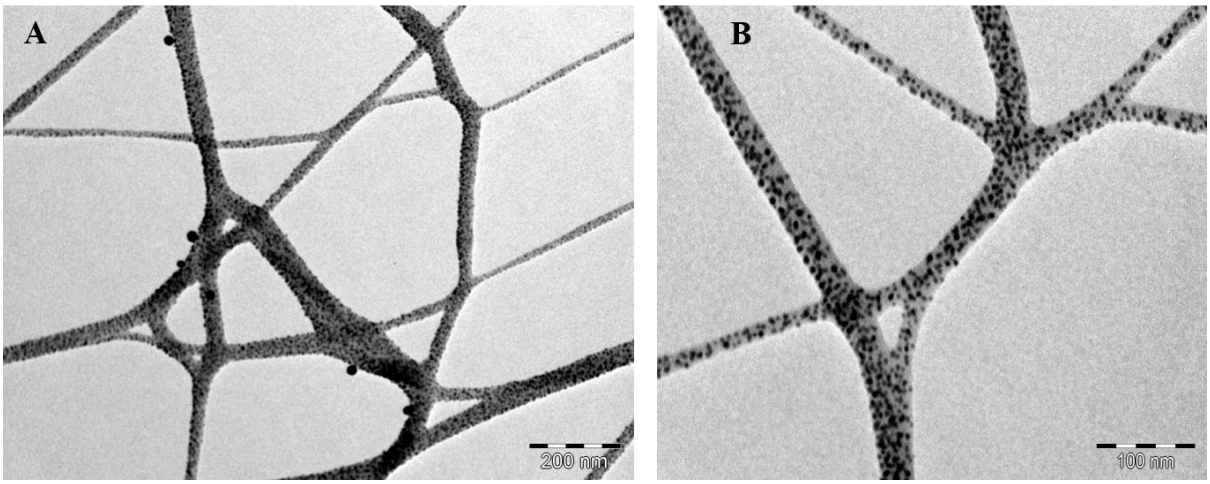

Figure 4.8.2: TEM images of the ex situ prepared CD–AuNPs +N6 nanofibre composite at different magnifications.

We went further on to try the *in situ* method since it proved to be effective in our previous studies. Firstly, a suitable order for adding the reagents that will make up the probe was investigated. The solution prepared by first dissolving N6 could not completely dissolve *β*–CD, as a result, the fibre mat exhibited a rough surface morphology. However, when *β*–CD was dissolved first followed by the addition of N6, both materials dissolved well hence this procedure was chosen for further studies.

The FTIR spectrum of the N6 containing the *in situ* prepared *β*–CD –AuNPs (**Fig. 4.8.3 blue**) did not change much from that of the *β*–CD + N6 nanofibre (**Fig. 4.8.3 brown)** except for the increase in intesity of the absorption peaks of both N6 and *β*–CD which was assumed to be due to the presence of the nanoparticles. This suggest that the functional groups of the two materials were responsible in the interaction with the AuNPs.

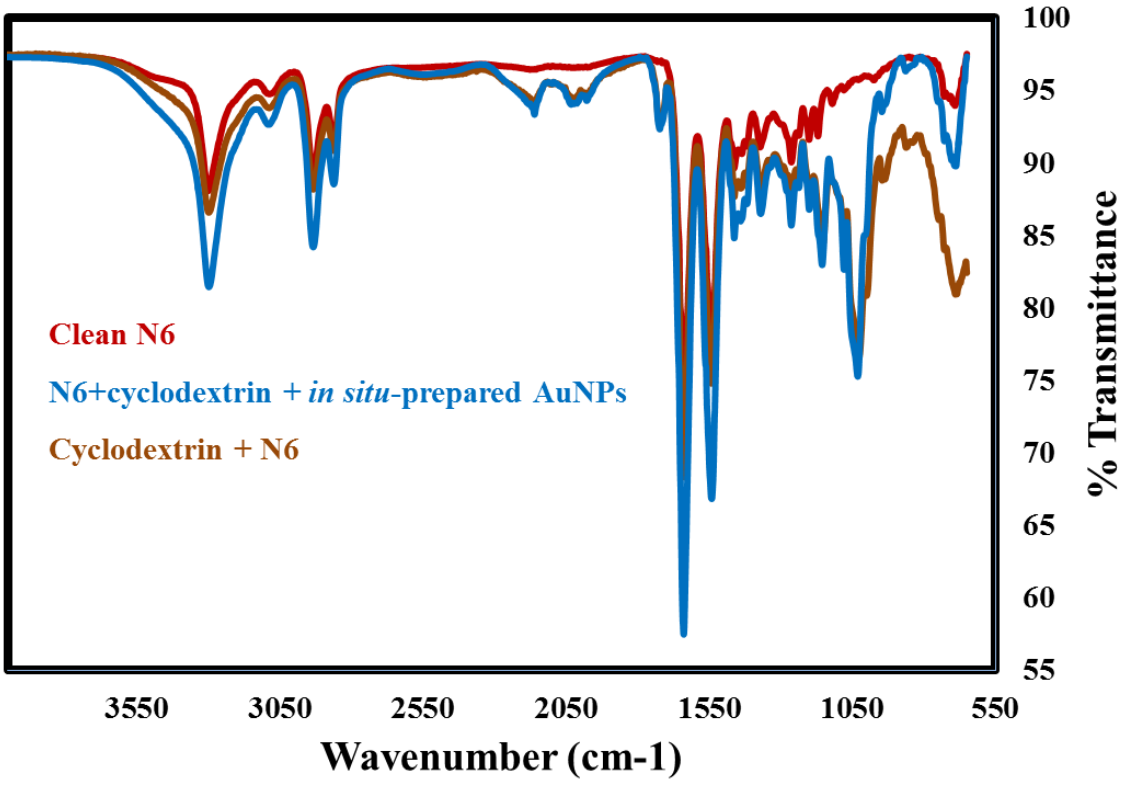

Figure 4.8.3: FTIR characterization of clean N6, N6 + AuNPs, N6 + Cyclodextrin + *in situ* prepared AuNPs and cyclodextrin + N6 nanofibres.

Fig. 4.8.4 shows that before DA, the in *situ* prepared *β*–CD –AuNPs were dispersed and encapsulated within the nanofibres (**Fig. 4.8.4A**) and in the presence of DA they formed aggregates on the surface of the nanofibre (**Fig. 4.8.4B**). The original colour of the nanofibre was brown. After 10 min exposure in EPI, DA, NORE and CAT they became purple while the colour remained unchanged in UA and AA (**Fig 4.8.5 top**). After 20 min, the fibres that were in EPI, DA, NORE and CAT became navy blue whereas the ones in AA became pink and remained brown in UA (**Fig. 4.8.5 bottom**).

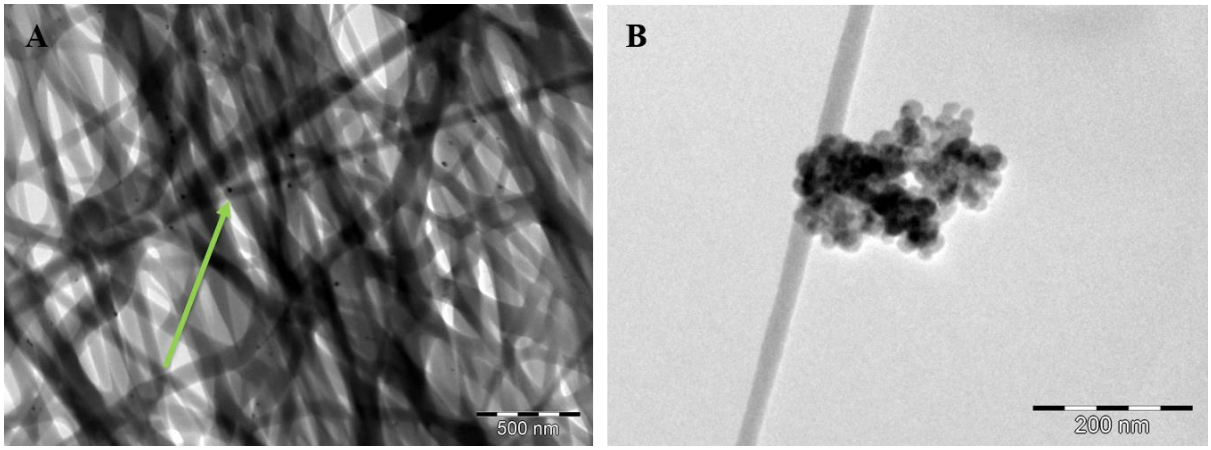

Figure 4.8.4: TEM images of the *in situ* prepared CD–AuNPs +N6 nanofibre composite before (A) and after (B) DA.

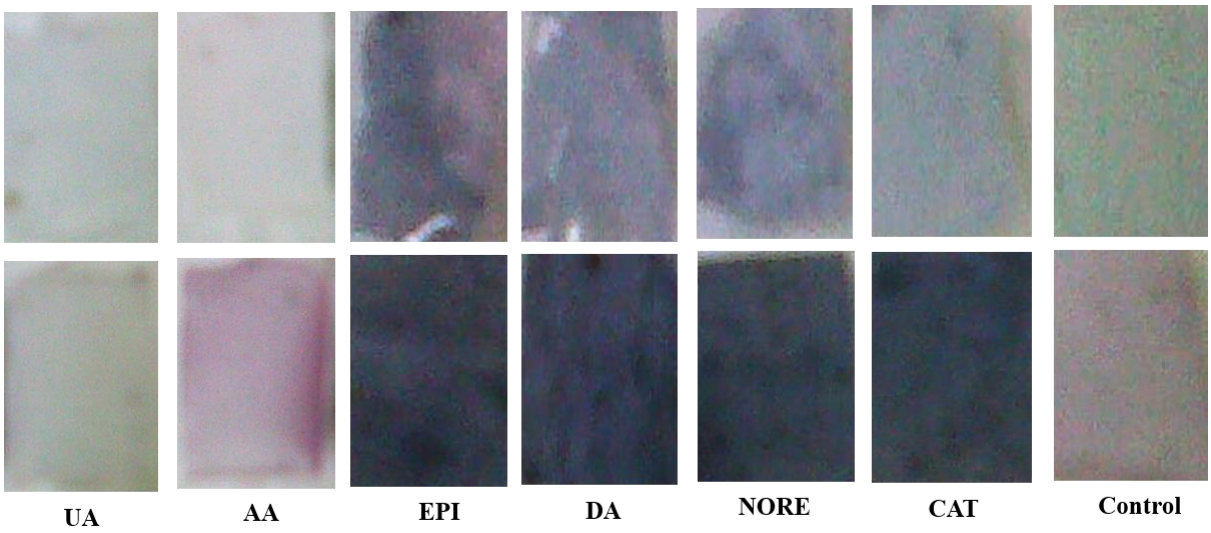

Figure 4.8.5: Preliminary evaluation of the nanofibres as probe in the presence of UA, AA, EPI, DA, NORE and CAT with after 10 min (top) and after 20 min (bottom).

Briefly, the *ex situ* method proved to be ineffective in the synthesis of a probe. However, the uniform distribution of the nanoparticles on the surface of the nanofibres can find application in other areas where such material are required such as in the design of biomedical devices and water purification. The *in situ* method gave a nanofibre that showed great potential to detect catecholamines simultaneously, indeed, a study worth looking at in the future.

Chapter 5: Summary and future prospects

Colorimetric probes for detecting DA were developed in both liquid and solid states. The novel probe for detecting DA was produced by utilizing UF–AuNPs. Due to DA being a good reducing agent of the UF–AuNPs, it induced growth and changes in the morphology of the nanoparticles which resulted in colour changes from pale green to orange then brown. Spectral shifts were observed from lower to higher wavelengths signalling the formation of large particles or aggregates. Under non–optimized pH conditions, colour change was observed from 0.5 µM. In the mixture of DA and AA, the probe could detect DA when the concentrations of AA were less than 200 times higher than those of DA. At very high concentrations of AA (200– higher times greater than DA), a deep purple colour with absorption maxima around 605 nm was observed showing the interference of AA. Under optimized pH conditions, colour change was observed from 5 nM DA and the detection limit was improved to 2.5 nM. The probe could selectively detect DA in whole blood sample. The practical simplicity of the probe demonstrated that it would be more useful in the development of new AuNPs based probes as it is safe (no use of toxic functionalities) and rapid. The developed probe also gave some insight on the synthesis of various shapes of AuNPs during the detection of DA, and this information is now being used in our lab to further develop sensitive probes with both free and immobilised nanoparticles.

The solid state probe in a form of a nanofibre produced via electrospinning and the UF–AuNPs were prepared following the *in−situ* reduction method of the $HAuCl_4$ in the N6 polymer solution. The fibres showed exceptional selectivity, sensitivity and fast response towards DA without contribution from any of the other interfering species. The probe was successfully applied in a whole blood sample and still showed high specificity towards DA. In solution it was observed that all the absorption peaks that were present in the original whole blood sample disappeared when the UF–AuNPs were added and the peaks that resulted corresponded to those that were observed in the standard DA solutions. For both the liquid and solid state, the necessity of using UF–AuNPs was investigated by preparing stabilized AuNPs and compared the findings. The UF–AuNPs showed very remarkable properties

during the detection of DA. In comparison to the probes mentioned in section 2.1.3.2, the probes developed in this study are easy to prepare, more sensitive and selective. Moreover, the solid state probe is portable. In order to investigate the need to introduce functionalities that will cater for selectivity towards DA during the development of the solid state probe, we evaluated the suitability of MIPs since they are known to be highly selective towards a targeted analyte. The results that were obtained showed that the MIPs were not playing any unique role since the control (NIPs) also showed selectivity towards DA.

For our future work, since DA is also found in urine and pharmaceuticals investigating the outstanding properties of the probe in these samples would also be sensible.

For the MIPs synthesized in the developed method to be used as components of the colorimetric probe, colour change by the NIP fibres would have to be circumvented for the merits of the MIPs to be clearly seen. Meaning, alterations would have to be made in the method. For instance, the AuNPs can be prepared separately followed by immersing the pre–synthesized polymer particles in the AuNPs solution for some time and then allow the polymer particles to dry before they are added to the polymer solution. Such a procedure may result in the NPs being attached on the surface of the polymer particles and their distribution will depend entirely on the distribution of the particles.

Preliminary studies were also done to see if the methods developed in this thesis could be used to make probes for other analytes. Using both un–functionalized and functionalized AuNPs housed in electrospun nanofibres two probes were synthesized. The probe based on UF–AuNPs showed that optimal conditions (in terms of reagents) can afford us a probe for other catecholamines such as norepinephrine. Meanwhile the probes based on AuNPs functionalized with β–cyclodextrin showed great potential to simultaneously detect all catecholamines in the presence of interfering substances such as AA and UA. This part of the work will form a major part of our future work.

References

1. Huang J, Liu Y, Hou H, You T: **Simultaneous electrochemical determination of dopamine, uric acid and ascorbic acid using palladium nanoparticle-loaded carbon nanofibers modified electrode**. *Biosens Bioelectron* 2008, **24**(Copyright (C) 2012 American Chemical Society (ACS). All Rights Reserved.):632-637.

2. Marsden CA: **Dopamine: the rewarding years**. *Br J Pharmacol* 2006, **147**(Copyright (C) 2013 American Chemical Society (ACS). All Rights Reserved.):S136-S144.

3. Fahn S: **The history of dopamine and levodopa in the treatment of Parkinson's disease**. *Mov Disord* 2008, **23 Suppl 3**(Copyright (C) 2013 U.S. National Library of Medicine.):S497-508.

4. Raj CR, Okajima T, Ohsaka T: **Gold nanoparticle arrays for the voltammetric sensing of dopamine**. *Journal of Electroanalytical Chemistry* 2003, **543**(2):127-133.

5. Wightman RM, May LJ, Michael AC: **Detection of dopamine dynamics in the brain**. *Anal Chem* 1988, **60**(Copyright (C) 2013 American Chemical Society (ACS). All Rights Reserved.):769A-770A, 772A, 774A-776A, 778A-779A.

6. Staal RGW, Rayport S, Sulzer D: **Amperometric detection of dopamine exocytosis from synaptic terminals**. In*: 2007*. CRC Press LLC: 337-352, 332 plates.

7. Kong B, Zhu A, Luo Y, Tian Y, Yu Y, Shi G: **Sensitive and Selective Colorimetric Visualization of Cerebral Dopamine Based on Double Molecular Recognition**. *Angew Chem, Int Ed* 2011, **50**(Copyright (C) 2012 American Chemical Society (ACS). All Rights Reserved.):1837-1840, S1837/1831-S1837/1838.

8. Zhuang Z, Li J, Xu R, Xiao D: **Electrochemical detection of dopamine in the presence of ascorbic acid using overoxidized polypyrrole/graphene modified electrodes**. *Int J Electrochem Sci* 2011, **6**(Copyright (C) 2013 American Chemical Society (ACS). All Rights Reserved.):2149-2161.

9. Kim Y-R, Bong S, Kang Y-J, Yang Y, Mahajan RK, Kim JS, Kim H: **Electrochemical detection of dopamine in the presence of ascorbic acid using**

graphene modified electrodes. *Biosensors and Bioelectronics* 2010, **25**(10):2366-2369.

10. Tian J, Xu J, Zhu F, Lu T, Su C, Ouyang G: **Application of nanomaterials in sample preparation**. *J Chromatogr A* 2013, **1300**(Copyright (C) 2013 American Chemical Society (ACS). All Rights Reserved.):2-16.

11. Ridgway K, Lalljie SPD, Smith RM: **Sample preparation techniques for the determination of trace residues and contaminants in foods**. *J Chromatogr A* 2007, **1153**(Copyright (C) 2013 American Chemical Society (ACS). All Rights Reserved.):36-53.

12. Smith RM: **Before the injection - modern methods of sample preparation for separation techniques**. *J Chromatogr A* 2003, **1000**(Copyright (C) 2013 American Chemical Society (ACS). All Rights Reserved.):3-27.

13. Baeyens WRG, Schulman SG, Calokerinos AC, Zhao Y, García Campaña AM, Nakashima K, De Keukeleire D: **Chemiluminescence-based detection: principles and analytical applications in flowing streams and in immunoassays**. *Journal of Pharmaceutical and Biomedical Analysis* 1998, **17**(6–7):941-953.

14. Li S-F, Zhang X-M, Yao Z-J, Yu R, Huang F, Wei X-W: **Enhanced chemiluminescence of the rhodamine 6G-cerium(IV) system by Au-Ag alloy nanoparticles**. *J Phys Chem C* 2009, **113**(Copyright (C) 2013 American Chemical Society (ACS). All Rights Reserved.):15586-15592.

15. Birks JW, Editor: **Chemiluminescence and Photochemical Reaction Detection in Chromatography**: VCH; 1989.

16. **Chemiluminescence** [<http://www.lumigen.com/detection_technologies/chemiluminescence/>] [06/10/14]

17. Maruyama W, Naoi M: **Cell death in Parkinson's disease**. *J Neurol* 2002, **249**(2):ii06-ii10.

18. Nozaki O, Iwaeda T, Kato Y: **Detection of substances with alcoholic or phenolic hydroxyl groups by generation of hydrogen peroxide with imidazole and**

peroxyoxalate chemiluminescence. *J Biolumin Chemilumin* 1995, **10**(Copyright (C) 2013 American Chemical Society (ACS). All Rights Reserved.):339-344.

19. Nozaki O, Iwaeda T, Kato Y: **Amines for detection of dopamine by generation of hydrogen peroxide and peroxyoxalate chemiluminescence**. *J Biolumin Chemilumin* 1996, **11**(Copyright (C) 2013 American Chemical Society (ACS). All Rights Reserved.):309-313.

20. Liu T, Zhang L, Song H, Wang Z, Lv Y: **Sonochemical synthesis of Ag nanoclusters: electrogenerated chemiluminescence determination of dopamine**. *Luminescence* 2013, **28**(Copyright (C) 2013 American Chemical Society (ACS). All Rights Reserved.):530-535.

21. Mathews S, Plaisance E, Kim T: **Imaging Systems for Westerns: Chemiluminescence vs. Infrared Detection**. In: *Protein Blotting and Detection.* Edited by Kurien BT, Scofield RH, vol. 536: Humana Press; 2009: 499-513.

22. Dubertret B, Skourides P, Norris DJ, Noireaux V, Brivanlou AH, Libchaber A: **In vivo imaging of quantum dots encapsulated in phospholipid micelles**. *Science (Washington, DC, U S)* 2002, **298**(Copyright (C) 2013 American Chemical Society (ACS). All Rights Reserved.):1759-1762.

23. Bruchez M, Jr., Moronne M, Gin P, Weiss S, Alivisatos AP: **Semiconductor nanocrystals as fluorescent biological labels**. *Science (Washington, D C)* 1998, **281**(Copyright (C) 2013 American Chemical Society (ACS). All Rights Reserved.):2013-2016.

24. Fan C, Plaxco KW, Heeger AJ: **High-efficiency fluorescence quenching of conjugated polymers by proteins**. *J Am Chem Soc* 2002, **124**(Copyright (C) 2013 American Chemical Society (ACS). All Rights Reserved.):5642-5643.

25. Mu Q, Xu H, Li Y, Ma S, Zhong X: **Adenosine capped QDs based fluorescent sensor for detection of dopamine with high selectivity and sensitivity**. *Analyst* 2013.

26. Ma Y, Yang C, Li N, Yang X: **A sensitive method for the detection of catecholamine based on fluorescence quenching of CdSe nanocrystals**. *Talanta*

2005, **67**(Copyright (C) 2013 American Chemical Society (ACS). All Rights Reserved.):979-983.

27. Larry GH: **Analytical chemistry principles and techniques**. Englewood Cliffs, New Jersey: Prentice-Hall, Inc.; 1988.

28. Nevado JJB, Gallego JML, Laguna PB: **Spectrophotometric determination of catecholamines with metaperiodate by flow-injection analysis**. *Analytica Chimica Acta* 1995, **300**(1–3):293-297.

29. El-Dien FAN, Zayed MA, Mohamed GG, El-Nahas RG: **Two spectrophotometric assays for dopamine derivatives in pharmaceutical products and in biological samples of schizophrenic patients using copper tetramine complex and triiodide reagent**. *J Biomed Biotechnol* 2005(Copyright (C) 2013 American Chemical Society (ACS). All Rights Reserved.):1-9.

30. Shishehbore MR, Asgharpoor A, Nasirizadeh N: **A novel kinetic spectrophotometric method for the determination of dopamine in biological and pharmaceutical samples**. *J Chem* 2013:819460, 819467 pp.

31. Nezhad MRH, Tashkhourian J, Khodaveisi J: **Sensitive spectrophotometric detection of dopamine, levodopa, and adrenaline using surface plasmon resonance band of silver nanoparticles**. *J Iran Chem Soc* 2010, **7**(Copyright (C) 2013 American Chemical Society (ACS). All Rights Reserved.):S83-S91.

32. Barnum DW: **Spectrophotometric determination of catechol, epinephrine, dopa, dopamine and other aromatic vic-diols**. *Analytica Chimica Acta* 1977, **89**(1):157-166.

33. Wang J: **Nanoparticle-based electrochemical DNA detection**. *Anal Chim Acta* 2003, **500**(Copyright (C) 2013 American Chemical Society (ACS). All Rights Reserved.):247-257.

34. Iost RM, Madurro JM, Brito-Madurro AG, Nantes IL, Caseli L, Crespilho FN: **Strategies of nano-manipulation for application in electrochemical biosensors**. *Int J Electrochem Sci* 2011, **6**(Copyright (C) 2013 American Chemical Society (ACS). All Rights Reserved.):2965-2997.

35. Wu L, Feng L, Ren J, Qu X: **Electrochemical detection of dopamine using porphyrin-functionalized graphene**. *Biosensors and Bioelectronics* 2012, **34**(1):57-62.

36. Shervedani RK, Alinajafi-Najafabadi HA: **Electrochemical determination of dopamine on a glassy carbon electrode modified by using nanostructure ruthenium oxide hexacyanoferrate/ruthenium hexacyanoferrate thin film**. *Int J Electrochem* 2011(Copyright (C) 2013 American Chemical Society (ACS). All Rights Reserved.):603135, 603111 pp.

37. Linthicum DS, Patel J, Cairns N: **Antibody-based fluorescence polarization assay to screen combinatorial libraries for sweet taste compounds**. *Comb Chem High Throughput Screening* 2001, **4**(Copyright (C) 2013 American Chemical Society (ACS). All Rights Reserved.):431-438.

38. Ito Y, Yamazaki S-i, Kano K, Ikeda T: **Escherichia coli and its application in a mediated amperometric glucose sensor**. *Biosens Bioelectron* 2002, **17**(Copyright (C) 2013 U.S. National Library of Medicine.):993-998.

39. Eteshola E, Leckband D: **Development and characterization of an ELISA assay in PDMS microfluidic channels**. *Sens Actuators, B* 2001, **72**(Copyright (C) 2013 American Chemical Society (ACS). All Rights Reserved.):129-133.

40. Goddard NJ, Singh K, Hulme JP, Malins C, Holmes RJ: **Internally-referenced Resonant Mirror devices for dispersion compensation in chemical sensing and biosensing applications**. *Sens Actuators, A* 2002, **100**(Copyright (C) 2013 American Chemical Society (ACS). All Rights Reserved.):1-9.

41. Pauwels R, Balzarini J, Baba M, Snoeck R, Schols D, Herdewijn P, Desmyter J, De Clercq E: **Rapid and automated tetrazolium-based colorimetric assay for the detection of anti-HIV compounds**. *Journal of virological methods* 1988, **20**(4):309-321.

42. Forzani ES, Zhang H, Chen W, Tao N: **Detection of Heavy Metal Ions in Drinking Water Using a High-Resolution Differential Surface Plasmon Resonance Sensor**. *Environ Sci Technol* 2005, **39**(Copyright (C) 2013 American Chemical Society (ACS). All Rights Reserved.):1257-1262.

43. Li H, Fan J, Song F, Zhu H, Du J, Sun S, Peng X: **Fluorescent probes for Pd2+ detection by allylidene-hydrazone ligands with excellent selectivity and large fluorescence enhancement**. *Chemistry* 2010, **16**(Copyright (C) 2013 U.S. National Library of Medicine.):12349-12356.

44. Xu X, Wang J, Yang F, Jiao K, Yang X: **Label-Free Colorimetric Detection of Small Molecules Utilizing DNA Oligonucleotides and Silver Nanoparticles**. *Small* 2009, **5**(Copyright (C) 2013 American Chemical Society (ACS). All Rights Reserved.):2669-2672.

45. Kim S, Eom MS, Kim SK, Seo SH, Han MS: **A highly sensitive gold nanoparticle-based colorimetric probe for pyrophosphate using a competition assay approach**. *Chem Commun (Camb)* 2013, **49**(Copyright (C) 2013 U.S. National Library of Medicine.):152-154.

46. Song Y, Wei W, Qu X: **Colorimetric Biosensing Using Smart Materials**. *Adv Mater (Weinheim, Ger)* 2011, **23**(Copyright (C) 2012 American Chemical Society (ACS). All Rights Reserved.):4215-4236.

47. Zhang D, Jin W: **Highly selective and sensitive colorimetric probe for hydrogen sulfide by a copper (II) complex of azo-dye based on chemosensing ensemble approach**. *Spectrochim Acta, Part A* 2012, **90**(Copyright (C) 2013 American Chemical Society (ACS). All Rights Reserved.):35-39.

48. Zheng F, Wu Z, Chen Y: **A quantitative method for the measurement of membrane affinity by polydiacetylene-based colorimetric assay**. *Anal Biochem* 2012, **420**(Copyright (C) 2013 American Chemical Society (ACS). All Rights Reserved.):171-176.

49. Mirkin CA, Letsinger RL, Mucic RC, Storhoff JJ: **A DNA-based method for rationally assembling nanoparticles into macroscopic materials**. *Nature (London)* 1996, **382**(Copyright (C) 2013 American Chemical Society (ACS). All Rights Reserved.):607-609.

50. Cheng Q, Stevens RC: **Charge-Induced Chromatic Transition of Amino Acid-Derivatized Polydiacetylene Liposomes**. *Langmuir* 1998, **14**(Copyright (C) 2013 American Chemical Society (ACS). All Rights Reserved.):1974-1976.

51. Ahn DJ, Chae E-H, Lee GS, Shim H-Y, Chang T-E, Ahn K-D, Kim J-M: **Colorimetric Reversibility of Polydiacetylene Supramolecules Having Enhanced Hydrogen-Bonding under Thermal and pH Stimuli**. *J Am Chem Soc* 2003, **125**(Copyright (C) 2013 American Chemical Society (ACS). All Rights Reserved.):8976-8977.

52. Lu Y, Yang Y, Sellinger A, Lu M, Huang J, Fan H, Haddad R, Lopez G, Burns AR, Sasaki DY *et al*: **Self-assembly of mesoscopically ordered chromatic polydiacetylene/silica nanocomposites**. *Nature (London, U K)* 2001, **410**(Copyright (C) 2013 American Chemical Society (ACS). All Rights Reserved.):913-917.

53. Wenzel M, Atkinson GH: **Chromatic properties of polydiacetylene films**. *J Am Chem Soc* 1989, **111**(Copyright (C) 2013 American Chemical Society (ACS). All Rights Reserved.):6123-6127.

54. Sun X, Chen T, Huang S, Li L, Peng H: **Chromatic polydiacetylene with novel sensitivity**. *Chem Soc Rev* 2010, **39**(Copyright (C) 2013 American Chemical Society (ACS). All Rights Reserved.):4244-4257.

55. Reppy MA: **Enhancing the emission of polydiacetylene sensing materials through fluorophore addition and energy transfer**. *J Fluoresc* 2008, **18**(Copyright (C) 2013 American Chemical Society (ACS). All Rights Reserved.):461-471.

56. Charych DH, Nagy JO, Spevak W, Bednarski MD: **Direct colorimetric detection of a receptor-ligand interaction by a polymerized bilayer assembly**. *Science (Washington, D C, 1883-)* 1993, **261**(Copyright (C) 2013 American Chemical Society (ACS). All Rights Reserved.):585-588.

57. Reichert A, Nagy JO, Spevak W, Charych D: **Polydiacetylene Liposomes Functionalized with Sialic Acid Bind and Colorimetrically Detect Influenza Virus**. *J Am Chem Soc* 1995, **117**(Copyright (C) 2013 American Chemical Society (ACS). All Rights Reserved.):829-830.

58. Ma B, Fan Y, Zhang L, Kong X, Li Y, Li J: **Direct colorimetric study on the interaction of Escherichia coli with mannose in polydiacetylene Langmuir-Blodgett films**. *Colloids Surf, B* 2003, **27**(Copyright (C) 2013 American Chemical Society (ACS). All Rights Reserved.):209-213.

59. Satchell DP, Sheynis T, Shirafuji Y, Kolusheva S, Ouellette AJ, Jelinek R: **Interactions of Mouse Paneth Cell α-Defensins and α-Defensin Precursors with Membranes. Prosegment Inhibition of Peptide Association with Biomimetic Membranes**. *J Biol Chem* 2003, **278**(Copyright (C) 2013 American Chemical Society (ACS). All Rights Reserved.):13838-13846.

60. Gill I, Ballesteros A: **Immunoglobulin-polydiacetylene sol-gel nanocomposites as solid-state chromatic biosensors**. *Angew Chem, Int Ed* 2003, **42**(Copyright (C) 2013 American Chemical Society (ACS). All Rights Reserved.):3264-3267.

61. Okada SY, Jelinek R, Charych D: **Induced color change of conjugated polymeric vesicles by interfacial catalysis of phospholipase A2**. *Angew Chem, Int Ed* 1999, **38**(Copyright (C) 2013 American Chemical Society (ACS). All Rights Reserved.):655-659.

62. Jelinek R, Kolusheva S: **Biomolecular sensing with colorimetric vesicles**. *Top Curr Chem* 2007, **277**(Copyright (C) 2013 American Chemical Society (ACS). All Rights Reserved.):155-180.

63. Kolusheva S, Molt O, Herm M, Schrader T, Jelinek R: **Selective Detection of Catecholamines by Synthetic Receptors Embedded in Chromatic Polydiacetylene Vesicles**. *J Am Chem Soc* 2005, **127**(Copyright (C) 2013 American Chemical Society (ACS). All Rights Reserved.):10000-10001.

64. Sun S, Anders S, Thomson T, Baglin JEE, Toney MF, Hamann HF, Murray CB, Terris BD: **Controlled Synthesis and Assembly of FePt Nanoparticles**. *J Phys Chem B* 2003, **107**(Copyright (C) 2013 American Chemical Society (ACS). All Rights Reserved.):5419-5425.

65. Chen Z, Zhang X, Cao H, Huang Y: **Chitosan-capped silver nanoparticles as a highly selective colorimetric probe for visual detection of aromatic ortho-trihydroxy phenols**. *Analyst (Cambridge, U K)* 2013, **138**(Copyright (C) 2013 American Chemical Society (ACS). All Rights Reserved.):2343-2349.

66. Song S, Qin Y, He Y, Huang Q, Fan C, Chen H-Y: **Functional nanoprobes for ultrasensitive detection of biomolecules**. *Chem Soc Rev* 2010, **39**(Copyright (C) 2013 American Chemical Society (ACS). All Rights Reserved.):4234-4243.

67. Liu D, Wang Z, Jiang X: **Gold nanoparticles for the colorimetric and fluorescent detection of ions and small organic molecules**. *Nanoscale* 2011, **3**(Copyright (C) 2013 American Chemical Society (ACS). All Rights Reserved.):1421-1433.

68. Zhang Y, Li B, Chen X: **Simple and sensitive detection of dopamine in the presence of high concentration of ascorbic acid using gold nanoparticles as colorimetric probes**. *Microchim Acta* 2010, **168**(Copyright (C) 2012 American Chemical Society (ACS). All Rights Reserved.):107-113.

69. Rai M, Yadav A, Gade A: **Silver nanoparticles as a new generation of antimicrobials**. *Biotechnology advances* 2009, **27**(1):76-83.

70. Kim JS, Kuk E, Yu KN, Kim J-H, Park SJ, Lee HJ, Kim SH, Park YK, Park YH, Hwang C-Y: **Antimicrobial effects of silver nanoparticles**. *Nanomedicine: Nanotechnology, Biology and Medicine* 2007, **3**(1):95-101.

71. Kumar A, Vemula PK, Ajayan PM, John G: **Silver-nanoparticle-embedded antimicrobial paints based on vegetable oil**. *Nature materials* 2008, **7**(3):236-241.

72. Chen Y, Aveyard J, Wilson R: **Gold and silver nanoparticles functionalized with known numbers of oligonucleotides per particle for DNA detection**. *Chem Commun (Cambridge, U K)* 2004(Copyright (C) 2013 American Chemical Society (ACS). All Rights Reserved.):2804-2805.

73. Li H, Cui Z, Han C: **Glutathione-stabilized silver nanoparticles as colorimetric sensor for Ni2+ ion**. *Sens Actuators, B* 2009, **B143**(Copyright (C) 2013 American Chemical Society (ACS). All Rights Reserved.):87-92.

74. Li Y, Schluesener HJ, Xu S: **Gold nanoparticle-based biosensors**. *Gold Bull (London, U K)* 2010, **43**(Copyright (C) 2013 American Chemical Society (ACS). All Rights Reserved.):29-41.

75. Nguyen DT, Kim D-J, Kim K-S: **Controlled synthesis and biomolecular probe application of gold nanoparticles**. *Micron* 2011, **42**(Copyright (C) 2013 American Chemical Society (ACS). All Rights Reserved.):207-227.

76. Wang L, Xing H, Zhang S, Ren Q, Pan L, Zhang K, Bu W, Zheng X, Zhou L, Peng W *et al*: **A Gd-doped Mg-Al-LDH/Au nanocomposite for CT/MR bimodal imagings**

and simultaneous drug delivery. *Biomaterials* 2013, **34**(Copyright (C) 2013 American Chemical Society (ACS). All Rights Reserved.):3390-3401.

77. Baptista P, Pereira E, Eaton P, Doria G, Miranda A, Gomes I, Quaresma P, Franco R: **Gold nanoparticles for the development of clinical diagnosis methods**. *Anal Bioanal Chem* 2008, **391**(Copyright (C) 2013 American Chemical Society (ACS). All Rights Reserved.):943-950.

78. Spain E, Kojima R, Kaner RB, Wallace GG, O'Grady J, Lacey K, Barry T, Keyes TE, Forster RJ: **High sensitivity DNA detection using gold nanoparticle functionalised polyaniline nanofibres**. *Biosensors and Bioelectronics* 2011, **26**(5):2613-2618.

79. Nam EJ, Kim EJ, Wark AW, Rho S, Kim H, Lee HJ: **Highly sensitive electrochemical detection of proteins using aptamer-coated gold nanoparticles and surface enzyme reactions**. *Analyst (Cambridge, U K)* 2012, **137**(Copyright (C) 2013 American Chemical Society (ACS). All Rights Reserved.):2011-2016.

80. Nikoobakht B, El-Sayed MA: **Evidence for Bilayer Assembly of Cationic Surfactants on the Surface of Gold Nanorods**. *Langmuir* 2001, **17**(Copyright (C) 2013 American Chemical Society (ACS). All Rights Reserved.):6368-6374.

81. Gole A, Murphy CJ: **Seed-Mediated Synthesis of Gold Nanorods: Role of the Size and Nature of the Seed**. *Chem Mater* 2004, **16**(Copyright (C) 2013 American Chemical Society (ACS). All Rights Reserved.):3633-3640.

82. Belloni J: **Metal nanocolloids**. *Curr Opin Colloid Interface Sci* 1996, **1**(Copyright (C) 2013 American Chemical Society (ACS). All Rights Reserved.):184-196.

83. Grunwaldt J-D, Kiener C, Wogerbauer C, Baiker A: **Preparation of supported gold catalysts for low-temperature CO oxidation via "size-controlled" gold colloids**. *J Catal* 1999, **181**(Copyright (C) 2013 American Chemical Society (ACS). All Rights Reserved.):223-232.

84. Schneider S, Halbig P, Grau H, Nickel U: **Reproducible preparation of silver sols with uniform particle size for application in surface-enhanced Raman spectroscopy**. *Photochem Photobiol* 1994, **60**(Copyright (C) 2013 American Chemical Society (ACS). All Rights Reserved.):605-610.

85. Sau TK, Pal A, Jana NR, Wang ZL, Pal T: **Size controlled synthesis of gold nanoparticles using photochemically prepared seed particles**. *J Nanopart Res* 2001, **3**(Copyright (C) 2013 American Chemical Society (ACS). All Rights Reserved.):257-261.

86. Watzky MA, Finke RG: **Nanocluster Size-Control and "Magic Number" Investigations. Experimental Tests of the "Living-Metal Polymer" Concept and of Mechanism-Based Size-Control Predictions Leading to the Syntheses of Iridium(0) Nanoclusters Centering about Four Sequential Magic Numbers**. *Chem Mater* 1997, **9**(Copyright (C) 2013 American Chemical Society (ACS). All Rights Reserved.):3083-3095.

87. Brown KR, Walter DG, Natan MJ: **Seeding of colloidal Au nanoparticle solutions. 2. Improved control of particle size and shape**. *Chem Mater* 2000, **12**(Copyright (C) 2013 American Chemical Society (ACS). All Rights Reserved.):306-313.

88. Grzelczak M, Perez-Juste J, Mulvaney P, Liz-Marzan LM: **Shape control in gold nanoparticle synthesis**. *Chem Soc Rev* 2008, **37**(Copyright (C) 2013 American Chemical Society (ACS). All Rights Reserved.):1783-1791.

89. Niu J, Zhu T, Liu Z: **One-step seed-mediated growth of 30-150 nm quasispherical gold nanoparticles with 2-mercaptosuccinic acid as a new reducing agent**. *Nanotechnology* 2007, **18**(Copyright (C) 2013 American Chemical Society (ACS). All Rights Reserved.):325607/325601-325607/325607.

90. Jana NR, Gearheart L, Murphy CJ: **Wet chemical synthesis of high aspect ratio cylindrical gold nanorods**. *J Phys Chem B* 2001, **105**(Copyright (C) 2013 American Chemical Society (ACS). All Rights Reserved.):4065-4067.

91. Jana NR, Gearheart L, Murphy CJ: **Evidence for seed-mediated nucleation in the chemical reduction of gold salts to gold nanoparticles**. *Chem Mater* 2001, **13**(Copyright (C) 2013 American Chemical Society (ACS). All Rights Reserved.):2313-2322.

92. Capek I: **Preparation of metal nanoparticles in water-in-oil (w/o) microemulsions**. *Advances in Colloid and Interface Science* 2004, **110**(1–2):49-74.

93. Zheng Y, Wang Y, Yang X: **Aptamer-based colorimetric biosensing of dopamine using unmodified gold nanoparticles**. *Sens Actuators, B* 2011, **B156**(Copyright (C) 2013 American Chemical Society (ACS). All Rights Reserved.):95-99.

94. Dang Y-Q, Li H-W, Wang B, Li L, Wu Y: **Selective Detection of Trace Cr3+ in Aqueous Solution by Using 5,5'-Dithiobis (2-Nitrobenzoic acid)-Modified Gold Nanoparticles**. *ACS Appl Mater Interfaces* 2009, **1**(Copyright (C) 2013 American Chemical Society (ACS). All Rights Reserved.):1533-1538.

95. Liu L, Li S, Liu L, Deng D, Xia N: **Simple, sensitive and selective detection of dopamine using dithiobis(succinimidylpropionate)-modified gold nanoparticles as colorimetric probes**. *Analyst (Cambridge, U K)* 2012, **137**(Copyright (C) 2012 American Chemical Society (ACS). All Rights Reserved.):3794-3799.

96. Feng J-J, Guo H, Li Y-F, Wang Y-H, Chen W-Y, Wang A-J: **Single Molecular Functionalized Gold Nanoparticles for Hydrogen-Bonding Recognition and Colorimetric Detection of Dopamine with High Sensitivity and Selectivity**. *ACS Appl Mater Interfaces* 2013, **5**(Copyright (C) 2013 American Chemical Society (ACS). All Rights Reserved.):1226-1231.

97. Lee H-C, Chen T-H, Tseng W-L, Lin C-H: **Novel core etching technique of gold nanoparticles for colorimetric dopamine detection**. *Analyst (Cambridge, U K)* 2012, **137**(Copyright (C) 2012 American Chemical Society (ACS). All Rights Reserved.):5352-5357.

98. Zheng Y, Wang Y, Yang X: **Aptamer-based colorimetric biosensing of dopamine using unmodified gold nanoparticles**. *Sensors and Actuators B: Chemical* 2011, **156**(1):95-99.

99. Wang Z, Bai Y, Wei W, Xia N, Du Y: **Magnetic Fe3O4-based sandwich-type biosensor using modified gold nanoparticles as colorimetric probes for the detection of dopamine**. *Materials* 2013, **6**(12):5690-5699.

100. Liu J-M, Wang X-X, Cui M-L, Lin L-P, Jiang S-L, Jiao L, Zhang L-H: **A promising non-aggregation colorimetric sensor of AuNRs-Ag+ for determination of dopamine**. *Sens Actuators, B* 2013, **176**:97-102.

101. Huck CW, Bonn GK: **Recent developments in polymer-based sorbents for solid-phase extraction**. *J Chromatogr A* 2000, **885**(Copyright (C) 2013 American Chemical Society (ACS). All Rights Reserved.):51-72.

102. Dąbrowska H, Dąbrowski Ł, Biziuk M, Gaca J, Namieśnik J: **Solid-phase extraction clean-up of soil and sediment extracts for the determination of various types of pollutants in a single run**. *Journal of Chromatography A* 2003, **1003**(1–2):29-42.

103. Gessner MO, Schmitt AL: **Use of solid-phase extraction to determine ergosterol concentrations in plant tissue colonized by fungi**. *Appl Environ Microbiol* 1996, **62**(Copyright (C) 2013 American Chemical Society (ACS). All Rights Reserved.):415-419.

104. Marumo A, Kumazawa T, Lee X-P, Hasegawa C, Suzuki O, Sato K: **Utility of disk solid-phase extraction for whole blood samples: analysis of some tetracyclic antidepressants by gas chromatography with nitrogen-phosphorus detection**. *Forensic Toxicol* 2008, **26**(1):13-18.

105. Schindler BK, Foerster K, Angerer J: **Quantification of two urinary metabolites of organophosphorus flame retardants by solid-phase extraction and gas chromatography-tandem mass spectrometry**. *Anal Bioanal Chem* 2009, **395**(Copyright (C) 2013 American Chemical Society (ACS). All Rights Reserved.):1167-1171.

106. Kang X-J, Chen L-Q, Wang Y, Zhang Y-Y, Gu Z-Z: **Design of packed-fiber solid-phase extraction device for analysis of the drug and its metabolite in plasma**. *Biomed Microdevices* 2009, **11**(Copyright (C) 2013 American Chemical Society (ACS). All Rights Reserved.):723-729.

107. Qi D, Kang X, Chen L, Zhang Y, Wei H, Gu Z: **Electrospun polymer nanofibers as a solid-phase extraction sorbent for the determination of trace pollutants in environmental water**. *Anal Bioanal Chem* 2008, **390**(Copyright (C) 2013 American Chemical Society (ACS). All Rights Reserved.):929-938.

108. Lucci P, Pacetti D, Frega NG, Núñez O: **Current Trends in Sample Treatment Techniques for Environmental and Food Analysis**; 2012.

109. Chen J, Duan C, Guan Y: **Sorptive extraction techniques in sample preparation for organophosphorus pesticides in complex matrices**. *J Chromatogr B: Anal Technol Biomed Life Sci* 2010, **878**(Copyright (C) 2013 American Chemical Society (ACS). All Rights Reserved.):1216-1225.

110. Bielicka-Daszkiewicz K, Voelkel A: **Theoretical and experimental methods of determination of the breakthrough volume of SPE sorbents**. *Talanta* 2009, **80**(Copyright (C) 2013 American Chemical Society (ACS). All Rights Reserved.):614-621.

111. Rodriguez-Mozaz S, Lopez de Alda MJ, Barceló D: **Advantages and limitations of on-line solid phase extraction coupled to liquid chromatography–mass spectrometry technologies versus biosensors for monitoring of emerging contaminants in water**. *Journal of Chromatography A* 2007, **1152**(1–2):97-115.

112. Chen Y, Guo Z, Wang X, Qiu C: **Sample preparation**. *Journal of Chromatography A* 2008, **1184**(1–2):191-219.

113. Yu Z, Westerlund D, Boos KS: **Evaluation of liquid chromatographic behavior of restricted-access media precolumns in the course of direct injection of large volumes of plasma samples in column-switching systems**. *J Chromatogr B Biomed Sci Appl* 1997, **704**(Copyright (C) 2013 U.S. National Library of Medicine.):53-62.

114. Hennion M-C: **Solid-phase extraction: method development, sorbents, and coupling with liquid chromatography**. *Journal of Chromatography A* 1999, **856**(1–2):3-54.

115. Maisonnette C, Simon P, Hennion M-C, Pichon V: **Selective immunoclean-up followed by liquid chromatography for the monitoring of a biomarker of exposure to polycyclic aromatic hydrocarbons in urine at the ngl-1 level**. *J Chromatogr A* 2006, **1120**(Copyright (C) 2013 American Chemical Society (ACS). All Rights Reserved.):185-193.

116. Ferrer I, Barcelo D: **Validation of new solid-phase extraction materials for the selective enrichment of organic contaminants from environmental samples**. *TrAC, Trends Anal Chem* 1999, **18**(Copyright (C) 2013 American Chemical Society (ACS). All Rights Reserved.):180-192.

117. Deinl I, Angermaier L, Franzelius C, Machbert G: **Simple high-performance liquid-chromatographic column-switching technique for the online immunoaffinity extraction and analysis of flunitrazepam and its main metabolites in urine**. *J Chromatogr B: Biomed Sci Appl* 1997, **704**(Copyright (C) 2013 American Chemical Society (ACS). All Rights Reserved.):251-258.

118. Nedved ML, Habibi-Goudarzi S, Ganem B, Henion JD: **Characterization of Benzodiazepine "Combinatorial" Chemical Libraries by Online Immunoaffinity Extraction, Coupled Column HPLC-Ion Spray Mass Spectrometry-Tandem Mass Spectrometry**. *Anal Chem* 1996, **68**(Copyright (C) 2013 American Chemical Society (ACS). All Rights Reserved.):4228-4236.

119. Haasnoot W, Schilt R, Hamers ARM, Huf FA, Farjam A, Frei RW, Brinkman UAT: **Determination of β-19-nortestosterone and its metabolite α-19-nortestosterone in biological samples at the sub parts per billion level by high-performance liquid chromatography with on-line immunoaffinity sample pretreatment**. *J Chromatogr, Biomed Appl* 1989, **489**(Copyright (C) 2013 American Chemical Society (ACS). All Rights Reserved.):157-171.

120. Wang Y, Zhang J, Zhu XX, Yu A: **Specific binding of cholic acid by cross-linked polymers prepared by the hybrid imprinting method**. *Polymer* 2007, **48**(Copyright (C) 2013 American Chemical Society (ACS). All Rights Reserved.):5565-5571.

121. Djozan D, Ebrahimi B: **Preparation of new solid phase micro extraction fiber on the basis of atrazine-molecular imprinted polymer: application for GC and GC/MS screening of triazine herbicides in water, rice and onion**. *Anal Chim Acta* 2008, **616**(Copyright (C) 2013 U.S. National Library of Medicine.):152-159.

122. Kim WJ, Chang JY: **Molecularly imprinted polyimide nanofibers prepared by electrospinning**. *Mater Lett* 2011, **65**(Copyright (C) 2013 American Chemical Society (ACS). All Rights Reserved.):1388-1391.

123. Vlatakis G, Andersson LI, Mueller R, Mosbach K: **Drug assay using antibody mimics made by molecular imprinting**. *Nature (London)* 1993, **361**(Copyright (C) 2013 American Chemical Society (ACS). All Rights Reserved.):645-647.

124. Song X, Li J, Wang J, Chen L: **Quercetin molecularly imprinted polymers: preparation, recognition characteristics and properties as sorbent for solid-phase extraction**. *Talanta* 2009, **80**(Copyright (C) 2013 U.S. National Library of Medicine.):694-702.

125. Tamayo FG, Turiel E, Martin-Esteban A: **Molecularly imprinted polymers for solid-phase extraction and solid-phase microextraction: Recent developments and future trends**. *J Chromatogr A* 2007, **1152**(Copyright (C) 2013 American Chemical Society (ACS). All Rights Reserved.):32-40.

126. Yan H, Row KH: **Characteristic and synthetic approach of molecularly imprinted polymer**. *Int J Mol Sci* 2006, **7**(Copyright (C) 2013 American Chemical Society (ACS). All Rights Reserved.):155-178.

127. Pan H-H, Lee W-C, Hung C-Y, Hwang C-C: **Synthesis of molecularly imprinted polymer and its molecular recognition properties of N-acetylneuraminic acid**. *E-J Chem* 2007, **4**(Copyright (C) 2013 American Chemical Society (ACS). All Rights Reserved.):611-619.

128. Zhang H, Ye L, Mosbach K: **Non-covalent molecular imprinting with emphasis on its application in separation and drug development**. *J Mol Recognit* 2006, **19**(Copyright (C) 2013 American Chemical Society (ACS). All Rights Reserved.):248-259.

129. Zhang H, Song T, Zong F, Chen T, Pan C: **Synthesis and characterization of molecularly imprinted polymers for phenoxyacetic acids**. *Int J Mol Sci* 2008, **9**(Copyright (C) 2013 American Chemical Society (ACS). All Rights Reserved.):98-106.

130. Wulff G, Sarhan A, Zabrocki K: **Enzyme-analogue built polymers and their use for the resolution of racemates**. *Tetrahedron Letters* 1973, **14**(44):4329-4332.

131. Wulff G, Grobe-Einsler R, Vesper W, Sarhan A: **Enzyme-analogue built polymers, 5. On the specificity distribution of chiral cavities prepared in synthetic polymers**. *Die Makromolekulare Chemie* 1977, **178**(10):2817-2825.

132. Chen L, Xu S, Li J: **Recent advances in molecular imprinting technology: current status, challenges and highlighted applications**. *Chem Soc Rev* 2011, **40**(Copyright (C) 2013 American Chemical Society (ACS). All Rights Reserved.):2922-2942.

133. Takeuchi T, Murase N, Maki H, Mukawa T, Shinmori H: **Dopamine selective molecularly imprinted polymers via post-imprinting modification**. *Org Biomol Chem* 2006, **4**(Copyright (C) 2013 American Chemical Society (ACS). All Rights Reserved.):565-568.

134. Arshady R, Mosbach K: **Synthesis of substrate-selective polymers by host-guest polymerization**. *Macromol Chem Phys* 1981, **182**(Copyright (C) 2013 American Chemical Society (ACS). All Rights Reserved.):687-692.

135. Mosbach K, Ramstroem O: **The emerging technique of molecular imprinting and its future impact on biotechnology**. *Bio/Technology* 1996, **14**(Copyright (C) 2013 American Chemical Society (ACS). All Rights Reserved.):163-170.

136. Turiel E, Martin-Esteban A: **Molecularly imprinted polymers for sample preparation: A review**. *Anal Chim Acta* 2010, **668**(Copyright (C) 2013 American Chemical Society (ACS). All Rights Reserved.):87-99.

137. Katz A, Davis ME: **Investigations into the Mechanisms of Molecular Recognition with Imprinted Polymers**. *Macromolecules* 1999, **32**(Copyright (C) 2013 American Chemical Society (ACS). All Rights Reserved.):4113-4121.

138. Turner NW, Piletska EV, Karim K, Whitcombe M, Malecha M, Magan N, Baggiani C, Piletsky SA: **Effect of the solvent on recognition properties of molecularly imprinted polymer specific for ochratoxin A**. *Biosens Bioelectron* 2004, **20**(Copyright (C) 2013 American Chemical Society (ACS). All Rights Reserved.):1060-1067.

139. Oral E, Peppas NA: **Dynamic studies of molecular imprinting polymerizations**. *Polymer* 2004, **45**(Copyright (C) 2013 American Chemical Society (ACS). All Rights Reserved.):6163-6173.

140. Piletska EV, Guerreiro AnR, Whitcombe MJ, Piletsky SA: **Influence of the Polymerization Conditions on the Performance of Molecularly Imprinted Polymers**. *Macromolecules* 2009, **42**(14):4921-4928.

141. Widstrand C, Yilmaz E, Boyd B, Billing J, Rees A: **Molecularly imprinted polymers: a new generation of affinity matrices**. *Am Lab (Shelton, CT, U S)* 2006, **38**(Copyright (C) 2013 American Chemical Society (ACS). All Rights Reserved.):12,14.

142. Crescenzi C, Bayoudh S, Cormack PAG, Klein T, Ensing K: **Determination of Clenbuterol in Bovine Liver by Combining Matrix Solid-Phase Dispersion and Molecularly Imprinted Solid-Phase Extraction Followed by Liquid Chromatography/Electrospray Ion Trap Multiple-Stage Mass Spectrometry**. *Anal Chem* 2001, **73**(Copyright (C) 2013 American Chemical Society (ACS). All Rights Reserved.):2171-2177.

143. Kaabi FB, Pichon V: **Different approaches to synthesizing molecularly imprinted polymers for solid-phase extraction**. *LCGC North Am* 2007, **25**(Copyright (C) 2013 American Chemical Society (ACS). All Rights Reserved.):732-739.

144. Shamsipur M, Fasihi J, Khanchi A, Hassani R, Alizadeh K, Shamsipur H: **A stoichiometric imprinted chelating resin for selective recognition of copper(II) ions in aqueous media**. *Anal Chim Acta* 2007, **599**(Copyright (C) 2013 American Chemical Society (ACS). All Rights Reserved.):294-301.

145. Koohpaei AR, Shahtaheri SJ, Ganjali MR, Forushani AR, Golbabaei F: **Application of multivariate analysis to the screening of molecularly imprinted polymers (MIPs) for ametryn**. *Talanta* 2008, **75**(Copyright (C) 2013 American Chemical Society (ACS). All Rights Reserved.):978-986.

146. Feas X, Seijas JA, Vazquez-Tato MP, Regal P, Cepeda A, Fente C: **Syntheses of molecularly imprinted polymers: Molecular recognition of cyproheptadine using original print molecules and azatadine as dummy templates**. *Anal Chim Acta* 2009, **631**(Copyright (C) 2013 American Chemical Society (ACS). All Rights Reserved.):237-244.

147. Kempe M, Fischer L, Mosbach K: **Chiral separation using molecularly imprinted heteroaromatic polymers**. *J Mol Recognit* 1993, **6**(Copyright (C) 2013 American Chemical Society (ACS). All Rights Reserved.):25-29.

148. Ramstrom O, Ansell RJ: **Molecular imprinting technology: challenges and prospects for the future**. *Chirality* 1998, **10**(Copyright (C) 2013 American Chemical Society (ACS). All Rights Reserved.):195-209.

149. Kempe M, Mosbach K: **Direct resolution of naproxen on a non-covalently molecularly imprinted chiral stationary phase**. *J Chromatogr A* 1994, **664**(Copyright (C) 2013 American Chemical Society (ACS). All Rights Reserved.):276-279.

150. Lai EPC, De MZ, Wu S: **Characterization of molecularly imprinted and nonimprinted polymer submicron particles specifically tailored for removal of trace 17β-estradiol in water treatment**. *J Appl Polym Sci* 2010, **116**(Copyright (C) 2013 American Chemical Society (ACS). All Rights Reserved.):1499-1508.

151. Xia WZ, Cook WD: **Exotherm control in the thermal polymerization of nona-ethylene glycol dimethacrylate (NEGDM) using a dual radical initiator system**. *Polymer* 2002, **44**(Copyright (C) 2013 American Chemical Society (ACS). All Rights Reserved.):79-88.

152. Haginaka J: **Molecularly imprinted polymers as affinity-based separation media for sample preparation**. *J Sep Sci* 2009, **32**(Copyright (C) 2013 American Chemical Society (ACS). All Rights Reserved.):1548-1565.

153. Haginaka J, Kagawa C: **Uniformly sized molecularly imprinted polymer for d-chlorpheniramine. Evaluation of retention and molecular recognition properties in an aqueous mobile phase**. *J Chromatogr A* 2002, **948**(Copyright (C) 2013 American Chemical Society (ACS). All Rights Reserved.):77-84.

154. Hosoya K, Yoshizako K, Shirasu Y, Kimata K, Araki T, Tanaka N, Haginaka J: **Molecularly imprinted uniform-size polymer-based stationary phase for high-performance liquid chromatography. Structural contribution of cross-linked polymer network on specific molecular recognition**. *J Chromatogr A* 1996, **728**(Copyright (C) 2013 American Chemical Society (ACS). All Rights Reserved.):139-147.

155. Haginaka J, Sakai Y: **Uniform-sized molecularly imprinted polymer material for (S)-propranolol**. *Journal of Pharmaceutical and Biomedical Analysis* 2000, **22**(6):899-907.

156. Perez-Moral N, Mayes AG: **Novel MIP formats**. *Bioseparation* 2001, **10**(Copyright (C) 2013 U.S. National Library of Medicine.):287-299.

157. Perez-Moral N, Mayes AG: **Comparative study of imprinted polymer particles prepared by different polymerisation methods**. *Anal Chim Acta* 2004, **504**(Copyright (C) 2013 American Chemical Society (ACS). All Rights Reserved.):15-21.

158. Jing T, Gao X-D, Wang P, Wang Y, Lin Y-F, Hu X-Z, Hao Q-L, Zhou Y-K, Mei S-R: **Determination of trace tetracycline antibiotics in foodstuffs by liquid chromatography-tandem mass spectrometry coupled with selective molecular-imprinted solid-phase extraction**. *Anal Bioanal Chem* 2009, **393**(Copyright (C) 2013 American Chemical Society (ACS). All Rights Reserved.):2009-2018.

159. Wang J, Cormack PAG, Sherrington DC, Khoshdel E: **Monodisperse, Molecularly Imprinted Polymer Microspheres Prepared by Precipitation Polymerization for Affinity Separation Applications**. *Angewandte Chemie International Edition* 2003, **42**(43):5336-5338.

160. Svec F, Tennikova TB, Deyl Z: **Monolithic Materials: Preparation, Properties and Applications. [In: J. Chromatogr. Libr., 2003; 67]**: Elsevier Science B.V.; 2003.

161. Matsui J, Kato T, Takeuchi T, Suzuki M, Yokoyama K, Tamiya E, Karube I: **Molecular recognition in continuous polymer rods prepared by a molecular imprinting technique**. *Anal Chem* 1993, **65**(Copyright (C) 2013 American Chemical Society (ACS). All Rights Reserved.):2223-2224.

162. Liu H, Row KH, Yang G: **Monolithic molecularly imprinted columns for chromatographic separation**. *Chromatographia* 2005, **61**(Copyright (C) 2013 American Chemical Society (ACS). All Rights Reserved.):429-432.

163. Pawliszyn J, Lord HL, Editors: **Handbook of Sample Preparation**: John Wiley & Sons, Inc.; 2010.

164. Saim Na, Dean JR, Abdullah MP, Zakaria Z: **Extraction of polycyclic aromatic hydrocarbons from contaminated soil using Soxhlet extraction, pressurised and atmospheric microwave-assisted extraction, supercritical fluid extraction and accelerated solvent extraction**. *Journal of Chromatography A* 1997, **791**(1–2):361-366.

165. Janoszka B, Blaszczyk U, Warzecha L, Strozyk M, Damasiewicz-Bodzek A, Bodzek D: **Clean-up procedures for the analysis of heterocyclic aromatic amines (aminoazaarenes) from heat-treated meat samples**. *J Chromatogr A* 2001, **938**(Copyright (C) 2013 American Chemical Society (ACS). All Rights Reserved.):155-165.

166. Pawliszyn J: **New directions in sample preparation for analysis of organic compounds**. *TrAC, Trends Anal Chem* 1995, **14**(Copyright (C) 2013 American Chemical Society (ACS). All Rights Reserved.):113-122.

167. [http://whale.wheelock.edu/bwcontaminants/analysis.html]

168. Long C, Mai Z, Yang Y, Zhu B, Xu X, Lu L, Zou X: **Determination of multi-residue for malachite green, gentian violet and their metabolites in aquatic products by high-performance liquid chromatography coupled with molecularly imprinted solid-phase extraction**. *J Chromatogr A* 2009, **1216**(Copyright (C) 2013 American Chemical Society (ACS). All Rights Reserved.):2275-2281.

169. Jiang T, Zhao L, Chu B, Feng Q, Yan W, Lin J-M: **Molecularly imprinted solid-phase extraction for the selective determination of 17β-estradiol in fishery samples with high performance liquid chromatography**. *Talanta* 2009, **78**(Copyright (C) 2013 American Chemical Society (ACS). All Rights Reserved.):442-447.

170. Benito-Pena E, Martins S, Orellana G, Moreno-Bondi MC: **Water-compatible molecularly imprinted polymer for the selective recognition of fluoroquinolone antibiotics in biological samples**. *Anal Bioanal Chem* 2009, **393**(Copyright (C) 2013 American Chemical Society (ACS). All Rights Reserved.):235-245.

171. Ramstroem O, Ye L, Mosbach K: **Artificial antibodies to corticosteroids prepared by molecular imprinting**. *Chem Biol* 1996, **3**(Copyright (C) 2013 American Chemical Society (ACS). All Rights Reserved.):471-477.

172. Valero-Navarro A, Salinas-Castillo A, Fernández-Sánchez JF, Segura-Carretero A, Mallavia R, Fernández-Gutiérrez A: **The development of a MIP-optosensor for the detection of monoamine naphthalenes in drinking water**. *Biosensors and Bioelectronics* 2009, **24**(7):2305-2311.

173. Du J, Shen L, Lu J: **Flow injection chemiluminescence determination of epinephrine using epinephrine-imprinted polymer as recognition material**. *Anal Chim Acta* 2003, **489**(Copyright (C) 2013 American Chemical Society (ACS). All Rights Reserved.):183-189.

174. Yu J, Wan F, Zhang C, Yan M, Zhang X, Wang S: **Molecularly imprinted polymeric microspheres for determination of bovine serum albumin based on flow injection chemiluminescence sensor**. *Biosensors and Bioelectronics* 2010, **26**(2):632-637.

175. Lu F, Li H, Sun M, Fan L, Qiu H, Li X, Luo C: **Flow injection chemiluminescence sensor based on core–shell magnetic molecularly imprinted nanoparticles for determination of sulfadiazine**. *Analytica Chimica Acta* 2012, **718**(0):84-91.

176. Kubo H, Nariai H, Takeuchi T: **Multiple hydrogen bonding-based fluorescent imprinted polymers for cyclobarbital prepared with 2,6-bis(acrylamido)pyridine**. *Chem Commun (Cambridge, U K)* 2003(Copyright (C) 2013 American Chemical Society (ACS). All Rights Reserved.):2792-2793.

177. Wandelt B, Turkewitsch P, Wysocki S, Darling GD: **Fluorescent molecularly imprinted polymer studied by time-resolved fluorescence spectroscopy**. *Polymer* 2002, **43**(Copyright (C) 2013 American Chemical Society (ACS). All Rights Reserved.):2777-2785.

178. Tong A, Dong H, Li L: **Molecular imprinting-based fluorescent chemosensor for histamine using zinc(II)-protoporphyrin as a functional monomer**. *Anal Chim Acta* 2002, **466**(Copyright (C) 2013 American Chemical Society (ACS). All Rights Reserved.):31-37.

179. Graham AL, Carlson CA, Edmiston PL: **Development and characterization of molecularly imprinted sol-gel materials for the selective detection of DDT**. *Anal Chem* 2002, **74**(Copyright (C) 2013 American Chemical Society (ACS). All Rights Reserved.):458-467.

180. Wang W, Gao S, Wang B: **Building fluorescent sensors by template polymerization: the preparation of a fluorescent sensor for D-fructose**. *Org Lett* 1999, **1**(Copyright (C) 2013 U.S. National Library of Medicine.):1209-1212.

181. Gao S, Wang W, Wang B: **Building fluorescent sensors for carbohydrates using template-directed polymerizations**. *Bioorg Chem* 2001, **29**(Copyright (C) 2013 American Chemical Society (ACS). All Rights Reserved.):308-320.

182. Claude B, Nehme R, Morin P: **Analysis of urinary neurotransmitters by capillary electrophoresis: Sensitivity enhancement using field-amplified sample injection and molecular imprinted polymer solid phase extraction**. *Anal Chim Acta* 2011, **699**(Copyright (C) 2013 American Chemical Society (ACS). All Rights Reserved.):242-248.

183. Wang X, Tan H, Qi K, Shao L, Li H, Xue X, Xie Y: **Determination of enrofloxacin residue in chicken muscle using molecular imprinted solid phase extraction-high performance capillary electrophoresis**. *Sepu* 2010, **28**(Copyright (C) 2013 American Chemical Society (ACS). All Rights Reserved.):1107-1110.

184. Matsui J, Akamatsu K, Nishiguchi S, Miyoshi D, Nawafune H, Tamaki K, Sugimoto N: **Composite of Au Nanoparticles and Molecularly Imprinted Polymer as a Sensing Material**. *Anal Chem* 2004, **76**(Copyright (C) 2013 American Chemical Society (ACS). All Rights Reserved.):1310-1315.

185. Park J-S: **Electrospinning and its applications**. *Adv Nat Sci: Nanosci Nanotechnol* 2010, **1**(Copyright (C) 2013 American Chemical Society (ACS). All Rights Reserved.):043002/043001-043002/043005.

186. Li F, Zhao Y, Song Y: **Core-shell nanofibers: nano channel and capsule by coaxial electrospinning**. In*: 2010*. InTech: 419-438.

187. Thavasi V, Singh G, Ramakrishna S: **Electrospun nanofibers in energy and environmental applications**. *Energy Environ Sci* 2008, **1**(Copyright (C) 2013 American Chemical Society (ACS). All Rights Reserved.):205-221.

188. Chronakis IS, Grapenson S, Jakob A: **Conductive polypyrrole nanofibers via electrospinning: Electrical and morphological properties**. *Polymer* 2006, **47**(Copyright (C) 2013 American Chemical Society (ACS). All Rights Reserved.):1597-1603.

189. Holopainen J, Penttinen T, Santala E, Ritala M: **Needleless electrospinning with twisted wire spinneret**. *Nanotechnology* 2015, **26**(2):25301.

190. Niu H, Lin T: **Fiber generators in needleless electrospinning**. *J Nanomater* 2012:725950, 725913 pp.

191. Varesano A, Rombaldoni F, Mazzuchetti G, Tonin C, Comotto R: **Multi-jet nozzle electrospinning on textile substrates: observations on process and nanofiber mat deposition**. *Polym Int* 2010, **59**(12):1606-1615.

192. Theron SA, Yarin AL, Zussman E, Kroll E: **Multiple jets in electrospinning: experiment and modeling**. *Polymer* 2005, **46**(9):2889-2899.

193. Lau KT, Edwards S, Diamond D: **Solid-state ammonia sensor based on Berthelot's reaction**. *Sensors and Actuators B: Chemical* 2004, **98**(1):12-17.

194. Lu B, Wang Y, Liu Y, Duan H, Zhou J, Zhang Z, Wang Y, Li X, Wang W, Lan W *et al*: **Superhigh-Throughput Needleless Electrospinning Using a Rotary Cone as Spinneret**. *Small* 2010, **6**(15):1612-1616.

195. Niu H, Wang X, Lin T: **Needleless electrospinning: influences of fibre generator geometry**. *J Text Inst* 2012, **103**(7):787-794.

196. Li X, Ding B, Lin J, Yu J, Sun G: **Enhanced Mechanical Properties of Superhydrophobic Microfibrous Polystyrene Mats via Polyamide 6 Nanofibers**. *J Phys Chem C* 2009, **113**(Copyright (C) 2013 American Chemical Society (ACS). All Rights Reserved.):20452-20457.

197. Miyauchi Y, Ding B, Shiratori S: **Fabrication of a silver-ragwort-leaf-like super-hydrophobic micro/nanoporous fibrous mat surface by electrospinning**.

Nanotechnology 2006, **17**(Copyright (C) 2013 American Chemical Society (ACS). All Rights Reserved.):5151-5156.

198. Wang L, Topham PD, Mykhaylyk OO, Howse JR, Bras W, Jones RAL, Ryan AJ: **Electrospinning pH-responsive block copolymer nanofibers**. *Adv Mater (Weinheim, Ger)* 2007, **19**(Copyright (C) 2013 American Chemical Society (ACS). All Rights Reserved.):3544-3548.

199. Huang Z-M, Zhang YZ, Kotaki M, Ramakrishna S: **A review on polymer nanofibers by electrospinning and their applications in nanocomposites**. *Compos Sci Technol* 2003, **63**(Copyright (C) 2013 American Chemical Society (ACS). All Rights Reserved.):2223-2253.

200. Thompson CJ, Chase GG, Yarin AL, Reneker DH: **Effects of parameters on nanofiber diameter determined from electrospinning model**. *Polymer* 2007, **48**(Copyright (C) 2013 American Chemical Society (ACS). All Rights Reserved.):6913-6922.

201. Pant HR, Nam K-T, Oh H-J, Panthi G, Kim H-D, Kim B-i, Kim HY: **Effect of polymer molecular weight on the fiber morphology of electrospun mats**. *Journal of Colloid and Interface Science* 2011, **364**(1):107-111.

202. Wannatong L, Sirivat A, Supaphol P: **Effects of solvents on electrospun polymeric fibers: Preliminary study on polystyrene**. *Polym Int* 2004, **53**(Copyright (C) 2013 American Chemical Society (ACS). All Rights Reserved.):1851-1859.

203. Theron SA, Zussman E, Yarin AL: **Experimental investigation of the governing parameters in the electrospinning of polymer solutions**. *Polymer* 2004, **45**(Copyright (C) 2013 American Chemical Society (ACS). All Rights Reserved.):2017-2030.

204. Yang D, Liu X, Jin Y, Zhu Y, Zeng D-D, Jiang X-Y, Ma H-W: **Electrospinning of Poly(dimethylsiloxane)/Poly(methyl methacrylate) Nanofibrous Membrane: Fabrication and Application in Protein Microarrays**. *Biomacromolecules* 2009, **10**(Copyright (C) 2013 American Chemical Society (ACS). All Rights Reserved.):3335-3340.

205. Ding B, Wang M, Yu J, Sun G: **Gas sensors based on electrospun nanofibers**. *Sensors* 2009, **9**(Copyright (C) 2013 American Chemical Society (ACS). All Rights Reserved.):1609-1624.

206. Ding B, Wang M, Wang X, Yu J, Sun G: **Electrospun nanomaterials for ultrasensitive sensors**. *Materials Today* 2010, **13**(11):16-27.

207. Shin C: **Filtration application from recycled expanded polystyrene**. *J Colloid Interface Sci* 2006, **302**(Copyright (C) 2013 American Chemical Society (ACS). All Rights Reserved.):267-271.

208. Homaeigohar SS, Buhr K, Ebert K: **Polyethersulfone electrospun nanofibrous composite membrane for liquid filtration**. *J Membr Sci* 2010, **365**(Copyright (C) 2013 American Chemical Society (ACS). All Rights Reserved.):68-77.

209. Onozuka K, Ding B, Tsuge Y, Naka T, Yamazaki M, Sugi S, Ohno S, Yoshikawa M, Shiratori S: **Electrospinning processed nanofibrous TiO2 membranes for photovoltaic applications**. *Nanotechnology* 2006, **17**(Copyright (C) 2013 American Chemical Society (ACS). All Rights Reserved.):1026-1031.

210. Bhattarai N, Edmondson D, Veiseh O, Matsen FA, Zhang M: **Electrospun chitosan-based nanofibers and their cellular compatibility**. *Biomaterials* 2005, **26**(Copyright (C) 2013 American Chemical Society (ACS). All Rights Reserved.):6176-6184.

211. Mahanta N, Valiyaveettil S: **In situ preparation of silver nanoparticles on biocompatible methacrylated poly(vinyl alcohol) and cellulose based polymeric nanofibers**. *RSC Adv* 2012, **2**(Copyright (C) 2013 American Chemical Society (ACS). All Rights Reserved.):11389-11396.

212. Park H, Lee KY, Lee SJ, Park KE, Park WH: **Plasma-treated poly(lactic-co-glycolic acid) nanofibers for tissue engineering**. *Macromol Res* 2007, **15**(Copyright (C) 2013 American Chemical Society (ACS). All Rights Reserved.):238-243.

213. Son WK, Youk JH, Lee TS, Park WH: **Preparation of antimicrobial ultrafine cellulose acetate fibers with silver nanoparticles**. *Macromol Rapid Commun* 2004, **25**(Copyright (C) 2013 American Chemical Society (ACS). All Rights Reserved.):1632-1637.

214. Shi Q, Vitchuli N, Nowak J, Noar J, Caldwell JM, Breidt F, Bourham M, McCord M, Zhang X: **One-step synthesis of silver nanoparticle-filled nylon 6 nanofibers and their antibacterial properties**. *J Mater Chem* 2011, **21**(Copyright (C) 2013 American Chemical Society (ACS). All Rights Reserved.):10330-10335.

215. Li D, McCann JT, Gratt M, Xia Y: **Photocatalytic deposition of gold nanoparticles on electrospun nanofibers of titania**. *Chemical Physics Letters* 2004, **394**(4–6):387-391.

216. Sawada K, Sakai S, Taya M: **Polyacrylonitrile-based electrospun nanofibers carrying gold nanoparticles in situ formed by photochemical assembly**. *J Mater Sci* 2014, **49**(13):4595-4600.

217. Chang H-C, Liu C-L, Chen W-C: **Flexible Nonvolatile Transistor Memory Devices Based on One-Dimensional Electrospun P3HT:Au Hybrid Nanofibers**. *Advanced Functional Materials* 2013, **23**(39):4960-4968.

218. Kim G-M, Wutzler A, Radusch H-J, Michler GH, Simon P, Sperling RA, Parak WJ: **One-Dimensional Arrangement of Gold Nanoparticles by Electrospinning**. *Chem Mater* 2005, **17**(Copyright (C) 2013 American Chemical Society (ACS). All Rights Reserved.):4949-4957.

219. Han G, Guo B, Zhang L, Yang B: **Conductive gold films assembled on electrospun poly(methyl methacrylate) fibrous mats**. *Adv Mater (Weinheim, Ger)* 2006, **18**(Copyright (C) 2013 American Chemical Society (ACS). All Rights Reserved.):1709-1712.

220. Liu Z, Zhou C, Zheng B, Qian L, Mo Y, Luo F, Shi Y, Choi MMF, Xiao D: **In situ synthesis of gold nanoparticles on porous polyacrylonitrile nanofibers for sensing applications**. *Analyst (Cambridge, U K)* 2011, **136**(Copyright (C) 2013 American Chemical Society (ACS). All Rights Reserved.):4545-4551.

221. Fang X, Ma H, Xiao S, Shen M, Guo R, Cao X, Shi X: **Facile immobilization of gold nanoparticles into electrospun polyethyleneimine/polyvinyl alcohol nanofibers for catalytic applications**. *J Mater Chem* 2011, **21**(Copyright (C) 2013 American Chemical Society (ACS). All Rights Reserved.):4493-4501.

222. Mahanta N, Valiyaveettil S: **In situ preparation of silver nanoparticles on biocompatible methacrylated poly(vinyl alcohol) and cellulose based polymeric nanofibers**. *RSC Adv* 2012, **2**(30):11389-11396.

223. Chronakis IS, Jakob A, Hagstroem B, Ye L: **Encapsulation and Selective Recognition of Molecularly Imprinted Theophylline and 17β-Estradiol Nanoparticles within Electrospun Polymer Nanofibers**. *Langmuir* 2006, **22**(Copyright (C) 2013 American Chemical Society (ACS). All Rights Reserved.):8960-8965.

224. Liu H, Lei X, Zhai Y, Li L: **Electrospun nanofiber membranes containing molecularly imprinted polymer (MIP) for rhodamine B (RhB)**. *Adv Chem Eng Sci* 2012, **2**(2):266-274.

225. Yoshimatsu K, Ye L, Lindberg J, Chronakis IS: **BIOMIMETIC NANOCOMPOSITES WITH SELECTIVE MOLECULAR ADSORPTION USING ELECTROSPUN NANOFIBER AFFINITY MEMBRANES**.

226. Lulinski P, Maciejewska D, Bamburowicz-Klimkowska M, Szutowski M: **Dopamine-imprinted polymers: template-monomer interactions, analysis of template removal and application to solid phase extraction**. *Molecules* 2007, **12**(Copyright (C) 2013 American Chemical Society (ACS). All Rights Reserved.):2434-2449.

227. Chen W, Deng H-H, Hong L, Wu Z-Q, Wang S, Liu A-L, Lin X-H, Xia X-H: **Bare gold nanoparticles as facile and sensitive colorimetric probe for melamine detection**. *Analyst (Cambridge, U K)* 2012, **137**(Copyright (C) 2012 American Chemical Society (ACS). All Rights Reserved.):5382-5386.

228. Huang X, Wu H, Liao X, Shi B: **One-step, size-controlled synthesis of gold nanoparticles at room temperature using plant tannin**. *Green Chem* 2010, **12**(Copyright (C) 2013 American Chemical Society (ACS). All Rights Reserved.):395-399.

229. Jeon EK, Seo E, Lee E, Lee W, Um M-K, Kim B-S: **Mussel-inspired green synthesis of silver nanoparticles on graphene oxide nanosheets for enhanced**

catalytic applications. *Chem Commun (Cambridge, U K)* 2013, **49**(Copyright (C) 2013 American Chemical Society (ACS). All Rights Reserved.):3392-3394.

230. Brown KR, Walter DG, Natan MJ: **Seeding of colloidal Au nanoparticle solutions. 2. Improved control of particle size and shape**. *Chem Mater* 2000, **12**(2):306-313.

231. Baron R, Zayats M, Willner I: **Dopamine-, L-DOPA-, Adrenaline-, and Noradrenaline-Induced Growth of Au Nanoparticles: Assays for the Detection of Neurotransmitters**. *Anal Chem* 2005, **77**(Copyright (C) 2013 American Chemical Society (ACS). All Rights Reserved.):1566-1571.

232. Min K, Gao H, Matyjaszewski K: **Use of Ascorbic Acid as Reducing Agent for Synthesis of Well-Defined Polymers by ARGET ATRP**. *Macromolecules (Washington, DC, U S)* 2007, **40**(Copyright (C) 2013 American Chemical Society (ACS). All Rights Reserved.):1789-1791.

233. Liao Y, Wang Y, Feng X, Wang W, Xu F, Zhang L: **Antibacterial surfaces through dopamine functionalization and silver nanoparticle immobilization**. *Materials Chemistry and Physics* 2010, **121**(3):534-540.

234. Nam K-T, Pant HR, Jeong J-w, Pant B, Kim B-i, Kim H-Y: **Solvent degradation of nylon-6 and its effect on fiber morphology of electrospun mats**. *Polym Degrad Stab* 2011, **96**(Copyright (C) 2013 American Chemical Society (ACS). All Rights Reserved.):1984-1988.

235. Pant HR, Bajgai MP, Nam KT, Seo YA, Pandeya DR, Hong ST, Kim HY: **Electrospun nylon-6 spider-net like nanofiber mat containing TiO2 nanoparticles: A multifunctional nanocomposite textile material**. *J Hazard Mater* 2011, **185**(Copyright (C) 2013 American Chemical Society (ACS). All Rights Reserved.):124-130.

236. Pant HR, Bajgai MP, Yi C, Nirmala R, Nam KT, Baek W-i, Kim HY: **Effect of successive electrospinning and the strength of hydrogen bond on the morphology of electrospun nylon-6 nanofibers**. *Colloids and Surfaces A: Physicochemical and Engineering Aspects* 2010, **370**(1–3):87-94.

237. Morales-Luckie RA, Sanchez-Mendieta V, Olea-Mejia O, Vilchis-Nestor AR, Lopez-Tellez G, Varela-Guerrero V, Huerta L, Arenas-Alatorre J: **Facile solventless**

synthesis of a nylon-6,6/silver nanoparticles composite and its XPS study. *Int J Polym Sci* 2013(Copyright (C) 2013 American Chemical Society (ACS). All Rights Reserved.):235850, 235859 pp.

238. Suedee R, Seechamnanturakit V, Suksuwan A, Canyuk B: **Recognition properties and competitive assays of a dual dopamine/serotonin selective molecularly imprinted polymer**. *Int J Mol Sci* 2008, **9**(Copyright (C) 2013 American Chemical Society (ACS). All Rights Reserved.):2333-2356.

239. Liao J, Zhang Y, Yu W, Xu L, Ge C, Liu J, Gu N: **Linear aggregation of gold nanoparticles in ethanol**. *Colloids Surf, A* 2003, **223**(Copyright (C) 2012 American Chemical Society (ACS). All Rights Reserved.):177-183.

240. Thanh NTK, Rosenzweig Z: **Development of an aggregation-based immunoassay for anti-protein A using gold nanoparticles**. *Anal Chem* 2002, **74**(Copyright (C) 2012 American Chemical Society (ACS). All Rights Reserved.):1624-1628.

241. **Catecholamines urine** [http://www.nlm.nih.gov/medlineplus/ency/article/003613.htm]

242. **Uric acid in urine** [http://www.webmd.com/a-to-z-guides/uric-acid-in-urine?page=2]

243. Zhuang Z, Li J, Xu R, Xiao D: **Electrochemical detection of dopamine in the presence of ascorbic acid using overoxidized polypyrrole/graphene modified electrodes**. *Int J Electrochem Sci* 2011, **6**(6):2149-2161.

244. Scampicchio M, Arecchi A, Mannino S: **Optical nanoprobes based on gold nanoparticles for sugar sensing**. *Nanotechnology* 2009, **20**(Copyright (C) 2014 American Chemical Society (ACS). All Rights Reserved.):135501/135501-135501/135505.

245. Bai J, Li Y, Yang S, Du J, Wang S, Zheng J, Wang Y, Yang Q, Chen X, Jing X: **A simple and effective route for the preparation of poly(vinyl alcohol) (PVA) nanofibers containing gold nanoparticles by electrospinning method**. *Solid State Commun* 2007, **141**(5):292-295.

246. Deniz AE, Vural HA, Ortac B, Uyar T: **Gold nanoparticle/polymer nanofibrous composites by laser ablation and electrospinning**. *Mater Lett* 2011, **65**(19-20):2941-2943.

247. Bai J, Yang Q, Li M, Wang S, Zhang C, Li Y: **Preparation of composite nanofibers containing gold nanoparticles by using poly(N-vinylpyrrolidone) and β-cyclodextrin**. *Mater Chem Phys* 2008, **111**(2-3):205-208.

248. Oprea S, Potolinca VO: **Synthesis and characterization of linear and cross-linked cyclodextrin polyurethane elastomers**. *Polymer-Plastics Technology and Engineering* 2013, **52**(15):1550-1556.

249. Babaei A, Mirzakhani S, Khalilzadeh B: **A sensitive simultaneous determination of epinephrine and tyrosine using an iron(III) doped zeolite-modified carbon paste electrode**. *Journal of the Brazilian Chemical Society* 2009, **20**:1862-1869.

250. Iversen LL: **The uptake and Storage of Noradrenaline in Sympathetic Nerves**: Cambridge Univ. Press; 1967.

251. Yu C, Luo M, Zeng F, Zheng F, Wu S: **Mesoporous silica particles for selective detection of dopamine with [small beta]-cyclodextrin as the selective barricade**. *Chemical Communications* 2011, **47**(32):9086-9088.

252. Abbaspour A, Noori A: **A cyclodextrin host–guest recognition approach to an electrochemical sensor for simultaneous quantification of serotonin and dopamine**. *Biosensors and Bioelectronics* 2011, **26**(12):4674-4680.

253. Sambasevam KP, Mohamad S, Sarih NM, Ismail NA: **Synthesis and characterization of the inclusion complex of β-cyclodextrin and azomethine**. *Int J Mol Sci* 2013, **14**:3671-3682.

254. Roik NV, Belyakova LA: **IR spectroscopy, X-ray diffraction and thermal analysis studies of solid "β-cyclodextrin - p-aminobenzoic acid" inclusion complex**. *Fiz Khim Tverd Tila* 2011, **12**(1):168-173.